Studying the Effect of Low Doses of Ionization Radiation on Senescence in Human Lung Fibroblasts.

By

Usha Kabilan

A thesis submitted in partial fulfilment of the requirements for the Master of Science degree in Biochemistry.

Department of Biochemistry, Microbiology, Immunology
Faculty of Medicine
University of Ottawa

Supervisor: Dr. Dmitry Klokov
Co-Supervisor: Dr. Tommy Alain

ABSTRACT

The exposure to high doses of ionizing radiation (>5Gy) is unequivocally associated with increased cancer risk. However, there is substantial experimental evidence showing that in response to low doses of ionizing radiation (LDR: <100mGy), cells and organisms are benefitted with delayed aging, improved immunity and reduced cancer growth. These intriguing findings have proposed the "Radiation Hormesis" hypothesis. Herein, I studied the senescence effects of LDR exposure to normal human HFL1 cells and examined transcriptional changes. I found that HFL1 cells exposed to 10 mGy of gamma radiation had delayed senescence measured at 12 weeks post-irradiation compared to unirradiated cells. Through qPCR array analysis, I found that genes involved in human cellular senescence functions are differentially regulated in 10 mGy exposed cells at 12 weeks compared to 1-week post-exposure. A nucleolar protein, SIRT7, that belongs to the family of proteins called *Sirtuins* with known roles in aging, was found to be upregulated transcriptionally in LDR-exposed HFL1 cells. Knocking out SIRT7 protein significantly accelerated senescence in HFL1 cells suggesting a direct role of SIRT7 in deceleration of senescence and potentially in mediating radiation hormesis. Furthermore, overexpression of the HRAS oncogene strongly accelerated senescence in HFL1 cells through gene expression of cell cycle regulators and checkpoint proteins. Together, my studies revealed that LDR induces unique transcriptional changes resulting in a potentially radio adaptive protective cellular response. I also discuss the HRAS overexpression system as a time-efficient cellular model that could be used to more rapidly study the effect of LDR on senescence using primary cultures.

ACKNOWLEDGMENTS

I thank Dr. Dmitry Klokov for believing in me and agreeing to let me work on this project. I also want to thank Dr. Tommy Alain whom irrespective of not working on senescence gave me full freedom and space in his lab to do my experiments and encouraged me to explore different aspects of this project. I also want to thank Dr. Tyson Graber, Huy-Dung Hoang, Jian-Jun Jia, and Vickey Gilchrist for the help in establishing my experiments and guiding me through this degree. I also want to thank my TAC members Dr. Michael Downey and Dr. Yi Wang for their support and guidance on this project. Finally, I thank the University of Ottawa for accepting me as a graduate student and letting me complete this degree on time. I also thank my mother for letting me focus on my career and pursue higher studies.

LIST OF ABBREVIATIONS:

Trp53/Tp53	Tumor Protein p53
TGFβ1	Transforming Growth Factor Beta 1
Nrf1	Nuclear Respiratory Factor 1
Nrf2	Nuclear Respiratory Factor 2
MAPK1	Mitogen-Activated Protein Kinase 1
Mn-SOD2	Manganese dependent Superoxide Dismutase 2
HO-1	Heme Oxygenase - 1
NQO1	NADPH Quinone Oxygenase - 1
NADPH	dihydroxy Nicotinamide Adenine Dinucleotide Phosphate
CD4	Cluster of Differentiation 4
CD8	Cluster of Differentiation 8
CXCL1	Chemokine (C-X-C) Ligand 1
CXCL5	Chemokine (C-X-C) Ligand 5
CREB	cAMP Response Element Binding protein
NF-κβ	Nuclear Factor Kappa-light chain enhancer of activated Beta Cells
C3H10T1/2	Sarcoma cells from C3H mice strain
CT scans	Computed Tomography
H3K18	Histone 3 Lysine 18
ATCC	American Type Culture collection

uPA/PLAU	Urokinase-type Plasminogen Activator
SERPINE1	Serine Protease Inhibitor E1
SERPINB1	Serine Protease Inhibitor B1
PAI-1	Plasminogen Activator inhibitor - 1
PAI-2	Plasminogen Activator inhibitor - 2
CREG1	Cellular Repressor E1
TBX2	TATA box Binding Factor -2
HMGB1	High Mobility Group Box 1
IGFBP3	Insulin-like Growth Factor Binding Protein 3
γ-H2AX	Gamma – Histone 2 A family member X
HFL1	Human Fetal Lung Fibroblasts 1 cells
HEK293T	Human embryonic Kidney 293T cells
DSB	Double-Strand Breaks
SSB	Single-Strand Breaks
WI – 38	Human fetal lung fibroblasts
IMR 90	Human fetal lung fibroblasts
SA-β-Gal	Senescence Associated Beta Galactosidase Assay

Table of Contents:

LIST OF FIGURES:

LIST OF TABLES:

Chapter 1 : INTRODUCTION

1.1 IONIZATION RADIATION (IR):

Ionization radiation is a form of energy that can interact with an atom to remove electrons from its orbitals, causing the formation of ions. This further can result in the breaking of chemical bonds and the production of free radicals which is one of the predominant causatives for cancers. X-rays and Gamma rays are the most common forms of ionization radiation that humans are exposed to. The application of ionization radiation is growing with the advancement of technology. Wide usage of ionization radiation for medical imaging and working in nuclear facilities leads to increased radiation exposure of humans. According to the World Health Organization (WHO), the medical use of ionization radiation constitutes 98% of the population dose from all available artificial radiation sources: 3600 million diagnostic radiological exams including 37 million nuclear medicinal procedures and 7.5 million radiotherapies are performed worldwide annually [1].

All naturally occurring radioactive elements such as Uranium and commonly occurring radioisotopes such as Carbon 14, potassium-40, etc., emit γ-radiation. Gamma-radiation being the most energetic form of radiation is highly penetrative in nature. Annually, an average individual receives 2.4 mSv of ionization radiation dose through both background and artificial ionization radiation exposures. The radiation dose can be expressed in two commonly used units: Gray (Gy) and Sieverts (Sv). The doses received by an organ or a tissue are the absorbed dose and are expressed in Gy. Sievert is the equivalent dose that accounts for the physical characteristics of a type of radiation. For X-rays and gamma-radiation, conversion between the two units is 1Gy=1Sv. The damage due to radiation depends on various factors such as dose, the dose rate, type of radiation, and the sensitivity of the organ. Studies have shown that exposure to high doses of ionization radiation leads to negative health outcomes due to excessive cellular damage ultimately leading to cancer. In cells, radiation causes double or single-strand breaks in the DNA, as well as other types of lesions[2]–[4]. Hence, through these studies, it is conclusive that high doses of

radiation can lead to deterministic effects on organisms. In contrast, at lower doses of radiation stochastic effects are observed that are related to probabilities of conversion of molecular and cellular damage to later health outcomes, such as cancer (Figure 2). The damage caused by low doses can be repaired by cellular defense mechanisms [5].

To evaluate such differential effects between low and high doses of ionization radiation on organisms, appropriate risk assessment models are needed to be established. This could help in defining the threshold dose of ionization radiation and also help in studying the biological responses under these effects.

1.2 RADIATION RISK ASSESSMENT MODELS:

The cancer risk assessment of radiation exposures is done using a commonly used model called the **Linear No-Threshold (LNT) model**. This model was a result of early studies by a Nobel Prize winner Dr. Hermann Muller who showed a linear dose-response for mutations in 1927 and was incorporated into an international system of radiation protection in 1966. The LNT postulates that the risk of cancer increases linearly with the increase in radiation dose. Many studies using high doses of radiation (above 1000 mGy) have been consistent with this model [6]. This model suggests that even at low doses of radiation (below 100mGy) there is a risk of cancer incidence in organisms. This model is adapted by various governing bodies that regulate radiation-related policies. The statistical and epidemiological studies have been performed to show that the LNT model is inconsistent with the results at a low dose of radiation [7]. Upon exposure to radiation, various types of DNA lesions, such as double-strand or single-strand breaks, are formed caused by direct interaction of photons with DNA and indirectly via reactive oxygen species formed by the interaction of photons with water molecules. This damage caused by the gamma rays triggers various DNA repair and anti-inflammatory pathways. If the damage was caused by low doses and cells could repair it, the resulting state also called primed, that is characterized by activated defense

mechanisms, can protect cells or tissues from further damage upon successive irradiation. This protective phenomenon observed in the cells or the whole organism following exposure to low doses of radiation is called Radiation Hormesis [8] (fig 1). When the priming low dose exposure is followed by a challenging high dose, this effect is commonly called a Radio-adaptive Response (RAR) [9]. Accounting for Radiation Hormesis when constructing the dose-response model results in a biphasic curve, with a clear distinction of effects at low vs high doses of radiation as shown in Fig. 1. According to such a biphasic model, the detrimental effects of radiation are not expected up to a certain threshold dose below which hormesis or protective effects can be observed.

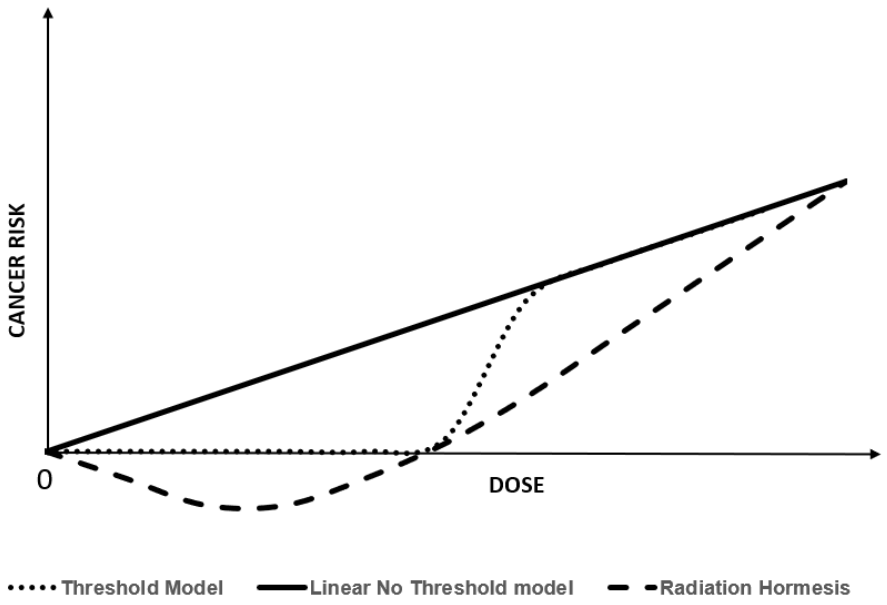

Figure 1: Graphical representation of radiation hormesis, a linear model, and the threshold model to access the health risk of ionization radiation. Linear No Threshold model (LNT) is a widely used model to access the health risk in humans. It states that any given radiation dose, even a very low dose, has a detrimental effect on organisms. In contrast, the Radiation Hormesis model and the Threshold model suggest the existence of a threshold at a lower dose below which radiation triggers the radio adaptive molecular mechanisms to boost the cellular responses towards the damage caused by low doses of IR. This results in triggering cellular DNA repair, inflammatory and Reactive Oxygen Species (ROS) signaling pathways resulting in enhanced DNA repair and antioxidant activities.

There are many cellular processes observed in organisms upon exposure to low doses of radiation which cumulatively give rise to a beneficial or hormesis effect (Figure 2). These processes include efficient repair of DNA damage, activation of the immune system of that organism, and increased antioxidant activity [10]–[12].

1.3 DNA DAMAGE REPAIR PATHWAYS UPON LOW DOSE RADIATION:

Exposure to ionization radiation results in a variety of DNA lesions. For instance, gamma-radiation induces 850 pyrimidine lesions, 450 purine lesions, 1000 single-strand breaks, and 20-40 double-strand breaks (DSBs)/cell/Gy [13]. Single strand breaks (SSBs) and Double-Strand Breaks (DSB) are the most common of the DNA lesions upon irradiation [13]. This can lead to genome instability in organisms and may also result in cancer. In response to these damages, cellular defense mechanisms are triggered by employing various types of proteins and pathways to arrest the cell cycle and rectify the damage [14]. The most common DSB repair pathways triggered are Homologous Recombination (HR), and Non-Homologous End Joining (NHEJ). In mammalian somatic cells, NHEJ, which is a low fidelity repair type, occurs in the G1 phase, whereas the high fidelity HR occurs in the S/G2 phase of the cell cycle [15]. The hormesis effect is often observed upon irradiation with doses ranging between 1- 100 mGy. Since DSB are the most deleterious type of DNA lesions and is often associated with genomic instability and cancer, it is DSB that is often measured in radiation studies to assess DNA damage and repair. One of the most common techniques used to detect DSB is the immune-detection of nuclear-DNA associated phosphorylated histone H2A variant X (H2AX). Large numbers of phospho-H2AX, also called γH2AX, form around a single DSB which is seen as distinct fluorescence foci using immunofluorescence microscopy. Tracking the formation and dissolution of the foci from the damaged sites with time after irradiation allows reconstructing the DSB formation and repair kinetics curves [16]. Studies show, among other mechanisms, that three processes could contribute to the hormesis effect: p53 dependent high-fidelity DNA repair; p53 dependent apoptosis, and p53 independent protective

apoptosis mediated (PAM) process [17]. PAM process occurs due to radiation-induced bystander effect. The bystander effect is a cellular response observed in cells that are not traversed by ionization tracks [18]. This effect occurs via the production of ROS and cytokines such as Transforming Growth Factor (TGF) β to specifically remove the damaged cells [17]. Hence, this and other studies suggest that pre-exposure to radiation leads to the protection of cells or organisms from further damage due to subsequent exposure to higher doses of radiation [19], [20]. Mild stress caused by LDR triggers the cellular defense mechanism leading to radioprotection or radio adaptive response. Irradiating male germ cells of Drosophila Melanogaster at 5 mGy of γ-radiation led to reduced mutation frequency compared to control and the flies treated with 10 Gy of IR [21]. Additionally, several apoptotic genes are observed to be upregulated along with reduced mutation frequency [21]. One of the possibilities that can explain the reduction in mutation frequency by LDR is that these upregulated apoptotic genes can lead to the elimination of damaged or pre-neoplastic cells which would otherwise result in transformed cells or cancer. Suppression of Expanded Simple Tandem Repeat is observed in mice pre-exposed to low doses of γ-radiation (100 mGy) explaining the adaptive response. The precise molecular pathways contributing to this observation are yet to be elucidated [22].

Similar effects are observed in various cancer cell lines. Low doses of radiation results in cellular adaptive responses by reducing both micronuclei count and neoplastic transformation in C3H 10T1/2 cells [23]. HeLa cells, when exposed to a cumulative dose as low as 100 mGy, show reduced neoplastic transformation compared to untreated cells, whereas a higher rate of transformation was seen upon 3 Gy of radiation. The study not only suggests that LDR results in adaptive responses in cells but also indicates that the effect of LDR seems to depend on the dose rate which in this case was ranging from 1-4mGy/day [24]. TGFβ1 signaling is a key player in regulating the defense mechanisms upon irradiation. It plays a role in inducing a protective bystander effect through signal transduction in non-irradiated cells when these cells are co-cultured

with cells pre-exposed to radiation. This effect occurs through the production of superoxide anions in nonirradiated cells. This implies that LDR helps in the release of cytokines from transformed cells resulting in signalling neighbouring cells triggering cellular defense mechanisms such as clearance of genetically compromised cells mediated through apoptosis or cellular senescence.

1.4 ANTIOXIDANT ACTIVITIES UPON LOW DOSE RADIATION:

High dose radiation damages cells through oxidative stress by producing Reactive Oxygen Species (ROS) and free radicals such as H_2O_2, superoxide anions (O_2^-), hydroxyl radicals (OH^-), etc. These free radicals are harmful to cells resulting in oxidation of various biomolecules and DNA damage [12]. Although an excessive amount of ROS and free radical in cells results in degenerative diseases and various types of cancer [25], experimental evidence suggests that low concentration of ROS results in the enhancement of oxidative stress resistance by acting as a signaling mediator for various molecular mechanisms in the cell [26]. ROS production due to low doses of radiation was shown to enhance antioxidant and anti-inflammatory activities in the organisms. These activities induced through redox signaling pathways, transcriptional factor activation, and gene and protein expressions result in radio adaptive responses [27]. In normal human epithelial cells, low doses of radiation resulted in the expression of major compounds of antioxidant systems such as glutathione peroxidases (GPx) which could result in an anti-inflammatory response [28].

Clearance of transformed cells by non-transformed cells through ROS/RNS signaling occurs in co-culture when cells are irradiated at doses as low as 2mGy up to 50mGy of gamma radiation [29]. The upregulation of antioxidant activity implies the beneficial effect of LDR to protect the cells by improving the defense mechanisms [30], [31]. Nrf1 and Nrf2 are two genes that regulate the cellular detoxification system [32]. Both genes respond to X-radiation with doses as low as 50 and 500 mGy in HS27 cells (human normal foreskin cells). Upon irradiation, the reactive oxygen species increase along with calcium flux and trigger the expression of Nrf1/2 genes in these cells through

the ERK1/2 signaling pathway. Although both Nrf1 and Nrf2 responded differently towards the radiation doses, Nrf1 being the most sensitive responding to a radiation dose of 50 and 500 mGy while Nrf2 translocated only 500 mGy. This, as suggested in the study, was due to the relative amount of ROS produced in the cell. Gene expression of Nrf1/2 also shown to promote the expression of Mn-SOD1, HO-1, and NQO1 genes that play a role in antioxidant activity [33]. Exposure of female Wistar rats to 200 mGy of X-radiation resulted in enhanced anti-oxidant activity through an increased level of glutathione S transferase (GST) and catalase. This exposure also led to an increase in whole blood lymphocytes and eosinophils in the body [34]. ROS mediated apoptosis is induced by normal embryonic fibroblasts through the TGFβ signaling pathway to selectively clear the transformed fibroblasts in vitro upon low doses of radiation. This reaction occurs through the release of superoxide ions which in return signals the non-transformed cells to elicit an autocrine ROS mediated signaling cascade in control of oncogenesis [35]. Exposure to low doses of gamma radiation creates a pro-inflammatory shift in humans in combination with the upregulation of antioxidant activity although the mechanistic role of these molecular changes is yet to be studied [36].

1.5 ANTI INFLAMMATION ACTIVITIES UPON LOW DOSE RADIATION:

Exposure to low doses of gamma radiation leads to anti-inflammatory effects in organisms. [28], [37], [38]. Increase in production of CD4(+) T cells and CD8 expression molecule, T cell activation by various cytokine production are observed under low dose exposure [39]. BPDE, Benzo(a)pyrene Diol epoxide, a potent inflammation triggering chemical in cigarette smoke results in the release of cytokines such as IL-6, CXCL1, and CXCL5 from human lung fibroblasts (HFL1). A single dose of 90 mGy of gamma radiation inhibited this secretion in the presence of BPDE. In the same study, upon the low dose of radiation, suppression of IL-6 mediated transformation in human bronchial epithelial cells (HBECs) was observed when cells were treated with BPDE treated

conditioned media [40]. Thus, low doses of radiation inhibit the transformation of normal cells into cancerous cells though suppressing IL-6 and CLF signaling pathways. A similar result was obtained in vivo studies using Benzo[a]pyrene, a precursor of BPDE. 600 mGy of gamma radiation showed suppression information of hyperplastic foci in the lungs (a risk factor for cancer progression) and inhibits the development of lung adenomas Benzo(a)pyrene exposed mouse [41]. Other studies reported enhanced anti-inflammatory activities such as enhanced production of Natural Killer (NK) cells, Interleukin 12 (IL-12), increasing cytotoxic activities of T lymphocytes following exposures to LDR [42]–[44]

MAPK signaling pathway is one of the inflammatory pathways influenced during the radio adaptive response caused by low doses of radiation [20]. CREB signaling and CREB associated pathways are also found to be responsive upon radiation in a dose-dependent manner. The murine hippocampus was subjected to doses of 6, 100, and 500 mGy of ionization radiation to study the hormesis effect of radiation. Unlike 6 and 100 mGy, 500 mGy is proven to be detrimental for mouse brain development. This was also seen in terms of microglia activation where 6 mGy reduced the activated microglia thus contributing anti-inflammatory effects while 500 mGy enhanced the activated microglia resulting in pro-inflammatory effects leading to neurodegeneration [38]. Another inflammatory pathway, NF-κβ signaling was reported in the inactivation of microglial cells upon high doses of radiation (16 Gy) [45].

Radiation-induced inflammation results in autoimmune diseases through increased production of cytokines. Impaired DNA repair upon high doses of ionization radiation can result in autoimmune diseases such as gastritis, type I diabetes, arthritis [46]. Collagen Induced Arthritis, CIA, one of the most common autoimmune model of rheumatoid arthritis [47]. In this condition, the secretion of Tumor Necrosis Factor (TNF) α, (IL-6), and interferon (IFN) γ plays a role. Low doses of radiation suppressed their secretion hence they ameliorate the pathological symptoms in CIA [48].

Many other inflammatory diseases can be alleviated upon exposure to LDR. For example, the current pandemic caused by the Severe Acute Respiratory Syndrome-Coronavirus-2 (SARS-CoV-2) virus. The virus affects various organs of the infected individual especially lungs causing an elevation in the secretion of cytokines such as IL6, TNF-A, and Monocyte chemoattractant protein – 1 (MCP1), etc [49], [50]. It targets the host cells of lungs i.e., alveolar cells by attacking the enzyme, Angiotensin-converting enzyme -2 (ACE2) which is present abundantly on these cells and in other organs such as heart, kidney and gastrointestinal organs [51], [52]. Among the clinical predictors for the SARS-CoV-2 in human beings, elevated IL6 protein is one of the strong predictors of the infection [53]. As studies have shown that LDR exposure produces a protecting effect from inflammation, studying, and understanding the biological relevance of Low dose radiation on these cytokines and proteins associated with SARS-CoV-2 in HFL1 cells could enable the use of LDR as an alternative cure for the disease [54].

A

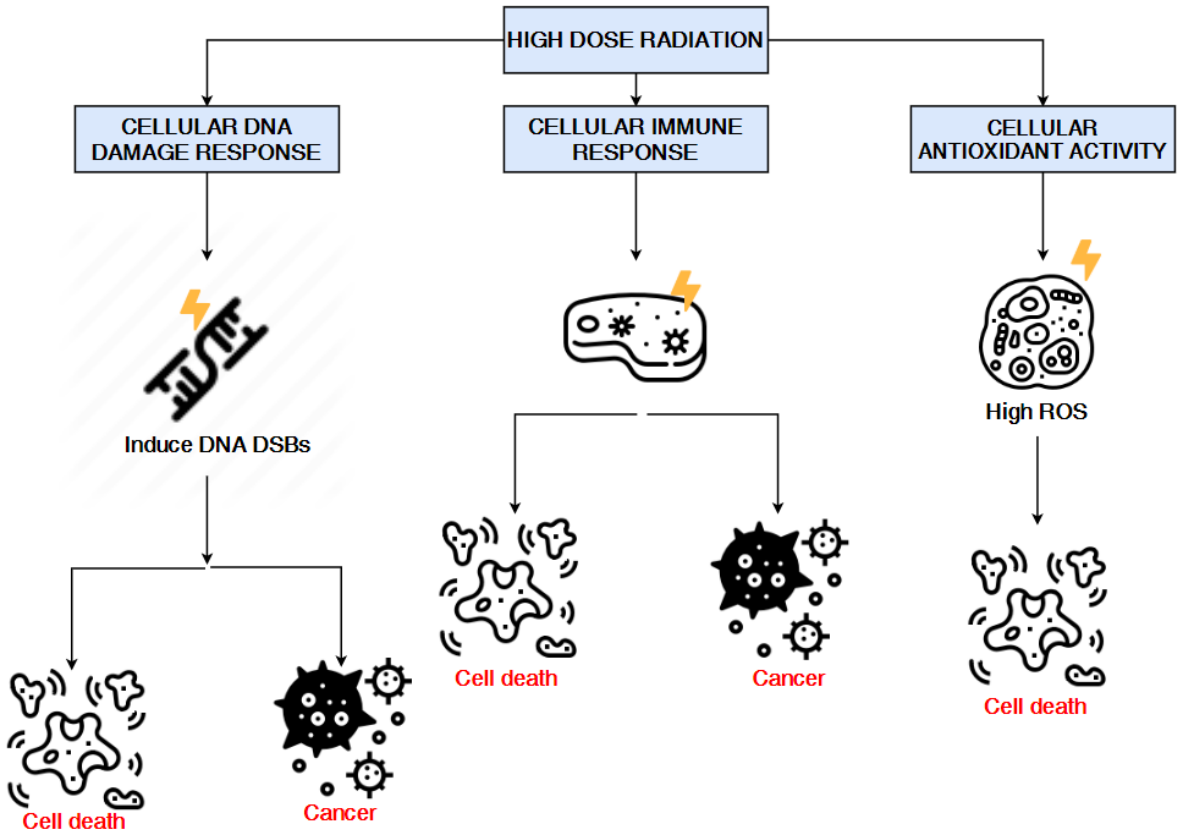
HIGH DOSE RADIATION
CELLULAR DNA DAMAGE RESPONSE
CELLULAR IMMUNE RESPONSE
CELLULAR ANTIOXIDANT ACTIVITY
Induce DNA DSBs
High ROS
Cell death
Cancer
Cell death
Cell death
Cancer

B

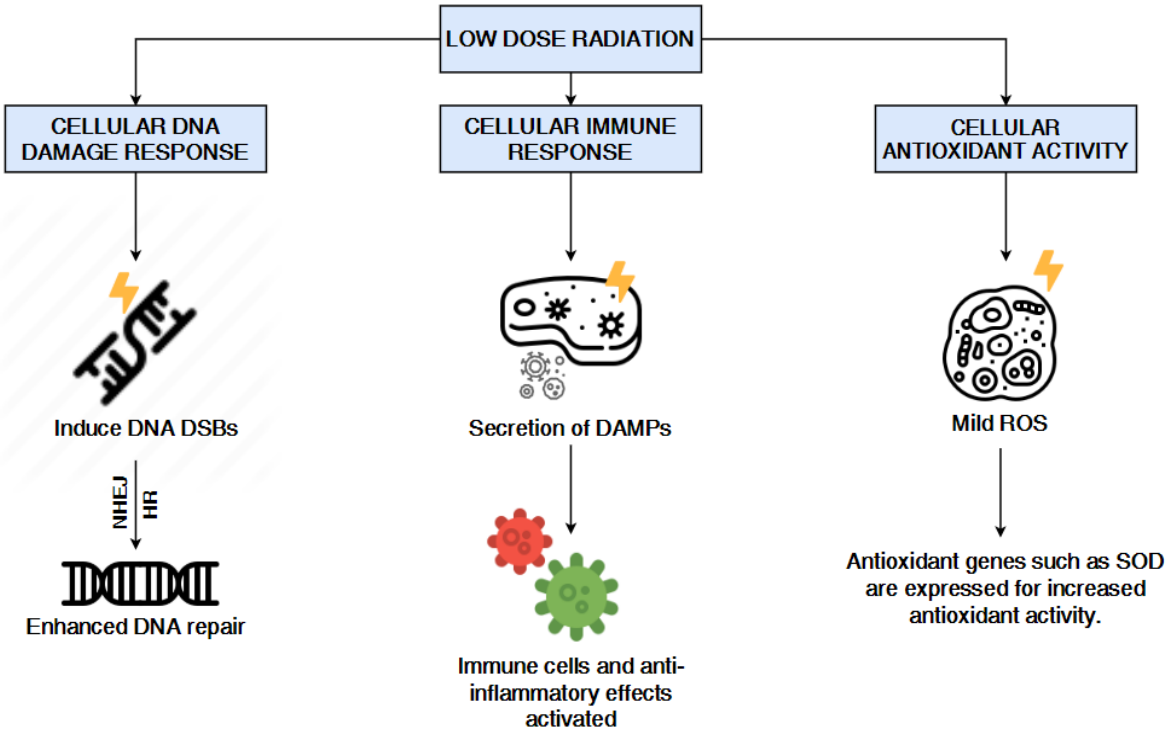
LOW DOSE RADIATION
CELLULAR DNA DAMAGE RESPONSE
CELLULAR IMMUNE RESPONSE
CELLULAR ANTIOXIDANT ACTIVITY
Induce DNA DSBs
Secretion of DAMPs
Mild ROS
NHEJ
HR
Enhanced DNA repair
Immune cells and anti-inflammatory effects activated
Antioxidant genes such as SOD are expressed for increased antioxidant activity.

Figure *2*: Schematic representation of the effect of ionization radiation at high and low doses on various cellular processes. Fig 2A shows the cellular response to high doses of radiation (HDR) which result in the induction of DNA double-strand breaks (DSBs) or suppression of immune response or antioxidant activity contributing to irreversible cell growth arrest (senescence), cell death (apoptosis) or cellular transformation leading to cancer. Fig 2B shows the cellular effect of low dose radiation which unlike HDR, triggers mechanisms that result in enhanced DNA repair and stimulates the immune response and cellular antioxidant activity.

1.6 CELLULAR SENESCENCE UPON LOW DOSE OF RADIATION:

Cells in culture undergo approximately 60-40 divisions in their lifespan after which they permanently lose the capacity to divide and enter the state called replicative senescence (RS) [55]. This phenomenon is termed the Hayflick Limit discovered by Dr. Leonard Hayflick in 1965. Primary cells can also undergo an irreversible cell cycle arrest called stress-induced premature senescence (SIPS) upon various environmental stressors. Various molecular pathways can contribute to senescence depending on the type of stressors and the exposure time. Well established senescence markers are used to study the senescence nature of cells. Senescence pathways are also introduced in normally proliferating cells through overexpression of Ras proteins, an oncogene protein family. Ras proteins are GTPases acting as molecular switches to drive a variety of cellular processes. It evokes intracellular signaling cascades in response to an external stimulus resulting in regulating various activities such as cellular proliferation and survival to suppress tumor progression. There are 3 isoforms of Ras proteins: HRas, KRas, and NRas [56]. Other than its oncogenic properties, activating or overexpression of Ras genes result in the induction of cellular senescence in mammalian cells. Oncogenic Ras promotes senescence in normal cells through BRAC1 mediated impaired DNA repair in lung fibroblasts exposed to 2 Gy of ionization radiation [57]. It will be interesting to explore this effect in these cells upon LDR.

High doses equivalent to or above 1 Gy of radiation result in DNA damage that triggers cellular processes that often lead to senescence or apoptosis to restrict transformation and cancer progression in organisms [58]. The damage caused by radiation is repaired through various DNA repair mechanisms in the cells. The efficiency of these repair mechanisms depends on the exposure time and the absorbed radiation dose. For example, irradiation of human foreskin fibroblasts with 1-4 Gy of gamma irradiation (6 - 20 mGy/hr for 7 days) increases cellular senescence through p53 signaling [59]. Whereas, at 30 mGy of gamma radiation, the normal human embryonic lung fibroblasts (HELF-104 cells) cells showed an increase in proliferation and delay in senescence

compared to the untreated cells and cells treated with 500 mGy [60]. Similarly, irradiating bone marrow mesenchymal stem cells displayed a delay in cellular senescence when exposed at 80 mGy, but not 1000 mGy of gamma radiation irrespective of elevated gamma H2AX foci in treated cells. Low doses of radiation equivalent to 50 - 80 mGy is widely used in medical diagnostics such as CT scans [61]. These and other studies show that there is a dose-independent hormesis effect of radiation. Hence, exploring molecular mechanisms underlying this delay of senescence upon low dose radiation can help in a better understanding of radiation and health risks and the application of radiation in fields such as medical diagnostics.

1.7 THE ROLE OF SIRT7 IN RADIO ADAPTIVE RESPONSE (RAR):

Sirtuin 7 belongs to the class of proteins called *Sirtuins* which functions in the presence of Nicotinamide Deacetylase (NAD+) enzymes. They are class III histone Deacetylases and play a role in human cellular aging. So far there are seven sirtuin proteins (SIRT1-SIRT7) identified in humans (Figure 3). The seventh protein of the family, SIRT7 localizes predominantly in the nucleolus which is a hub for ribosome biogenesis [62]. The protein is known for its rDNA transcription and ribosome biogenesis which consumes a major portion of cellular energetics [63]. It is also implicated in various disorders such as ovarian and prostate cancers. SIRT7-/- prostate cell lines show an inhibitory cellular proliferation and thorough Androgen Receptor (AR) Signaling [64]. In ovarian cancer patients, SIRT7 expression correlates with a good prognosis and was suggested to be one of the prognostic predictors in these patients [65]. Sirtuins take part in protecting the cells from damage received from various stressors. The depletion of SIRT7 in mice resulted in partial lethality and poor double-stranded DNA repair efficiency. DSB DNA damage is one of the most common and dangerous DNA lesions contributing to genome stability upon irradiation. SIRT7 protein is recruited to the DNA damage site to interact with 53BP1 and to deacetylate, H3K18 facilitating the removal of DNA damage [66]. Sirtuins also play a role in brain aging and neurodegenerative disorders such as Alzheimer's disease. SIRT7 also plays a role in the

regenerative capacity of hematopoietic stem cells via regulation of mitochondrial stress signaling [67], [68].

On the whole, SIRT7 is a relatively new protein in the family compared to SIRT1-6. Further studies are required to specifically elucidate and understand the role of SIRT7 in aging and its response to stressors especially upon exposure to low dose radiation.

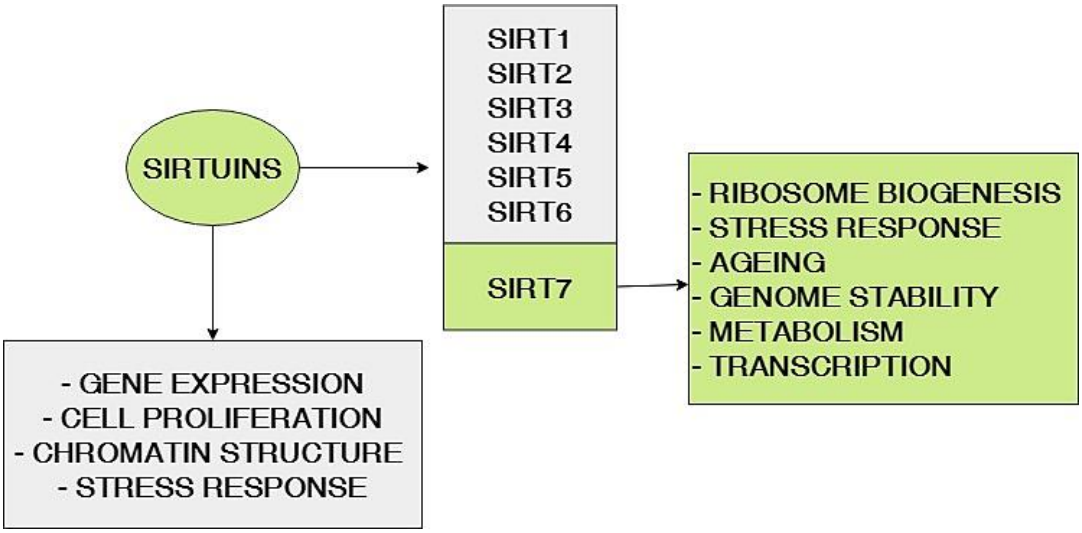

Figure 3: Schematic representation of the protein family of Sirtuins and their role in various cellular processes. It contains 7 Sirtuin proteins localized at different parts of a mammalian cell to perform their role. SIRT7 is predominantly in the nucleoli of a cell and plays a role in rDNA transcription and genome stability.

1.8 HYPOTHESIS, STATEMENT OF OBJECTIVE AND SIGNIFICANCE:

The impact of radiation on human health varies with the exposure time, dose, and dose rate. High doses can cause cancer and death, but the effects of low doses (<100 mGy) exposure is controversial as to whether they are toxic or favourable. Many studies report that low doses of radiation induce beneficial effects such as delaying senescence, improving immunity, and repair mechanisms in organisms. **I hypothesize that exposure of normal human lung fibroblasts to low doses of gamma-radiation results in radiation hormesis displayed as a delay in cellular senescence that is driven by transcriptional changes. Furthermore, I propose that this effect can be mediated by SIRT7, a regulator of senescence and a facilitator of DNA repair mechanisms.**

There are three objectives to test my hypotheses:

1. To study the delay of cellular senescence in HFL1 cells upon exposure to low dose gamma-radiation.
2. to investigate the role of SIRT7 in low dose induced senescence modulation in HFL1 cells.
3. To explore the possibility of using the Oncogene Induced Senescence (OIS) as a time-efficient model for mechanistic studies of the effects of low-dose radiation on senescence

Accomplishing the first objective will lead to some validation of the proposed radiation hormesis hypothesis in human lung fibroblast cells. This will be examined using various senescence assays and gene expression analyses at different time points after LDR exposure. Through the second objective, the gene expression of SIRT7 will be assessed in cells exposed to LDR at various time points following radiation exposure. In parallel, the role of SIRT7 protein in regulating senescence in HFL1 cells will be studied using RNAi gene know-down technology. Since SIRT7 plays a role in mammalian cellular senescence, this objective will help understand its role in the hormesis effect induced by low dose radiation. Oncogene induced senescence (OIS) is a strategy used to study the molecular mechanisms involved in replicative senescence (RS) contributing to aging humans. The

third objective of this study is to establish this method for studying potential mechanisms of deceleration of cellular senescence by low dose radiation. The utility of OIS vs. RS is substantially shorter times required for experimentation allowing for transient transfection experiments that are otherwise not useful for long-term RS experiments. In this last objective, it will be examined whether OIS leads to a similar pattern of gene expression changes compared to RS. This objective will lead to a better understanding of how different pathways and genes drive senescence in HFL1 cells. Since the precise molecular mechanisms that drive aging humans are not fully understood, studying cellular senescence in HFL1 cells using various approaches can help identify the genes and mechanisms that are influenced specifically in human aging.

Chapter 2 : MATERIALS AND METHODS

2.1 Cell Culture and Culture Conditions:

2.1.1: Human Fetal Lung Fibroblasts:

Human lung fibroblasts, HFL1, passage 3 were obtained from ATCC (ATCC - CCL- 153). These cells were cultured in a specialized medium that has reduced sodium bicarbonate level called F-12K (Kaighn's modification of Ham's F-12 medium) which was also obtained from ATCC (ATCC-30-2004). The culturing media was supplemented with 1% of sodium pyruvate, 10% Fetal Bovine Serum (Gibco, Thermo scientific). The culture conditions were 37ºC incubator with 5% CO_2 in the air and 80% humidity.

2.1.2: Human Embryonic Kidney 293T cells:

HEK293T cells were obtained from ATCC (ATCC CRL 3216) and cultured in Dulbecco's Modified Eagle's Medium (DMEM) obtained from Sigma Aldrich with 10% Fetal Bovine Serum (Gibco, Thermo Scientific) incubated in 37ºC incubator with 5% CO_2 in the air. The cells were transformed with adenovirus E1a and contain temperature-sensitive T antigen in their genome.

2.1.3: Phoenix Retroviral Packaging Cells:

This helper free packaging cell system was used for the production of retrovirus expressing the gene of interest through plasmid transduction. These cells were obtained from *Gentaur Molecular products*, Germany (Cat No: RVK_10001). Briefly, the phoenix cells were HEK293T cells which can produce the packaging proteins required for successful retroviral transduction and expression of the gene of interest. These cells were grown in DMEM obtained from Sigma Aldrich with 10% Fetal Bovine Serum (Gibco, Thermo Scientific) incubated in 37ºC incubator with 5% CO_2 in the air.

Once 80% confluence is reached, they were split at 1:4 – 1:6 ratio depending on the required confluency and the time of further experiments. To passage the cells, media was aspirated and the

cells were washed with 1X Phosphate Buffer Saline (PBS) solution. The cells were then treated with trypLE express (Gibco Lifetech), recombinant trypsin which helps the cells to detach. The trypsin treatment was done by incubating the cells in a 37ºC incubator with 5% CO_2 for 5 minutes. Following that, the cells were resuspended in warm media of 9 ml (for a 10 mm plate, Coring, USA) and cells counted manually for obtaining appropriate seeding density. The media was changed every 2-3 days from the date of seeding depending on the cell death and the culture was monitored periodically for contamination and cell death.

2.2 Irradiation Method, Dose, and Dose Rates:

Cobalt-60was used as a source for gamma radiation of HFL1 cells at Canadian Nuclear Laboratories, Chalk River, Ontario, Canada and the dose rate used for the irradiation experiments was 7mGy/sec, with total cumulative doses of 0 (sham-irradiation), 10 and 100 mGy.

Frozen HFL1 cells were retrieved from liquid nitrogen containers and cultured at the normal culturing condition. Before irradiation, these cells undergo at least one passage. Once reaching about 80% confluency, the cells were split into plated of various surface areas with appropriate seeding density for further experimentation (Fig 4 and 5) and irradiation. For 0, 6 hrs., and 24 hrs. time points, the cells were seeded such that they were available with 80-90% confluency for sampling after irradiation.

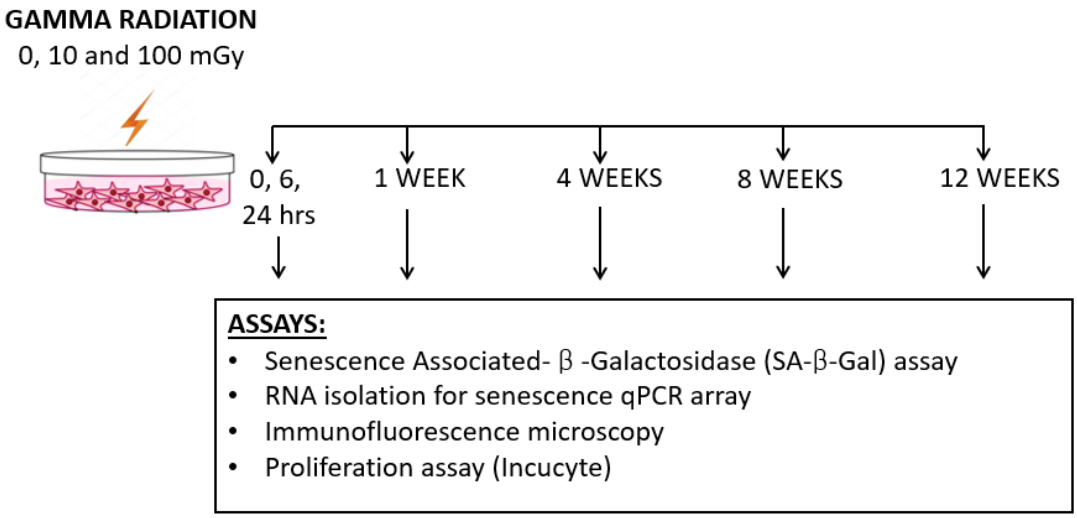

Figure 4: Experimental design to study the effect of LDR on senescence in HFL1 cells. The cells will be followed up to 12 weeks which was when they reach senescence. At different time points such as 1 week, 4, 8, and 12 weeks, cells were harvested for assays such as Senescence Associated □-galactosidase assay (SA-β-Gal), RNA isolation, Immunofluorescence Microscopy (IFM), proliferation assay, and polysome profiling assay.

A

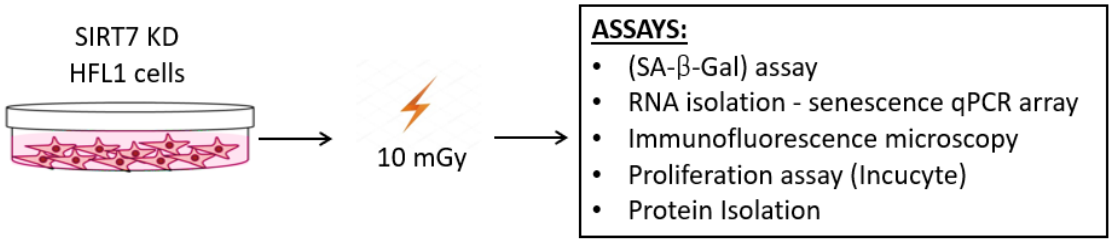

B

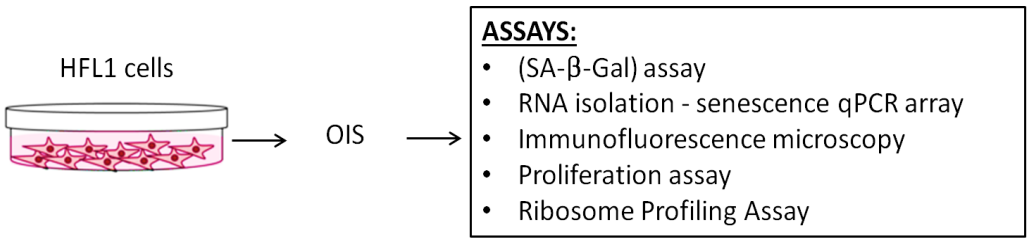

Figure 5: Experimental design to study the role of SIRT7 in senescence in HFL1 cells (A) and the Oncogene Induced Senescence (OIS) in HFL1 cells (B). Early passage of HFL1 cells for the respective interventions and the assays such as Senescence Associated-B-Galactosidase (SA-β-Gal) assay, RNA, and protein isolation, Immunofluorescence microscopy and proliferation assay will be performed.

2.3 Senescence Associated- β -Galactosidase Assay:

As cells reach senescence, they gradually accumulate □-galactosidase in lysosomes making it one of the most widely used biomarkers for studying cellular senescence in various mammalian systems. In this study, this process was identified in HFL1 cells using the SA- β-Gal assay kit (Cat No. 9860) from *Cell Signaling Technology* at different time points of the cell cultures as explained in the experimental design until they cease to proliferate (100% senescent). The kit protocol was followed to perform this experiment. Briefly, 10^5 cells were seeded in 35 mm *Mattek* disposable plastic Petri plates (Cat No. P35G-1.5-14-C) which contain No 1.5 coverslip with 14mm glass diameter. Cells were then cultured under normal growth conditions until the 50-60% confluency was reached. The media was aspirated and cells were washed twice with 1X phosphate Buffer Saline (PBS) solution. Cells were treated with 1 ml of 1X fixing solution made from 10X glutaraldehyde using a 1X phosphate Buffer Saline (PBS) solution for 20 minutes. Meanwhile, a 1X staining solution was made from a 10X staining solution along with solutions A, B, and 20mg/ml of X-galactosidase. After 20 minutes of incubation, the cells were washed twice with 1X phosphate Buffer Saline (PBS) solution. The washed cells were treated with a 1X staining solution. The plate was sealed with parafilm to avoid evaporation. The cells were incubated in a 37ºC dry incubator for 16 - 18 hours in a dark environment. After incubation, the cells were washed thrice with 1X phosphate Buffer Saline (PBS) solution. The cells were also stained with Hoechst 33342 staining kit (Cat No. R37605) obtained from Thermo Scientific. 10µl of staining solution was added to the 1ml of 1X phosphate Buffer Saline (PBS) solution for 20 minutes to visualize the nuclei of cells to score the total number of cells in the field. The imaging for this assay was done using an Olympus Microscope under Brightfield mode (for senescent positive cells) and DAPI mode (total cell number count using their nuclei). The blind scoring of β galactosidase positive cells was done manually using ImageJ software and images were randomized by creating random IDs against the original IDs.

2.4 RNA Isolation and Real-Time Polymerase Chain Reaction (RT-qPCR):

To harvest cell lysate or for RNA isolation, approximately 6-8 x 10^5 cells were seeded into a 60 mm sterile tissue culture graded Petri plate and grown in normal culturing conditions. Upon 80-90% confluency, the media was aspirated and cells were washed twice with 1X PBS solution. The cells were treated with 500µl of TRIzol (Invitrogen, Cat No. 15596018) for 5 minutes and collected in a sterile 1ml microcentrifuge tube. Following this, 300 ul of chloroform was mixed with the cell lysates, and samples were suspended in TRIzol and mixed well-using vortex mixer. The mixture was incubated at room temperature for 3 minutes and centrifuged at 13000 RPM for 20 minutes at 4ºC. The supernatant (clear liquid) was carefully transferred to fresh 1ml microcentrifuge tubes and ice-cold isopropanol was added (volume equals to 70% volume of the supernatant) to the supernatant. The mixture was incubated at -20ºC overnight for RNA precipitation and centrifuged the following day at 13000 RPM for 15 minutes at 4ºC. This step results in RNA pellet formation which was washed with 70% ethanol (first wash) and 100% ethanol (second wash) by centrifuging it at 13000 RPM for 5 mins at 4ºC respectively. The pellet was air-dried and 20 ul of nuclease-free water was added to it and incubated in a water bath set at 40ºC for dissolving. The quality and quantification of RNA were checked with the help of Nanodrop 2000 (Thermo scientific) looking at the 260/280 ratio.

2.5.1: cDNA synthesis and qPCR:

500 ng of total RNA was used to synthesize cDNA for performing qPCR. Qiagen RT2 First Strand cDNA synthesis kit (Cat No. 330404) was used for cDNA synthesis and the kit protocol was followed. In a nutshell, 500ng of RNA was treated with 10 µl of Genomic DNA Elimination (GE) buffer for removal of residual genomic DNA in the RNA sample before reverse transcription. This step involves incubating the RNA and GE buffer at 42ºC for 5 mins in a PCR machine. Following this step, RNA was reverse transcribed using the appropriate volume of reverse transcriptase enzyme and the buffers in the kit by incubating at 95ºC for 5 minutes and 42ºC for 15 minutes. The total mixture was diluted with 91µl of nuclease-free water and proceeded for setting up the qPCR

reaction. A similar set of reactions without Reverse transcriptase enzyme and template respectively were also performed to be used as Reverse Transcription Control (RTC) and No Template Control (NTC) while performing qPCR.

For all the qPCRs performed in this study, the 2X SYBR green qPCR master mix (Bimake, Cat. No. 21203) was used. It was a DNA Taq Polymerase that enabled hot-start activation. The primers used for qPCR experiments (Table 1) and the list of genes screened in human cellular senescence qPCR array kit (Fig 6A) was shown in fig 6. 200nM of primer concentration was used for all the reactions along with 2X SYBR green master mix and nuclease-free water to make the volume of 20µl per reaction. The reaction cycle starts with a denaturing step of 95ºC for 10 minutes; 39 cycles of 95ºC for 1 minute; respective annealing temperature optimized for each primer for 30 seconds; extension temperature of 72ºC for 30 seconds followed by a final extension step of 72ºC for 5 minutes and plate reading step. The reaction was set up in the Bio-Rad CFX 96-well qPCR machine and for the qPCR array, the reaction was set up in Bio-Rad CFX 384 well qPCR machine. The Qiagen Human Cellular Senescence (HCS) 384 qPCR array plate (Qiagen, RT2 profiler PCR array, Cat. No. 330231 PAHS-050ZA) was used for screening 84 top hits genes of cellular senescence (fig 6A) in humans with RNA samples. The Cq values and relative quantity of RNA expression was calculated using Bio-Rad CFX manager software. The housekeeping genes such as β-actin (for individual qPCRs) and *ACTB, B2M, GAPDH, HPRT1,* and *RPLP0* genes were used for the qPCR array, No Template Control (NTC) and Reverse transcription Control (RTC) for individual RNA samples are used for all the qPCR experiments done in this study.

Genes	Forward Primer	Reverse Primer
p16^{INK4A}	5'-CCCAACGCACCGAATAGTT-3'	5'-GTCGTGCACGGGTCGG-3'
SIRT7	5'-GGGCCCTAATGGAGTGTGG-3'	5'-GCTCATGCAGACGGGTGAT-3'
HMGB1	5'-ATATGGCAAAAGCGGACAAG-3'	5'-GCAACATCACCAATGGACAG-3'
NRF2	5'-TGTGGCATCACCAGAACACT-3'	5'-TGACACTTCCAGGGGCACTA-3'
FOXO3A	5'-GAACAGACCAGCCACCTTCT-3'	5'-TGAAGCAAGCAGGTCTTGGA-3'
MnSOD2	5'-GTTGGGGTTGGCTTGGTTTC-3'	5'-GTTCCTTGCAGTGGATCCTG-3'
IL6	5'-GCCCAGCTATGAACTCCTTCT-3'	5'-GAAGGCAGCAGGCAACAC-3'
IL8	5'-AGACAGCAGAGCACACAAGC-3'	5'-ATGGTTCCTTCCGGTGGT-3'
β-ACTIN	5'-AGAGCTACGAGCTGCCTGAC-3'	5'-AGCACTGTGTTGGCGTACAG-3'

Table 1: List of genes and primers used for performing qPCR:

ABL1	**CHEK2**	**IRF3**	**SIRT1**
AKT1	**CITED2**	**IRF5**	**SOD1**
ALDH1A3	**COL1A1**	**IRF7**	**SOD2**
ATM	**COL3A1**	**MAP2K1**	**SPARC**
BMI1	**CREG1**	**MAP2K3**	**TBX2**
CALR	**E2F1**	**MAP2K6**	**TBX3**
CCNA2	**E2F3**	**MAPK14**	**TERF2**
CCNB1	**EGR1**	**MDM2**	**TERT**
CCND1	**ETS1**	**MORC3**	**TGFB1**
CCNE1	**ETS2**	**MYC**	**TGFB1I1**
CD44	**FN1**	**NBN**	**THBS1**
CDC25C	**GADD45A**	**NFKB1**	**TP53**
CDK2	**GLB1**	**NOX4**	**TP53BP1**
CDK4	**GSK3B**	**PCNA**	**TWIST1**
CDK6	**HRAS**	**PIK3CA**	**VIM**
CDKN1A	**ID1**	**PLAU**	**ACTB**
CDKN1B	**IFNG**	**PRKCD**	**B2M**
CDKN1C	**IGF1**	**PTEN**	**GAPDH**
CDKN2A	**IGF1R**	**RB1**	**HPRT1**
CDKN2B	**IGFBP3**	**RBL1**	**RPLP0**
CDKN2C	**IGFBP5**	**RBL2**	**HGDC**
CDKN2D	**IGFBP7**	**SERPINB2**	**RTC**
CHEK1	**ING1**	**SERPINE1**	**PPC**

Table 2 shows the list of genes screened through the Qiagen human cellular senescence qPCR array kit. Genes highlighted in blue are the inhibitors of senescence; Orange are the activators of senescence; Black represents housekeeping genes; HGDC represents Human genomic DNA control; RTC represents Reverse Transcriptase control; PPC represents PCR positive control.

2.5 Protein Isolation and Western Blotting:

To harvest cell lysate or for protein isolation, approximately 6-8 x 10^5 cells were seeded into a 60 mm sterile tissue culture graded Petri plate and grown in normal culturing conditions. Upon 80-90% confluency, the media was aspirated and cells were washed twice with 1X PBS solution. The cells were treated with 500µl of freshly prepared RIPA buffer (including 10mM of (Sodium Fluoride) NaF, 10 mM of (sodium Orthovanadate) Na_2VO_3 and cOmplete protease inhibitor cocktail (Roche)) for 5 minutes and the lysate was collected in a sterile 1ml microcentrifuge tube. The tubes were centrifuged at 14000 RPM for 5 minutes to separate the cell debris from the protein (supernatant). The protein quantification was performed on a 96 well sterile microplate using DC Protein Assay (Bio-Rad, Cat No. 5000116). The kit protocol was followed to prepare the sample for quantification. Briefly, the standard BSA (Bovine Serum Albumin) solutions were diluted in a range between 0-2mg/ml of concentration, and 2ul of each protein sample was used. Each sample and standard will contain 25µl of the tartrate-carbonate buffer, 0.5µl of copper sulfate solution, and 200µl of bicinchoninic acid. The samples were then incubated for 3-5 minutes at room temperature and the plate was read on SpectraMax Plus 384 microplate reader (Molecular Devices, Cat. No. 8254-30-1011). The protein quantification was performed by the machine based on the slope obtained from the optical density values of standard BSA solutions.

2.6.1 Sample Preparation and Western Blotting:

20-30µg of protein per lane was used based on its concentration to perform western blotting. The appropriate concentration of protein samples was mixed with 5X loading buffer containing bromophenol blue (0.25%), Dithiothreitol (0.5M), Glycerol (50%), Sodium dodecyl sulfate 10%, Tris-HCl (0.25 M, pH 6.8). The mixture was then incubated at 95ºC for 5 minutes for protein denaturation. All western blotting in this study was performed using 10% Sodium Dodecyl Sulphate gel. The separated protein was transferred to the nitrocellulose membrane. The membrane was blocked with 5% skimmed milk solution prepared in 1X TBS-T buffer (10mM Tris, 50mM

NaCl, 0.1% Tween-20, pH7.5). The following primary antibody and dilutions were used: anti-SIRT7 (Santa Cruz, sc-365344; 1:500), anti-GAPDH (Abcam, ab8245, 1:5000)

2.6 shRNA, Lentiviral, and Retroviral Production:

shRNA obtained from Sigma Aldrich was used for knockdown of the SIRT7 gene in HFL1 cells: SHC002 (shC), TRCN0000359663 (sh 3), and TRCN0000359594 (sh 4). sh3 and sh4 were two sequences targeting the SIRT7 gene at different sites. was aging. For lentiviral production, HEK293T cells were grown in 100mm well plate up to 50% confluency and the plasmids containing shRNA along with helper plasmids (pLP1, pLP2, and pLP/VSVG packaging plasmids (Thermo Scientific)) were added to the cells supplemented DMEM media. The lentiviral containing media was collected from HEK293T cells after 48 and 72 hours of post-transfection and filtered through a 0.45 μm filter. The filtrate was added to the 293T and early passages of HFL1 cells. After 72 hours, the media was changed and supplied with optimized concentrations of puromycin for HEK293T (6 μg/ml) and HFL1 (2 μg/ml) cells for clonal selection for 4 days. For the production of Retrovirus expressing the HRAS gene, a similar protocol was followed except the virus production was done using phoenix cells as these cells produce the packaging plasmids within their system for successful viral production. HFL1 cells underwent at least 2 passages before performing assays to study the role of SIRT7 in cellular senescence.

2.7 Proliferation Assay:

The proliferation rate of SIRT7 knockdown cells and Oncogene induced senescence were studied using the *Incucyte* proliferation assay. The cell proliferation was obtained by monitoring the confluency percentage over time by creating a confluency mask on the *Incucyte* live-cell imaging system (Sartorius). 2500-3000 cells were seeded on to a 96-well plate and incubated in the imaging system for 6 days post-seeding under normal growth conditions. The media was changed every 3 days. The proliferation curves were plotted using GraphPad Prism 5.

2.8 Statistics Analysis:

All experiments in this study were done on at least two independent biological replicates with at least 2 or more technical replicates with each dose or treatment group unless otherwise specified. The statistical analysis used for all experiments in this study was One-way ANalysis Of VAriance (ANOVA) with Post-hoc with Tukey's Honestly Significant Difference (HSD)

Chapter 3 : RESULTS

3.1 Effect of Low Dose Radiation (LDR) on Human Lung Fibroblasts (HFL1).

Previously, our group has shown that radiation doses equivalent to 30 mGy decelerate cellular senescence in Human Embryonic Lung Fibroblasts (HELF-104) cells [60]. Here, we sought to study was the underlying molecular pathways that result in the delay of cellular senescence upon exposure to was LDR in HFL1 cells.

3.1.1 LDR decelerates senescence in normal HFL1 cells.

To study if the low dose radiation induces deceleration of senescence in HFL1 cells as previously demonstrated in HELF-104 cells, early passages (P3) of HFL1 cells were exposed to 0, 10, and 100 mGy of gamma irradiation and kept in culture for 12 weeks following irradiation. Senescence associated - β - Galactosidase (SA-β-Gal) assay was performed at time points of 1, 4, 8, and 12 weeks post-irradiation. In Fig 7, the overall SA-β-Gal shows deceleration of senescence at the 12^{th} week in HFL1 cells irradiated at 10 mGy. This effect is not seen with cells that are irradiated at 100mGy which shows a similar pattern of senescence to that of untreated HFL1 cells (sham irradiated). This result is consistent with and similar to the previous results obtained by Velegzhaninov et al [60]. Fig 6B and 6C show the bright-field microscopic images of young proliferating (P5) and senescent (P14) HFL1 cells. The blue staining of β-galactosidase activity marks senescent cells. The accumulation of β-galactosidase is a biomarker of senescence in mammalian cell culture [69]. Hence, upon exposure to 10 mGy of radiation, the HFL1 cells show a delay in senescence compared to the control and the 100 mGy treatment group. This delayed senescence may be associated with a more general phenomenon of hormesis induced by low doses of radiation.

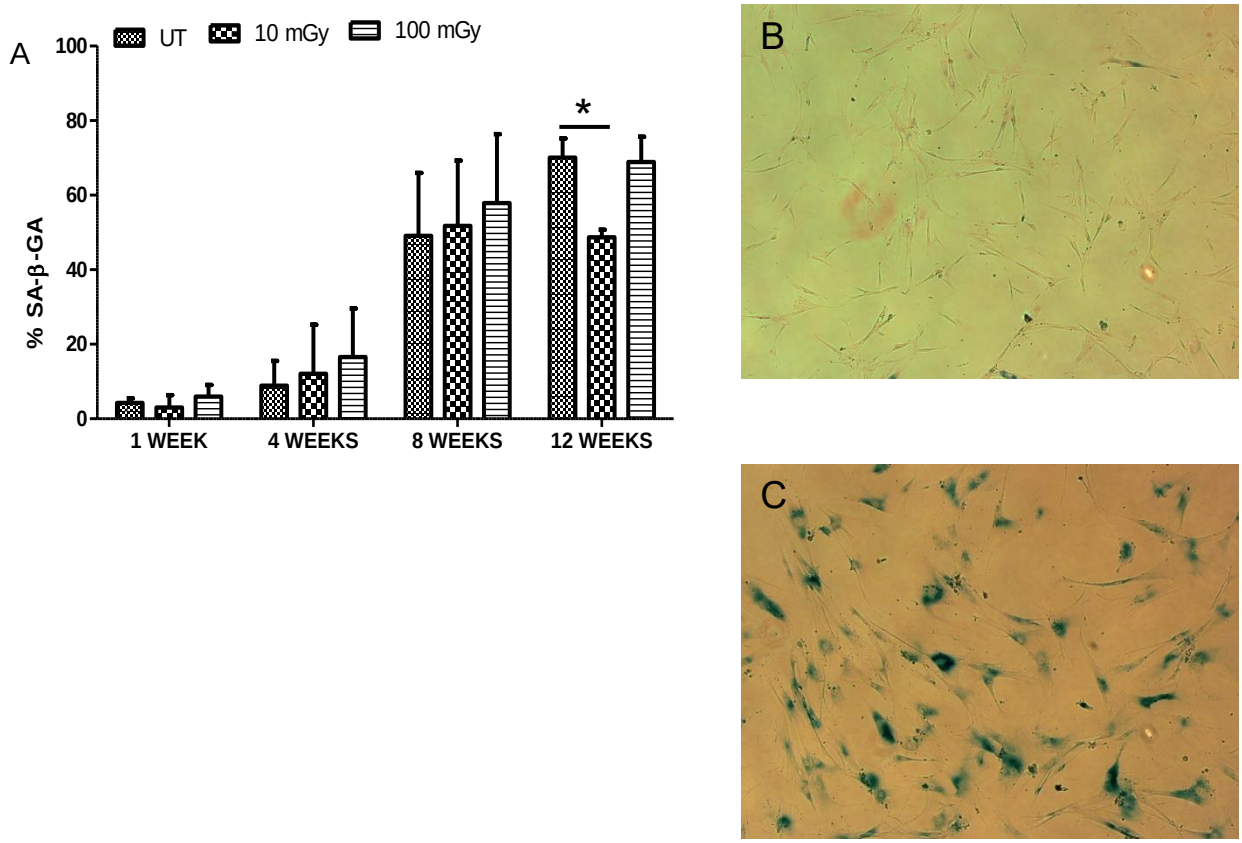

Figure 6: <u>Cells exposed to 10 mGy display delayed senescence</u>. Fig 6A - (SA-β-Gal) assay was done on normal Human fetal lung fibroblasts cells. The cells irradiated with 10 mGy showed a delay in senescence compared to the untreated cells and cells treated with 100 mGy. **Fig 6 B and C** – Bright field microscope images (10X) of young (P5) and old (P14) cells stained for SA-β-Gal assay. Data show the mean ± S.D of two independent biological replicates. Comparison between samples are made using one-way ANOVA with Post-hoc with Tukey's Honestly Significant Difference (HSD) using a totality of 4 replicates (2 biological x 2 technical); * $p<0.05$, ** $p<0.01$.

3.1.2 qPCR array analysis: Differential genes expressed upon LDR in HFL1 cells.

Human cellular senescence 384-well qPCR array kit from Qiagen is used to screen 84 highly influential genes involved in aging humans. The list of genes used in this screening is shown in Table 2. One week and 12 weeks post-irradiation HFL1 cells exposed to doses of 10 and 100 mGy were used for this experiment. Fig 7 A shows the scatter plots for gene expression regulation. One-week post-irradiation, not much change in the expression of the genes between untreated and 10 mGy and untreated and 100 mGy of gamma radiation was seen. In contrast, more regulation was observed at 12 weeks post-irradiation (Fig 7B). The threshold fold change of genes relative to the untreated cells is set to 2. Fig 7 A and B represent the distribution plot of differentially expressed genes shown in Table 3 (in Appendix) in two independent biological replicates. Figure 7 C and D shows the commonly regulated genes between 10 and 100 mGy in 1 week or 12 weeks post-irradiation HFL1 cells.

HFL1 cells irradiated at 10 mGy displays a higher proportion of gene regulation in qPCR array in both the time points compared to 100 mGy. From the Venn Diagram shown in Figure 7C and D, HFL1 cells with one-week post-irradiation with 10 mGy 32 genes can be seen that are regulated while 100 mGy lead to alterations in the expression of 8 genes among which 6 genes are commonly regulated between the two-dose groups. Similarly, 10 mGy differentially regulated 62 genes in HFL1 cells at 12 weeks post-irradiation and 100 mGy resulted in regulation of 31 genes in these cells among which the 22 genes are commonly regulated between the two-dose groups. To gain an insight into the biological significance of these gene expression changes, all genes were categorized into activators or suppressors of senescence. Then the number of suppressors down-regulated and activators up-regulated (collectively, these changes would promote senescence) vs. suppressors up-regulated and activators down-regulated (collectively, these changes would suppress senescence) was plotted against each other (Figure 7 E). It can again be seen that the magnitude of gene

expression changes is greater with 100 mGy vs 10 mGy at both time points. Also, for both doses, changes at 12 weeks post-irradiation are greater than those at 1 week, suggesting long-term rearrangement of the genetic aging program. Lastly, opposite to the expectation, no clear trend is seen in terms of the magnitude of gene expression changes that suppress (green bars) vs. activate (orange) senescence after 10 mGy. This analysis leads to a suggestion that transcriptional changes involved in a 10 mGy induced suppression of senescence are complex, with some signaling pathways that may have greater weight in the overall phenotypic change. To this end, it could be noted that most of the genes that are upregulated upon 10 mGy, belong to the family of transcriptional factors that inhibit cellular senescence (e.g.TBX2, TBX3, etc.). Further examination of the individual genes altered upon LDR could reveal their role in regulating cellular senescence. In consistent with the results from this study, genes such as p16, P19 and p21 is also mediates senescence in normal mammalian cells [70]. p21 is an antiproliferative factor and cell cycle inhibitors in normal cells which is upregulated during senescence through p53 dependent and independent pathways [71], [72]. Similarly, p16 and p19 genes also show higher expression with progressive aging in normal cells [73], [74]. Ultimately, these genes can be studied in various age-related disease models in the context of the potential use of LDR for therapy.

A

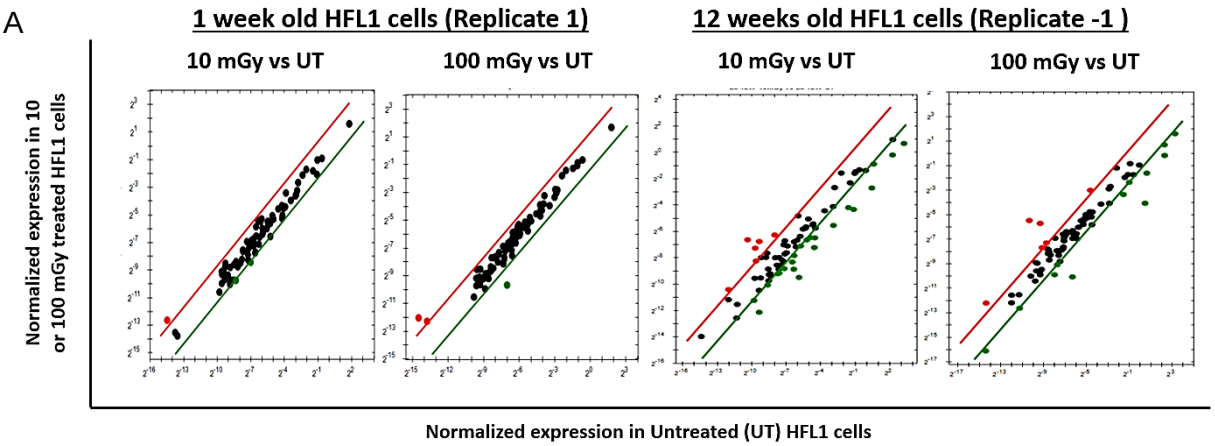
1 week old HFL1 cells (Replicate 1)
12 weeks old HFL1 cells (Replicate -1)
10 mGy vs UT
100 mGy vs UT
10 mGy vs UT
100 mGy vs UT
Normalized expression in 10 or 100 mGy treated HFL1 cells
Normalized expression in Untreated (UT) HFL1 cells

B

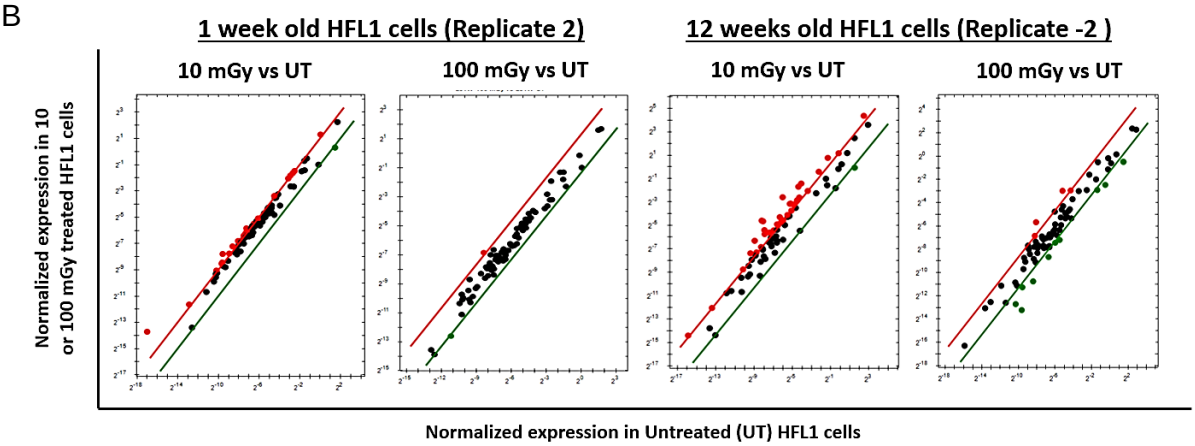
1 week old HFL1 cells (Replicate 2)
12 weeks old HFL1 cells (Replicate -2)
10 mGy vs UT
100 mGy vs UT
10 mGy vs UT
100 mGy vs UT
Normalized expression in 10 or 100 mGy treated HFL1 cells
Normalized expression in Untreated (UT) HFL1 cells

C

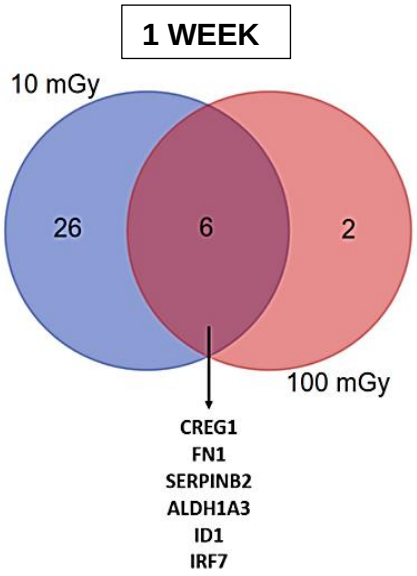
1 WEEK
10 mGy
26
6
2
100 mGy
CREG1
FN1
SERPINB2
ALDH1A3
ID1
IRF7

D

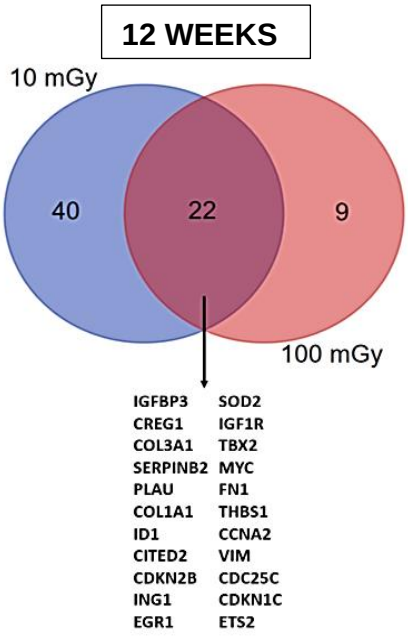
12 WEEKS
10 mGy
40
22
9
100 mGy
IGFBP3
CREG1
COL3A1
SERPINB2
PLAU
COL1A1
ID1
CITED2
CDKN2B
ING1
EGR1
SOD2
IGF1R
TBX2
MYC
FN1
THBS1
CCNA2
VIM
CDC25C
CDKN1C
ETS2

E

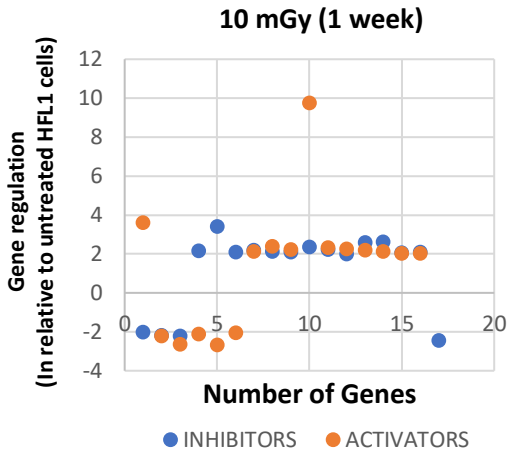
10 mGy (1 week)
Gene regulation
(In relative to untreated HFL1 cells)
12
10
8
6
4
2
0
-2
-4
0
5
10
15
20
Number of Genes
INHIBITORS
ACTIVATORS

F

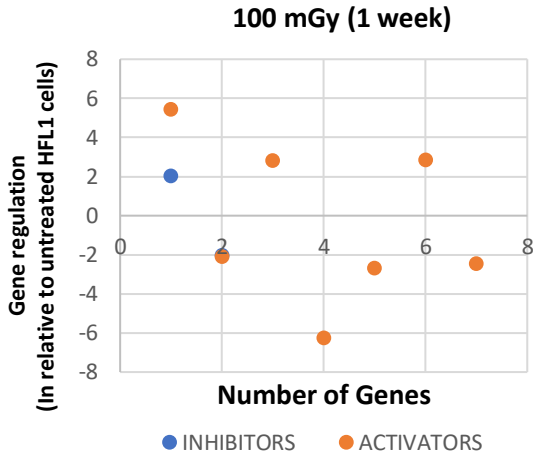
100 mGy (1 week)
Gene regulation
(In relative to untreated HFL1 cells)
8
6
4
2
0
-2
-4
-6
-8
0
2
4
6
8
Number of Genes
INHIBITORS
ACTIVATORS

G

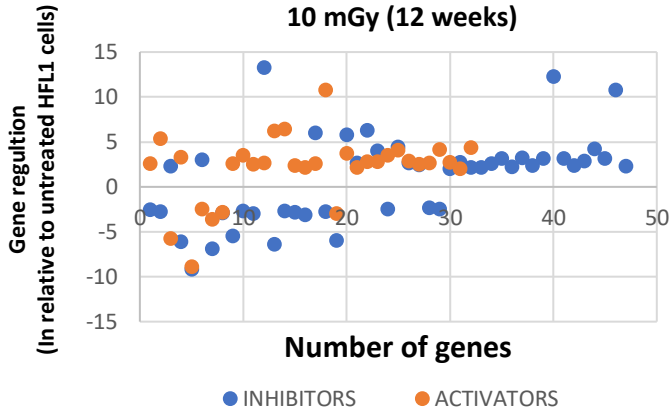
10 mGy (12 weeks)
Gene regulation
(In relative to untreated HFL1 cells)
15
10
5
0
-5
-10
-15
0
10
20
30
40
50
Number of genes
INHIBITORS
ACTIVATORS

H

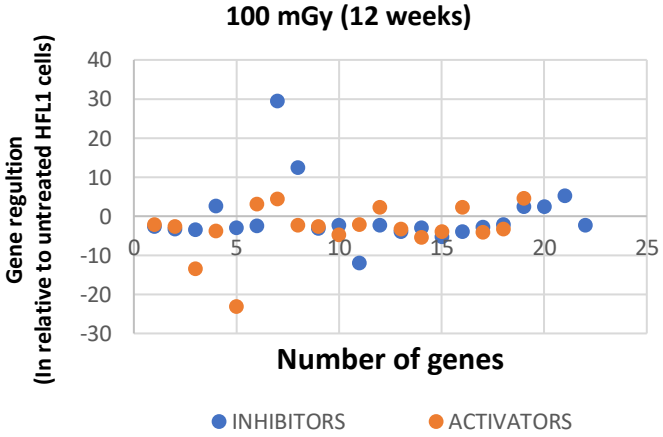
100 mGy (12 weeks)
Gene regulation
(In relative to untreated HFL1 cells)
40
30
20
10
0
-10
-20
-30
0
5
10
15
20
25
Number of genes
INHIBITORS
ACTIVATORS

Figure 7: <u>Higher number of genes altered at 10 mGy compared to 100 mGy:</u> Fig 7A and B represent the scatter plots for two independent biological replicates at 0,10, and 100 mGy of gamma radiation at 1 week and 12 weeks post-irradiation. The regulation threshold = 2-fold. Red highlight – upregulated; Green highlight – downregulation. **Fig 7C** and **D** show genes that are commonly regulated in 1-week and 12 weeks post-irradiation between 10 and 100 mGy. Figure 7 E – H shows the gene regulation of activators and inhibitors of senescence in HFL1 cells between 10 mGy and 100 mGy and between 1 week and 12 weeks time point. (Replicate 1 and 2 are the two independent biological replicates used for these experiments). Data show the mean ± S.E.M of two independent biological replicates.

3.2 Role of SIRT7 protein in delaying senescence in HFL1 cells upon LDR.

Sirtuins are a family of proteins that are known to regulate human cellular senescence by involving in various age-related molecular pathways. It contains 7 proteins localized in various organelles within the eukaryotic cell. Unlike other sirtuin proteins, SIRT7 is localized predominantly in nucleoli. SIRT7 is known to safeguard the mammalian cells from senescence through epigenetic silencing of rDNA instability. SIRT7 knockout WI 38 cells (human normal lung cells) show accelerated senescence compared to the control group [75]. Similarly, old IMR90 (human fetal lung) cells show a decrease in total SIRT7 protein concentration implying that SIRT7 plays a role in protection from cellular senescence [76].

3.2.1 SIRT7 gene is differentially expressed upon LDR in HFL1 cells.

Specific human primers were designed as given in Table 1 and the annealing temperature is optimized through qPCR standardization to study its role in deceleration of senescence by LDR in HFL1 cells. HFL1 cells one-week post-irradiation did not show any significant difference in SIRT7 gene expression between the dose groups while the 12-week old HFL1 cells irradiated at 10mGy shows a significantly higher expression of SIRT7 gene compared to the control and cells treated with 100mGy of radiation (Figure 8).

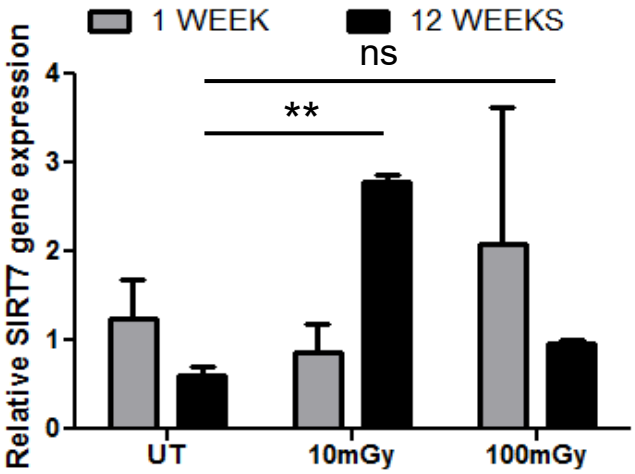

Figure 8: <u>LDR leads to upregulation of Sirt7 at long, but not short terms after exposure</u>: Relative SIRT7 gene expression at 1 week and 12 weeks post-irradiation in HFL1 cells. The expression is normalized with β – Actin. Data show the mean ± S.D from all technical replicates of two independent biological replicates. Comparison between samples are made using one-way ANOVA with Post-hoc with Tukey's Honestly Significant Difference (HSD); * $p<0.05$, ** $p<0.01$.

3.2.2 Specific genes upregulated upon LDR in HFL1 cells.

To further explore this SIRT7 gene regulation specifically by 10 mGy, but not 10 mGy, at 12 weeks post-IR, other genes that are reported for its interaction with sirtuins and involved in the regulation of cellular senescence in humans were searched in published literature reviews. The resulting list of genes that were selected for use in this study is given in Table 1. Collectively, HMGB1 [77], IL6 [78], and IL8 [78] are selected to study the inflammatory response; NRF2 [33], and MnSOD2 [79] are selected to study the antioxidative response and FOXO3A and $p16^{INK4A}$ are selected for its role in driving the senescence [80]. Primers were designed for RT-qPCR and used to measure mRNA in our HFL1 cells. Similar to SIRT7 expression, some of these genes are also differentially regulated at 10 mGy of gamma radiation compared to untreated and 100 mGy treated HFL1 cells at 1 week and 12 weeks post-irradiation. For example, IL6 and $p16^{INK4a}$ show significantly lower and higher expression compared to the control and 100 mGy.

LDR induces changes in the inflammatory pathways in HFL1 cells. Interleukin – 6, a prominent cytokine secreted in senescence-associated secretory phenotype (SASP) which influences inflammatory pathways leading to tissue repair and tumor progression. Studies show that IL6 secretion increases by suggesting its role in age-related inflammatory diseases [81], [82]. In this study, HFL1 cells 12 weeks post-irradiation of 10 mGy showed a significant decrease in IL6 mRNA expression compared to other groups (Figure 9). The reduced gene expression could contribute to the delay in senescence in HFL1 cells by regulating various inflammatory pathways. Consistent with this, lowering IL6 expression in mice resulted in the protection of articular tissues through adipsin deficiency which gives rise to osteoarthritis progression [83]. Also, as discussed earlier, elevated IL6 protein expression is a clinical predictor for SARS-CoV-2 mortality in humans [53]. Significant reduction in IL6 mRNA expression in HFL1 cells with LDR 12 weeks post-irradiation is a good indicator to emphasize that LDR can be used as an alternative treatment to cure SARS-CoV-2 infection. Other genes such as IL8, another cytokine associated with SASP, Mn-SOD2, and

NRF2 which plays a role in regulating antioxidant signaling and ROS scavenging activities also showed differential gene expressions upon 10 mGy in HFL1 cells (Figure 9).

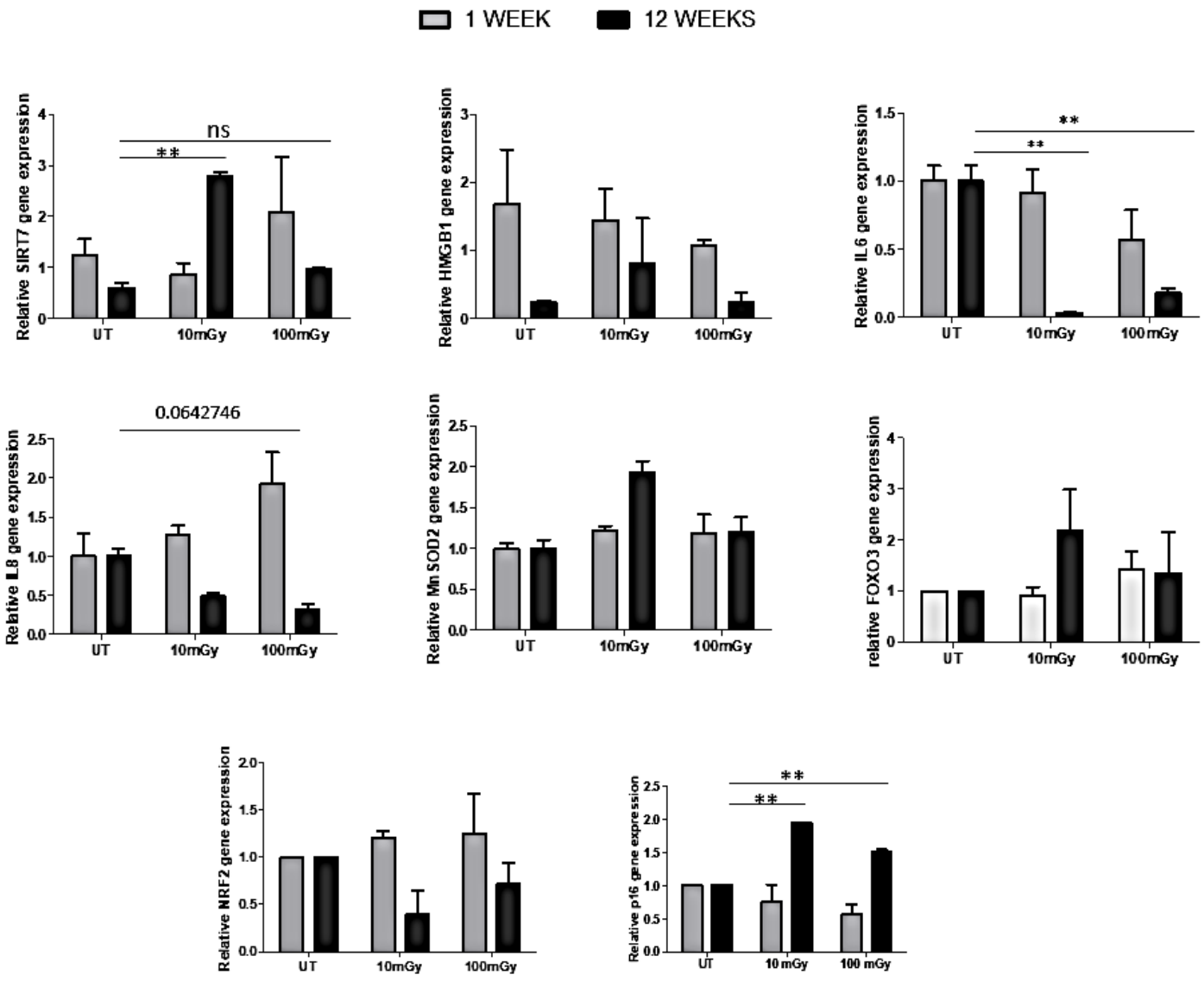

Figure 9: <u>LDR differentially regulates the genes associated with inflammation and antioxidant activity in HFL1 cells 12-week post-irradiation</u>. Genes such as IL6 and IL8 are significantly down-regulated in HFL1 cells exposed to 10 mGy of LDR. $P16^{INK4A}$ is expressed significantly higher in these cells while other genes associated with antioxidant activity such as NRF2 and SOD2 also expressed higher in these cells upon 10 mGy of LDR. Data show the mean ± SEM of two independent biological replicates. Comparison between samples are made using one-way ANOVA with Post-hoc with Tukey's Honestly Significant Difference (HSD); ns – non-significant, * $p<0.05$, ** $p<0.01$.

3.3 SIRT7 Knockdown HFL1 cells and its characterization.

To study the role of SIRT7 gene on cellular senescence and proliferation of HFL1 cells, SIRT7 knockdown HFL1 cells were created using a lentiviral transduction system. shRNA is obtained from the Sigma-Aldrich repository from the Research Institute – II of Children's' Hospital of Eastern Ontario (CHEO). Two sequences of different target sites on the SIRT7 gene were selected and using the lentiviral shRNA knockdown system, these two sequences were used to knock down the SIRT7 gene in HEK293T cells (Fig 10 A and B). After successful knockdown of SIRT7 in these cells with more than 50% knockdown efficiency, a similar protocol is used on an early passage (P3) HFL1 cells for knockdown of the SIRT7 gene. Successful knockdown of SIRT7 gene in HFL1 cells is shown in Fig 10 C and D through SIRT7 protein and mRNA expression. GAPDH and Actin were used for normalization for protein and mRNA expression, respectively. SIRT7 knockdown sequence 3 (sh 3) chosen to be used for further assays as it showed the most efficient knockdown of SIRT7 at both mRNA and protein levels. HFL1 cells were grown in F12K media supplemented with 1μg/ml of puromycin (optimized in titration experiment) for selecting the positive knockdown cells.

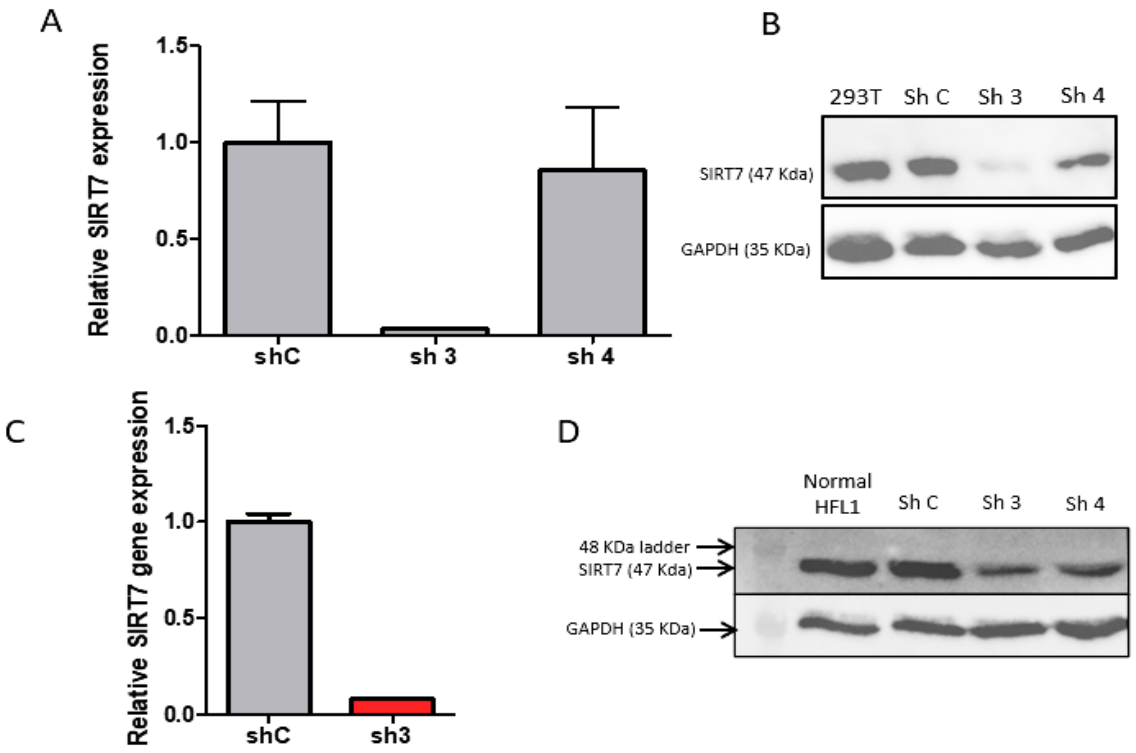

Figure 10: <u>SIRT7 Knock Down in HEK293T and HFL1 cells</u>. Fig 10A represents relative SIRT7 gene expression between control (shC) and two SIRT7 Knock Down sequences sh3 and sh4 respectively. The gene expression is normalized with β – Actin. Fig 10B shows the protein expression in the HEK293T normal, control, and two sequences used for knocking down the SIRT7 gene. Error bar represents the standard error of the mean from three technical replicates. Fig 10C and D show the relative SIRT7 mRNA expression and SIRT7 protein expression in SIRT7 KD HFL1 cells and that of HFL1 cells expressing scrambled control vector.

3.3.1 SIRT7KD affects cellular proliferation and drives senescence in HFL1 cells.

Following successful Knockdown of SIRT7 in HFL1 cells and selecting transduced HFL1 cells using puromycin, cells have undergone one passage. Assays to study the role of SIRT7 in cellular proliferation and senescence rate were performed using *Incucyte* proliferation assay and senescence-associated β-Galactosidase (SA-β-Gal) assay. Approximately 2500 cells of each treatment group in triplicates were seeded in 96 well plates and followed until 6 days from the day of seeding. Figure 11 A shows the proliferation rate of SIRT7 KD-HFL1 cells are affected and they proliferate at a slower rate compared to the control (shC) and normal HFL1 cells of the same passage. The Figure also shows that the concentration of puromycin (1 μg/ml) used for the selection of SIRT7 Knockdown HFL1 cells after 72 hours post-transfection. Figure 11 B shows that the SIRT7 knockdown HFL1 cells show a significantly higher senescence rate compared to the control and untreated or normal HFL1 cells. These results suggest that SIRT7 does have a pronounced effect on cellular proliferation in HFL1 cells and regulates senescence in these cells.

A

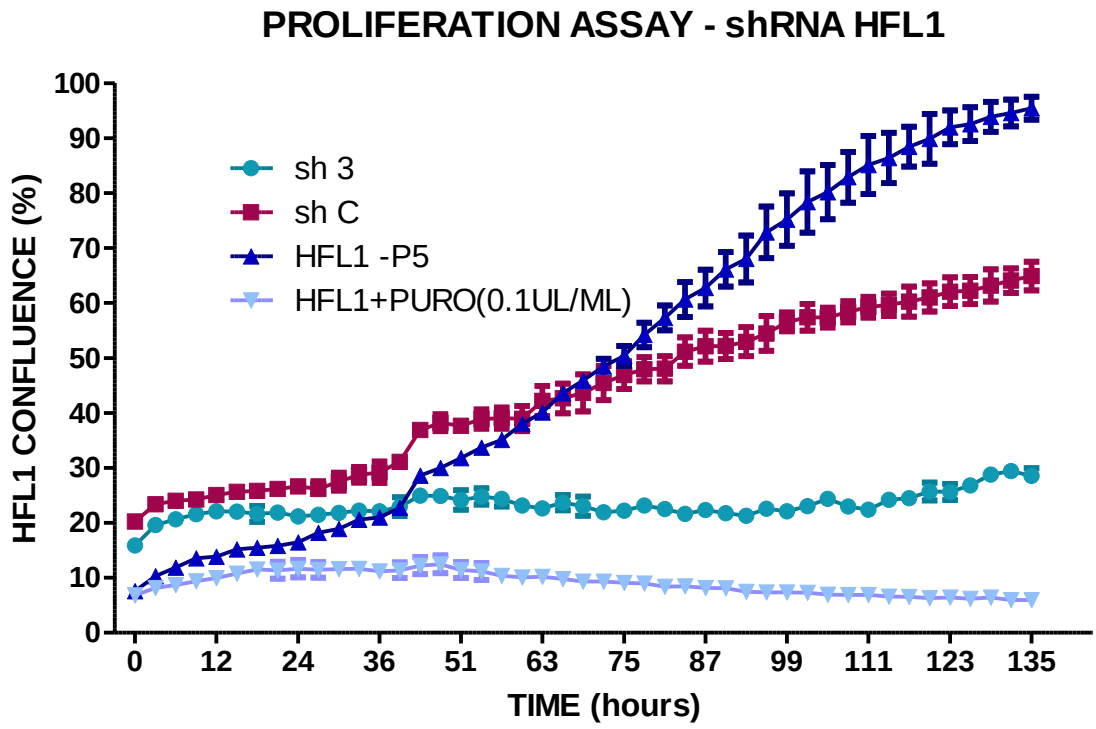
PROLIFERATION ASSAY - shRNA HFL1
HFL1 CONFLUENCE (%)
TIME (hours)
sh 3
sh C
HFL1 -P5
HFL1+PURO(0.1UL/ML)
0
10
20
30
40
50
60
70
80
90
100
0
12
24
36
51
63
75
87
99
111
123
135

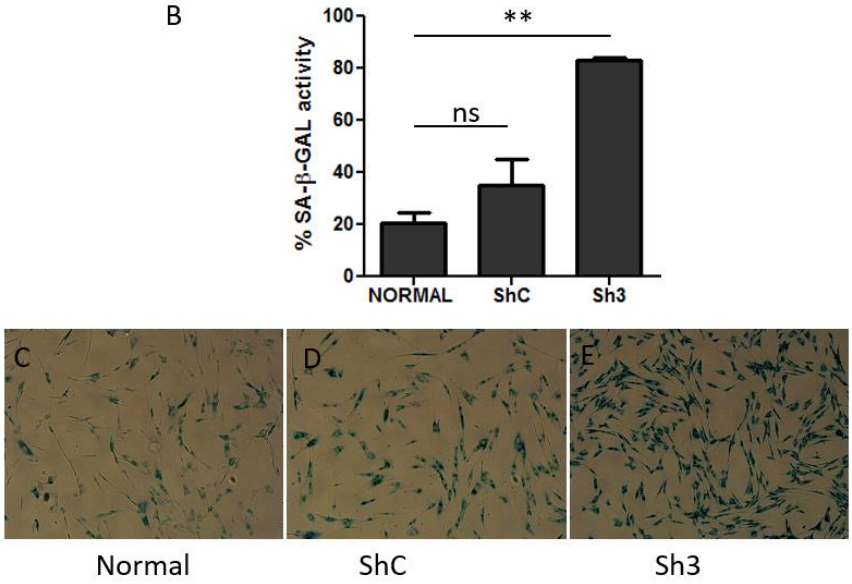
B
% SA-β-GAL activity
**
ns
NORMAL
ShC
Sh3
C
D
E
Normal
ShC
Sh3

Figure 11: <u>SIRT7 knockdown induces senescence in HFL1 cells</u>. Fig 11 A shows the proliferation rate of non-transfected HFL1 cells of passage 5 (P5); transfection control (shC); SIRT7 knockdown (sh3) and puromycin treated normal HFL1 cells. Fig 11 B shows the percentage of senescence of each treatment group. The SA- β -Gal assay is done in two independent biological replicates. Fig 11 C-E shows microphotographs of HFL1 cells expressing SA-b-gal (blue cells) after processing with a b-gal assay kit. Fig 11 G shows the common differentially expressed genes between 10 mGy and SIRT7 KD (knockdown) HFL1 cells. Shown are means ± standard error of the mean from at least three technical replicates (n= 1000 cells/replicate). ** $p<0.01$

3.3.2 qPCR array analysis: Differential genes expressed in SIRT7KD HFL1 cells.

To study if knocking down the SIRT7 gene in HFL1 cells affects the expression of senescence genes especially those that are regulated by low dose radiation (shown in Figure 7 C, D and 9), the RNA of SIRT7 knockdown HFL1 cells was isolated and cDNA was synthesized for each treatment group. Using Qiagen human cellular senescence qPCR 384-well array, we found that certain genes were up and downregulated in SIRT7 knockdown HFL1 cells compared to control (shC) HFL1 cells as shown in Figure 12 A-C. Among all the genes that are differentially regulated in SIRT7 knockdown cells, IGFBP3 is strongly downregulated and it is an insulin-like growth factor-binding protein that plays an important role in cellular senescence and aging in mammalian cells. Reduced mRNA expression of IGFBP3 is a biomarker for cellular senescence and aging [84]. This emphasizes that SIRT7 is required to regulate cellular senescence in these cells. Further, these cells also show a significant decrease in another frequently used senescence marker $p16^{INK4A}$ (Figure 12 D). Surprisingly, the data in this study suggests that SIRT7 regulates cellular senescence in HFL1 cells through $p16^{INK4A}$ gene expression. More replicates are needed to test the interplay of SIRT7 and p16 gene expression in regulating senescence in HFL1 cells.

SERPINE1, also known as Plasminogen Activator Inhibitor – 1 (PAI-1) plays a role in regulating thrombosis [85]. In SIRT7 knockdown HFL1 cells it is seen to be downregulated. mRNA of PAI-1, along with another gene called SPARC (secreted protein acidic and rich in cysteine) are co-expressed and control the expression of IGFBP3 in old human dermal fibroblasts. This suggests that they play a coordinative role in cellular senescence [86]. In this study, SIRT7 knockdown resulted in the down-regulation of both genes which hints that SIRT7 may play a role in the expression of PAI-1 and SPARC which in return induce a strong downregulation of the IGFBP3 gene. Exploring this aspect of SIRT7 effects on mRNA and protein levels of these genes may help understand diseased conditions such as thrombosis and other inflammatory diseases such as acute lung injury which is widely seen in SARS-Cov-19 affected patients [87]. Unlike PAI-1, PAI-2 also

known as SERPINB2 is upregulated in SIRT7 KD HFL1 cells. The unique feature of PAI-2 is that it is expressed predominantly by macrophages and detectable only during pregnancy due to increased activity of thrombosis and also known to play an important role in adaptive immunity [88]. Strikingly in this study, SIRT7 knockdown resulted in a detectable level of PAI-2 upregulation in HFL1 cells suggesting that SIRT7 loss triggers inflammatory signals which could be specific to lung fibroblasts.

Other genes that are downregulated include various cyclin and cyclin-dependent kinases (CDKs) such as CDK6, CDKN1A, CDKN2A, CDKN2B, CCNB1, CCND1and CCNE1. This suggests another role of SIRT7 as a mediator of cell cycle gene expression during senescence in HFL1 [89], [90]. TBX3, a TATA box binding protein 3, is known for direct interaction with these cell cycle regulators [91]–[94]. In the absence of SIRT7, upregulation of TBX3 in HFL1 cells may inhibit of cell cycle regulators resulting in senescence in these cells. Along with this gene, other transcriptional factor genes such as TWIST1, Interferon regulatory factors (IRF) 3 and 5, that were upregulated in SIRT7 knockdown HFL1 cells are known to drive cellular senescence through various cellular pathways [95]–[97]. MAPK signaling pathways commonly regulate senescence in normal human cells [98]. MAP2K6 signaling involved in senescence by inhibiting cell cycle progression through activation of various transcriptional factors [99]–[103]. This suggests that loss of SIRT7 in HFL1 cells results in this activation of MAP2K6 leading to the downregulation of various cell cycle regulators for accelerating senescence in HFL1 cells. The upregulation of the ATM gene is also seen in SIRT7 knockdown HFL1 cells, signifying its role in senescence [104]. Telomere length and expression of TERT should decrease with the aging process. In this study, TERT expression is shown to be upregulated in the absence of SIRT7 in HFL1 cells. This could be because of downregulation of SERPINE1 results in increasing telomere activity resulting in telomere independent senescence [105]–[108].

As explained earlier in Figure 12, there are differentially regulated genes by low doses of gamma radiation. To understand if SIRT7 knockdown in HFL1 has any effect on the expression of these genes, individual qPCRs were performed using the cDNA of SIRT7 knockdown HFL1 cells. Genes such as MnSOD2, NRF2, IL6, and HMGB1 are differentially expressed in SIRT7 knockdown HFL1 cells. Superoxide Dismutase 2, SOD2, a protein that expressed predominantly in mitochondria that is responsible for cellular antioxidant activity [79]. The expression of the SOD2 gene in HFL1 cells treated with 10 mGy showed an upregulation similar to SIRT7 gene expression upon LDR in 12 weeks post irradiated HFL1 cells. The knockdown of SIRT7 gene in these cells results in the downregulation of SOD2 in both qPCR array and individual qPCR assay (figure 12 C and E). In the absence of SIRT7 expression, SOD2 is downregulated while the upregulation of SOD2 is observed in 12-week old HFL1 cells treated with 10 mGy in the presence of SIRT7. This suggests that SIRT7 and SOD2 coordinate cellular senescence in HFL1 cells and are responsive to LDR, through an antioxidant regulatory role. Another antioxidant gene, NRF2 is transiently downregulated in SIRT7 knockdown HFL1 cells compared to the control of HFL1 cells. At 10 mGy treatment of 12-weeks old HFL1 cells, the mRNA level of NRF2 is lower compared to other dose groups suggesting that SIRT7 gene expression has either no or little effect on NRF2 gene expression and its activity in regulating cellular senescence. Inflammation associated genes such as HMGB1 and IL6 is also up and down-regulated in SIRT7 knockdown HFL1 cells. HMGB1 is a secretory cytokine result in the signal transduction process during inflammatory diseases [109], [110]. HMGB1 shows a strong upregulation compared to the control in SIRT7 knockdown cells suggesting that SIRT7 loss in these cells leads to senescence-associated secretory phenotype (SASP) which often observed in inflammation and age-related inflammatory diseases [78], [111], [112]. Similarly, another cytokine gene, IL6, is a secreted cytokine in SASP during age-related inflammatory diseases [113]. IL6 gene expression in the absence of SIRT7 is downregulated in HFL1 cells. This is similar to the IL6 gene expression profile in HFL1 cells 12 weeks post-irradiation of 10 mGy where upregulation of SIRT7 suppresses IL6 gene expression in HFL1 cells

12 weeks post-irradiation. This could be due to the indirect involvement of SIRT7 to down-regulate IL6 gene expression in SIRT7 Knockdown HFL1 cells.

Figure 12E shows the shared transcriptional profile between 10 mGy treated HFL1 cells and SIRT7 knockdown HFL1 cells. 21 genes are commonly regulated between these two subsets of HFL1 cells. Among these, genes such as TWIST1, PRKCD, CDK6, CDKN2B, CDKN2A, CDKN1A, SOD2, MYC, CCNE1, CCND1, IGFBP7 require SIRT7 expression for their transcriptional induction and activity. IGFPB3 is an exception that showed stronger downregulation in the absence of SIRT7 expression. These genes can be further studied in detail to understand their role in delaying senescence in 10 mGy treated HFL1 cells through their modulation by SIRT7.

A

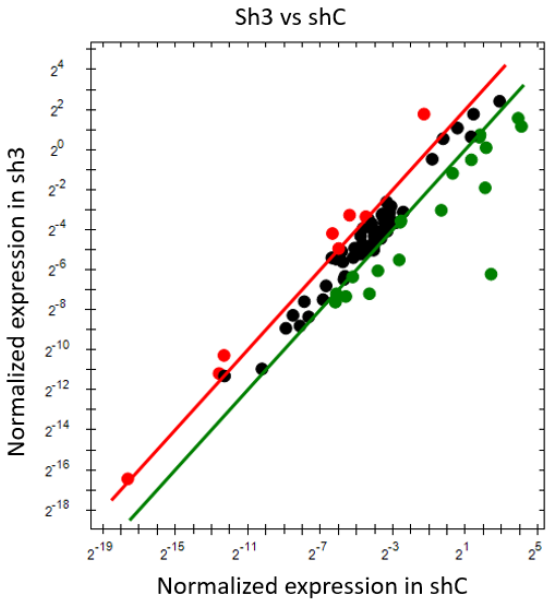
Sh3 vs shC
Normalized expression in sh3
Normalized expression in shC

B

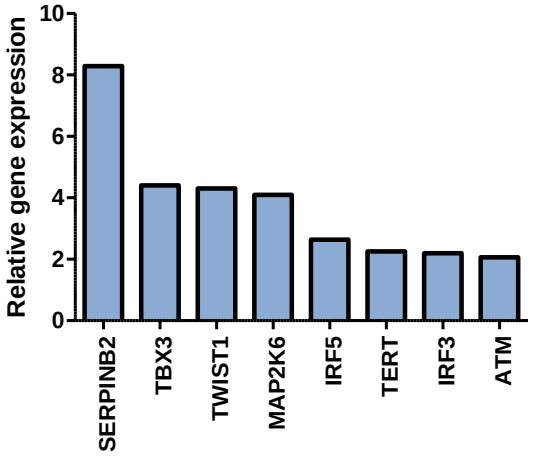
Relative gene expression
SERPINB2
TBX3
TWIST1
MAP2K6
IRF5
TERT
IRF3
ATM

C

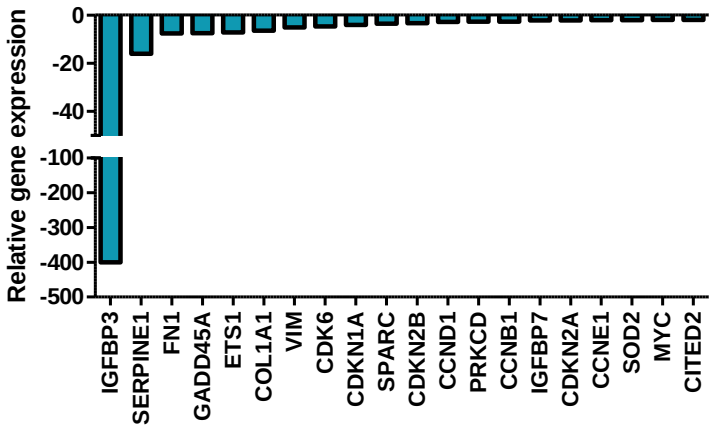
Relative gene expression
IGFBP3
SERPINE1
FN1
GADD45A
ETS1
COL1A1
VIM
CDK6
CDKN1A
SPARC
CDKN2B
CCND1
PRKCD
CCNB1
IGFBP7
CDKN2A
CCNE1
SOD2
MYC
CITED2

D

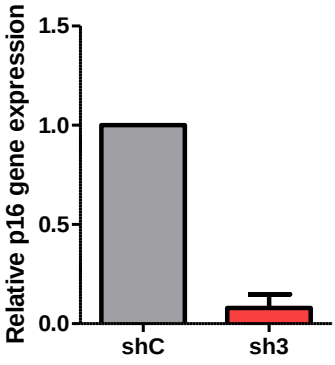
Relative p16 gene expression
shC
sh3

E

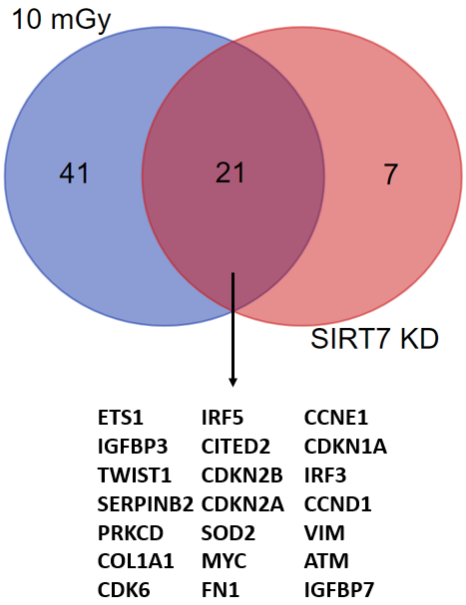
10 mGy
41
21
7
SIRT7 KD
ETS1 IRF5 CCNE1
IGFBP3 CITED2 CDKN1A
TWIST1 CDKN2B IRF3
SERPINB2 CDKN2A CCND1
PRKCD SOD2 VIM
COL1A1 MYC ATM
CDK6 FN1 IGFBP7

F

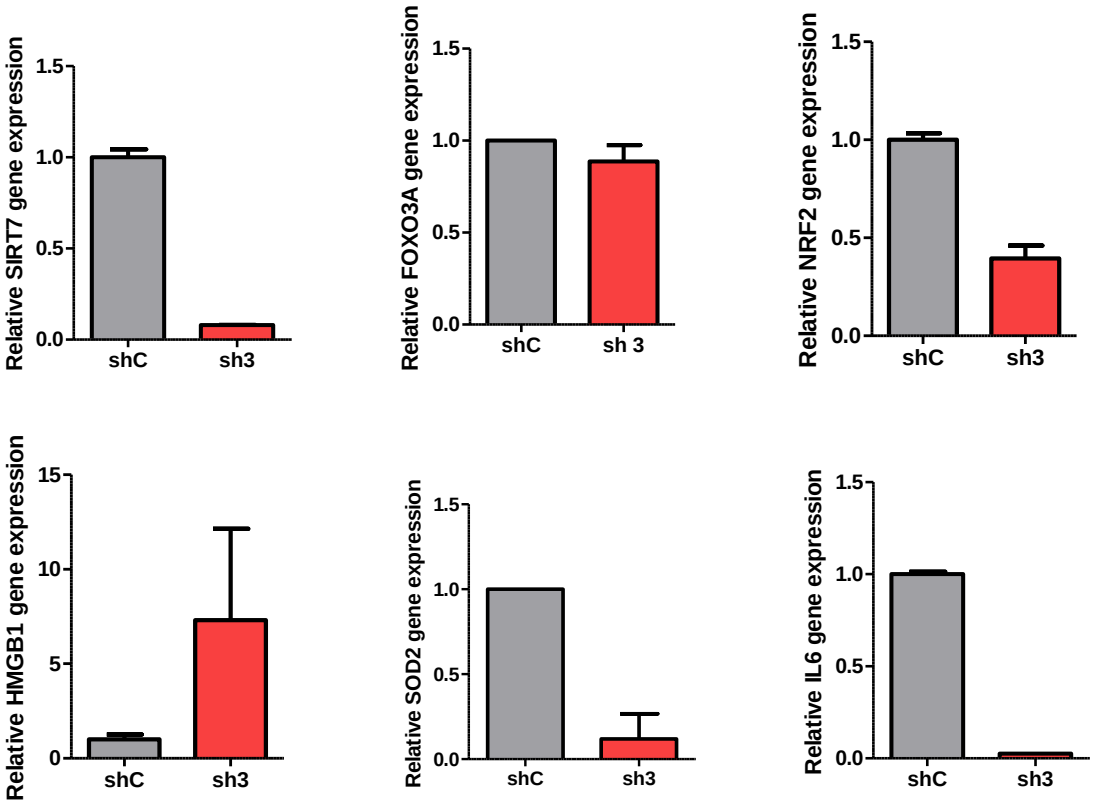
Relative SIRT7 gene expression
1.5
1.0
0.5
0.0
shC
sh3
Relative FOXO3A gene expression
1.5
1.0
0.5
0.0
shC
sh 3
Relative NRF2 gene expression
1.5
1.0
0.5
0.0
shC
sh3
Relative HMGB1 gene expression
15
10
5
0
shC
sh3
Relative SOD2 gene expression
1.5
1.0
0.5
0.0
shC
sh3
Relative IL6 gene expression
1.5
1.0
0.5
0.0
shC
sh3

Figure 12: <u>Differentially expressed genes in SIRT7 knockdown HFL1 cells.</u> Fig 12A shows the scatter plot of 84 genes screened using Qiagen Human cellular senescence qPCR 384-well array kit. Fig 12 B and C show the upregulated and downregulated genes, respectively. Fig 12 D shows the expression of $p16^{INK4A}$ in SIRT7 knockdown HFL1 cells relative to control (shC) cells. Fig 12 E shows the common differentially expressed genes between 10 mGy and SIRT7 KD (knockdown) HFL1 cells. Fig 12 F shows the expression of genes that are selected through a literature review due to their role in human cellular senescence. Data show the mean ± SEM of three technical replicates. Comparison between samples are made using one-way ANOVA with Post-hoc with Tukey's Honestly Significant Difference (HSD); ns – non-significant, * $p<0.05$, ** $p<0.01$.

3.4 Oncogene Induced senescence (OIS).

OIS is induced through overexpression of the HRAS gene that induces premature senescence and involves senescence signaling mechanisms similar to that of replicative senescence [114]. Previous studies have shown that overexpression of the HRAS gene induced premature senescent in mammalian cells through downregulation of cell cycle regulators in p53 and $p16^{INK4A}$ dependent manner and thus giving rise to cell cycle arrest [115]. The objective is to establish a time-efficient approach to study the effect of LDR on cellular senescence and to study if OIS can regulate similar molecular pathways that are found in HFL1 cells treated with LDR. This will help us to understand whether OIS can be used as a model to explore the deceleration of senescence by LDR.

To establish a time-efficient assay to study cellular senescence and to study if the LDR rescues the oncogene-induced premature senescence in HFL1 cells, the HRAS v12 gene was overexpressed in an early passage (P7) HFL1 cells through retroviral gene transfer system. The HRAS overexpressing HFL1 cells were selected through puromycin selection and the resultant cells underwent at least two passages before subjecting them to various assays. Figure 13 A shows the overexpression of the endogenous HRAS gene in HFL1 cells. The expression of the HRAS gene is 9- fold higher than in the control (pEmpty) HFL1 cells. Figure 13 B shows the activity of B-galactosidase, senescence marker in HRAS overexpressed (pRas) HFL1 cells. The degree of senescence is significantly higher in HRAS overexpressed (pRas) cells compared to normal and control (pE or pEmpty) HFL1 cells. As stated earlier, the expression of the HRAS gene and its capacity to promote senescence is dependent on $p16^{INK4A}$ expression. Indeed, it was found that $p16^{INK4A}$ was overexpressed in HRAS cells suggesting that HRAS induced senescence via $p16^{INK4A}$ dependent pathway (Figure 13 C). Figure 13 D-F shows microphotographs of senescence detected as SA-b-gal positive cells (stained blue) in non-transduced, control (pEmpty), and HRAS overexpressing (pRas) HFL1 cells.

To study the effect of HRAS gene overexpression on proliferation, the *Incucyte* live imaging system was used to track confluency change in live HFL1 cells over 5 days of growth under normal conditions. Figure 14 shows the proliferative nature of non-transfected, control (pEmpty), HRAS overexpressing (pRas) cells, and non-transfected HFL1 cells treated with puromycin. The concentration of puromycin used for selection is similar to the concentration used for selecting SIRT7 knockdown cells.

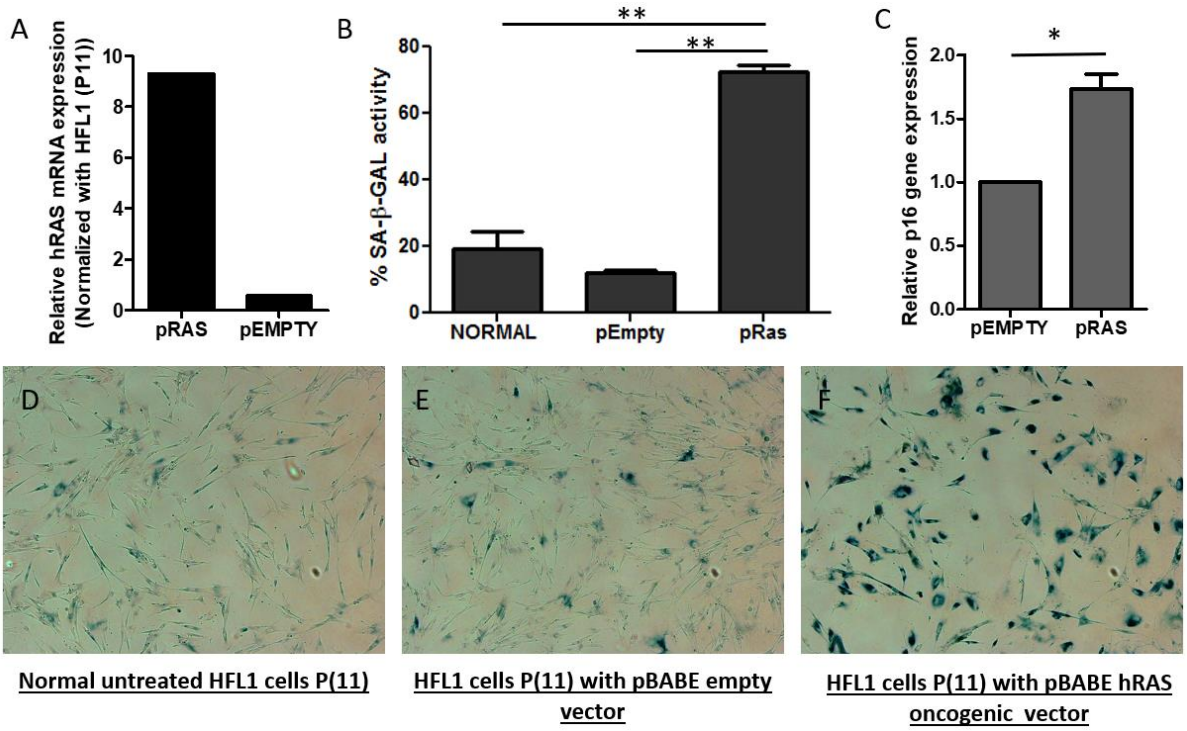

Normal untreated HFL1 cells P(11)

HFL1 cells P(11) with pBABE empty vector

HFL1 cells P(11) with pBABE hRAS oncogenic vector

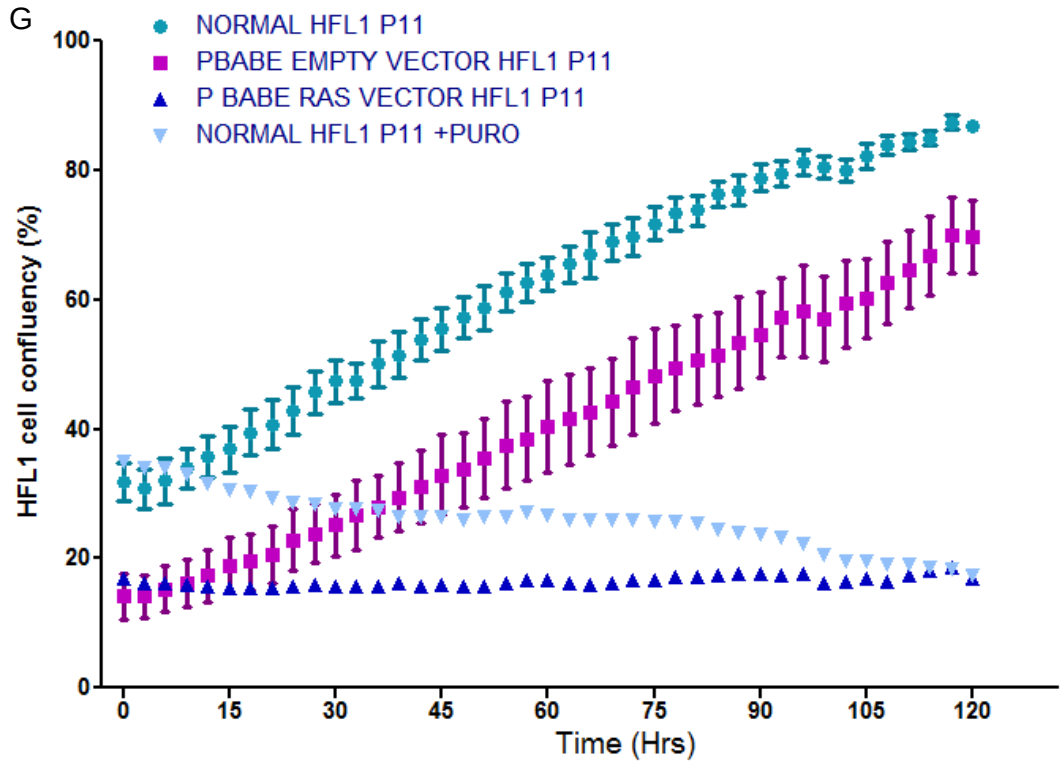

Figure 13: <u>Overexpression of the HRAS gene accelerates senescence in HFL1 cells.</u> A show the HRAS gene expression in HFL1 cells treated with pBABE-HRAS vector and pEmpty vector. **B** shows the SA-β-Gal activity (n=1000 cells) in non-transfected, Control (pEmpty), and HRAS overexpressed (pRas) HFL1 cells (P11). **C** the relative $p16^{INK4A}$ (senescence marker) gene expression in OIS cells. **D-F** is the pictorial representation of SA-β-Gal activity. G shows the proliferation rate of HFL1 cells of each treatment group. Data show the mean ± SEM of two independent biological replicates. Comparison between samples are made using one-way ANOVA with Post-hoc with Tukey's Honestly Significant Difference (HSD); ns – non-significant, * $p<0.05$, ** $p<0.01$.

3.4.1 qPCR array analysis: Differential genes expressed in OIS in HFL1 cells.

To understand how overexpression of the HRAS gene is influencing the senescence genes, Qiagen human cellular senescence qPCR array is used. This assay may reveal the gene circuits involved in driving the premature senescence in HFL1 cells and help in a comparative study of the HRAS gene expression between LDR treated HFL1 cells, and HRAS overexpressed cells (Figure 14). HFL1 cells upon low dose radiation show an increase in HRAS gene expression (Figure 14A). HRAS belongs to Ras subfamily which regulates cellular signaling transduction between cells during premature senescence [116]. HRAS expression controls cellular proliferation and its growth by regulating the cell cycle-associated checkpoint proteins [117], [118]. This data (Figure 14A-C) suggests that, although overexpression of the HRAS gene in HFL1 cells leads to premature senescence while transient upregulation of the HRAS gene could give rise to various signaling cascades that help in triggering cellular mechanisms to rectify the DNA damage induced by the low doses of radiation.

To confirm if the checkpoint genes are involved in driving OIS, the Qiagen human cellular senescence kit is used which contains an array of cell cycle and checkpoint genes influenced in cellular senescence. Figure 14 F and G show various genes affected by HRAS overexpression. The majority of these genes are cell cycle regulators and checkpoint genes as anticipated based on the results of previous studies [115]. Figure 14 H shows that overexpressing HRAS in HFL1 cells leads to the upregulation of $p16^{INK4A}$. This is also proven by other studies where they have shown that senescence induced by HRAS overexpression is dependent on $p16^{INK4A}$ in various human cancer cell lines and fibroblasts. The cells with impaired or loss of $p16^{INK4A}$ gene show resistance to OIS and gene expression of $p16^{INK4A}$ is required to drive cells to OIS through G1 cell cycle arrest. [115], [119]–[121].

Along with cell cycle regulators, genes such as HMGB1, NRF2 is also affected and HRAS overexpression decreases the expression of the SIRT7 gene in these cells. Studies have found that OIS results in cytokine and chemokines secretion as a part of Senescence Associated Secretory Phenotype (SASP) to inhibit the primary cells from transformation [122]–[124]. HMGB1 is one such cytokine that is a member of proteins involved in Damage Associated Molecular Patterns observed during inflammation and in age-related inflammatory diseases [77], [125]–[127]. Figure 14 H shows that the gene expression of HGMB1 is higher in HRAS overexpressing HFL1 cells. This emphasizes that OIS drives senescence through SASP where HGMB1 is one of the secreted cytokines regulating senescence-related cellular signal transduction in HFL1 cells.

Other genes such as FOXO3A and NRF2 also seem to be downregulated in these cells. NRF2 is widely known for its antioxidant role during the cellular stress response and also plays a role in inflammation. This activity of NRF2 declines with ageing[33], [128], [129]. On the other hand, upregulated NRF2 promotes senescence results in maintaining cancer-associated fibroblastic phenotype in vivo suggesting the dual role of NRF2 in fibroblasts [130]. Oncogene overexpression suppresses this function of the NRF2 gene in driving senescence in HFL1 cells. Hence, to identify the altered genes expression between LDR and OIS in HFL1 cells, a comparative qPCR array analysis was made between these two groups and with genes regulated in SIRT7 knockdown HFL1 cells.

The transcriptional profile during replicative senescence in normal HFL1 cells and HRAS overexpression is compared to be able to use OIS as an experimental approach to study radiation hormesis upon LDR in HFL1 cells. Figure 14 E shows that most of the genes that are altered due to HRAS overexpression is commonly shared with the replicative senescence (12 weeks old) HFL1 cells. The common genes are PCNA, CCNB1, RBL1, EGR1, IGFBP3, CDKN2C, CDKN2D, CHEK1, SERPINE1, CDK2, SERPINB2, CCND1, E2F1, ALDH1A3, CCNA2, VIM, ID1, CDC25C and CDKN1C.

Figure 15A-C (in the appendix) shows the genes that are commonly regulated between 10 mGy treated 12-weeks old HFL1 cells, OIS, and SIRT7 knockdown HFL1 cells. Out of 84 genes screened using qPCR array, only 7 genes (SERPINB2, SERPINE1, VIM, CCNB1, CCNE1, CCND1, and IGFBP3) are commonly regulated between SIRT7 knockdown and OIS HFL1 cells (pRAS). SERPINB2 and IGFBP3 show an upregulation and downregulation respectively between the groups while other genes are differentially regulated. This indicates that SIRT7 and HRAS overexpression has its unique regulatory pathways in regulating senescence in HFL1 cells. In comparison, with10 mGy treated HFL1 cells (12 weeks) and OIS HFL1 cells, 20 genes are commonly regulated out of which 15 genes display a similar pattern of regulation between 10 mGy and pRAS HFL1 cells (Figure 15B in the appendix). 5 genes among these are commonly regulated between these groups and SIRT7 knockdown cells (Figure 15C in the appendix).

The major difference between the senescence due to SIRT7 known down and HRAS overexpression is that SIRT7 knockdown in HFL1 cells leads to differential expression of various transcriptional factors such as ETS1, TWIST1, TBX3, SPARC, IRF3 and IRF5 which seems to occur through MAP kinase pathway via upregulation of MAP2K6 gene expression. While HRAS overexpression leads to differentially express a variety of cell cycle regulators and checkpoint genes which is not implicated by SIRT7 loss in HFL1 cells. This could be one of the reasons for the absence of a major overlap between the gene regulation between these two groups. This also emphasizes their unique nature in driving senescence in these cells. Adding to this, SIRT7 knockdown and 10 mGy treated HFL1 cells (12-weeks) share a higher portion of genes which is differentially regulated between them. This indicates that SIRT7 is required for transcriptional expression of various genes that maintain the genome stability leading to delay in senescence and thus suppressing SASPs. This is consistent which another study where SIRT7 is reported to protect the cells from cellular stress by maintaining the genome stability [75].

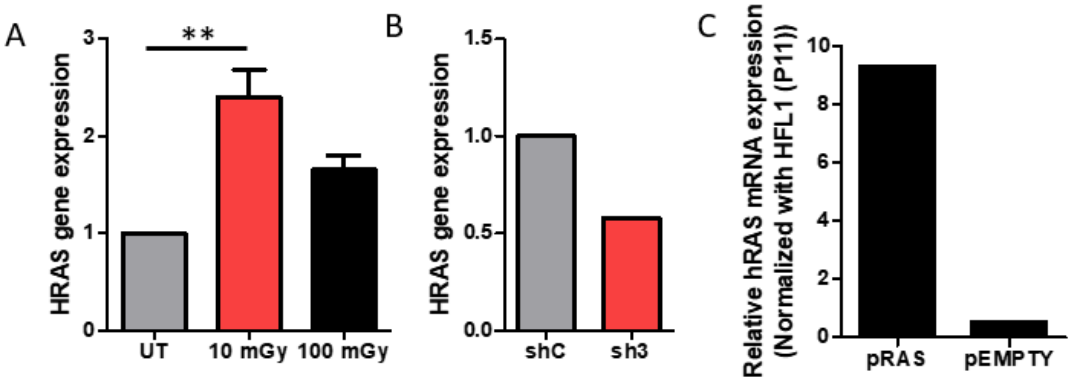
A
**
HRAS gene expression
3
2
1
0
UT
10 mGy
100 mGy
B
HRAS gene expression
1.5
1.0
0.5
0.0
shC
sh3
C
Relative hRAS mRNA expression
(Normalized with HFL1 (P11))
10
8
6
4
2
0
pRAS
pEMPTY

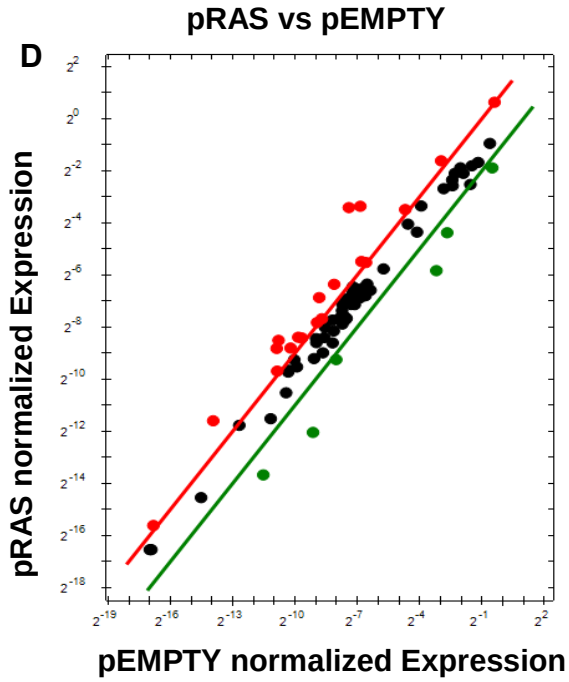
pRAS vs pEMPTY
D
pRAS normalized Expression
pEMPTY normalized Expression

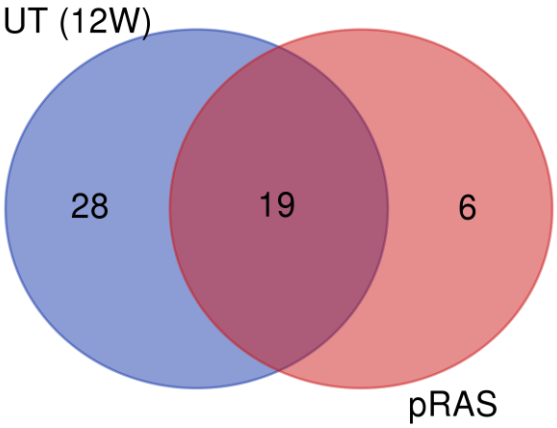
E
UT (12W)
28
19
6
pRAS

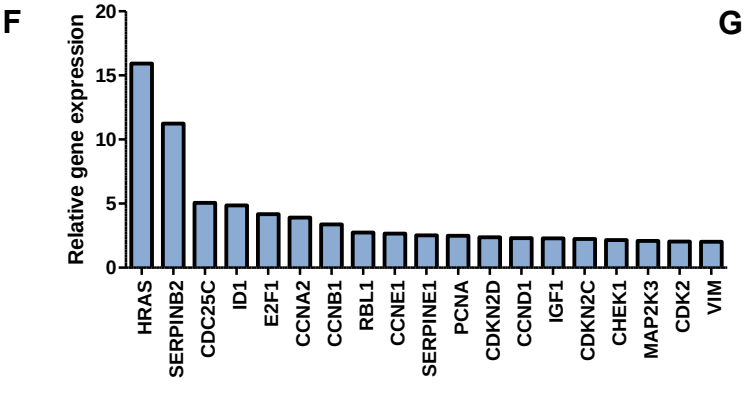
F
Relative gene expression
20
15
10
5
0
HRAS
SERPINB2
CDC25C
ID1
E2F1
CCNA2
CCNB1
RBL1
CCNE1
SERPINE1
PCNA
CDKN2D
CCND1
IGF1
CDKN2C
CHEK1
MAP2K3
CDK2
VIM

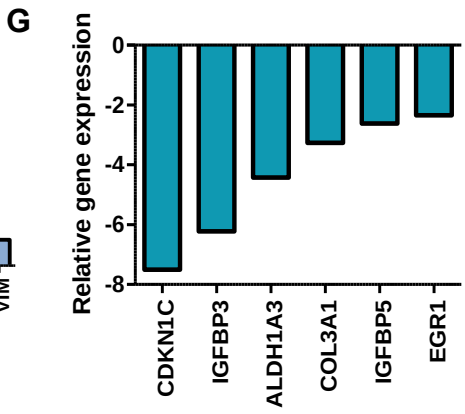
G
Relative gene expression
0
-2
-4
-6
-8
CDKN1C
IGFBP3
ALDH1A3
COL3A1
IGFBP5
EGR1

H

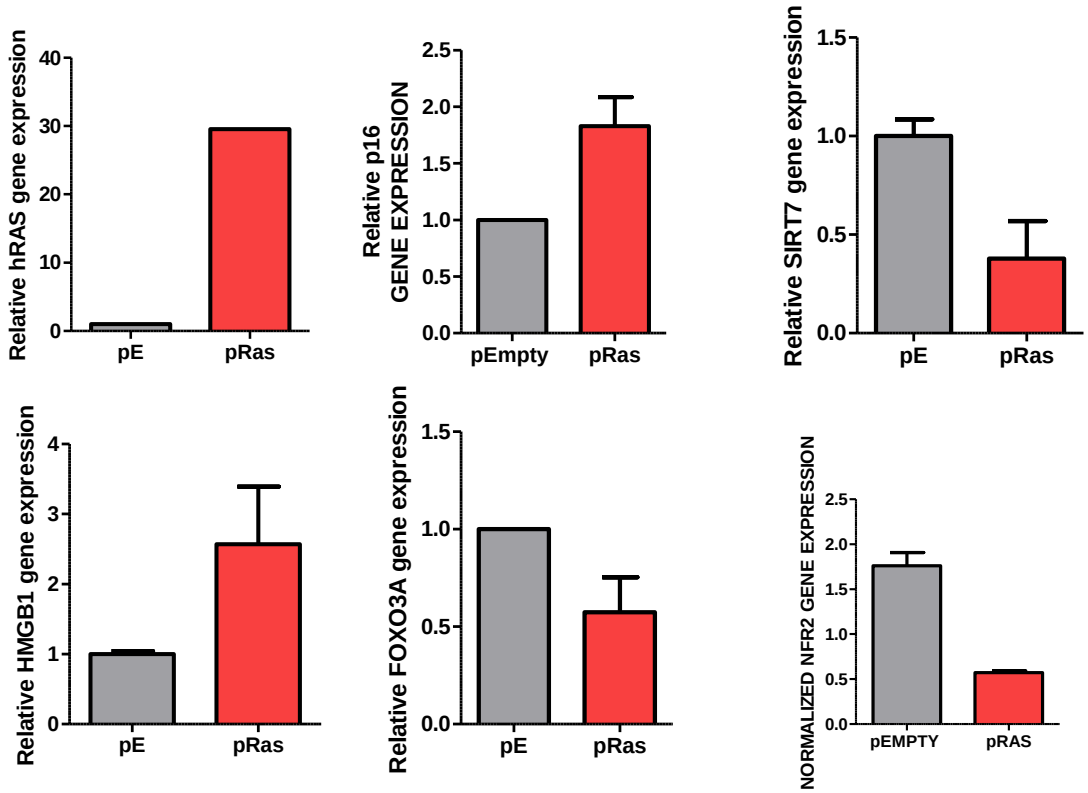

Figure 14: <u>Overexpression of the HRAS gene drives senescence in HFL1 cells through regulating genes associated with checkpoints and cell cycle regulators</u>. Fig 14 A-C shows relative HRAS expression in HFL1 cells treated with LDR; SIRT7 knockdown HFL1 cells and HRAS overexpressed cells. **Fig 14 D** shows the distribution plot of the top hit genes in OIS cells screened using Qiagen 384 well qPCR array. **Fig 14 E** shows the commonly regulated genes between 12 weeks old and in HRAS overexpressed HFL1 cells. **Fig 14 F-G** shows upregulated and downregulated genes in OIS HFL1 cells respectively. **Fig 14 H** shows the expression of genes selected through literature review, between control (pEmpty) and HRAS overexpressed (pRas) HFL1 cells. Error bars derived from Mean ± S.E.M of technical replicates of two independent replicates. * $p<0.05$; ** $p<0.01$.

Chapter 4 : DISCUSSION

Previously in the lab, a delay in senescence of HELF 104 (human embryonic lung fibroblasts) has been demonstrated following exposure to low doses of gamma radiation. Compared to high dose exposure (2 Gy), low doses of radiation such as 30 and 50 mGy also resulted these cells retain its proliferative nature [60], [131]. This has led me to question the molecular pathways and genes that are triggered in response to low doses of radiation resulting in these potential hormesis effects. The main objective of my study was to validate the delay in cellular senescence in human fetal lung fibroblasts (HFL1) cells and to identify genes and molecular pathways that mediate this phenomenon. Using Senescence Associated – β – Galactosidase assay, a deceleration in senescence is observed in HFL1 cells at 12 weeks post-irradiation with 10mGy compared to untreated or cells exposed to 100 mGy of gamma radiation (Fig 6 A-C). Similar results were reported in muscle stem cells and human fibroblasts upon LDR [132]. This capability of LDR to trigger various defense mechanisms to cope with the radiation damage may result in a delay in cellular senescence.

Since delay of senescence is evident in LDR exposed HFL1 cells as they age, I was interested in examining the changes induced in transcriptional profile caused by 10 mGy of radiation in HFL1 cells. This could reveal genes that are differentially expressed upon LDR to delay senescence in this cell's aging. For this, the expression of 84 senescence-associated genes was analyzed at different time points post-exposure using Qiagen 384 well qPCR array. Fig 7 and Table 3 (in Appendix) show the regulation of differentially expressed genes in HFL1 cells irradiated with gamma radiation.

Among 84 senescence-associated genes screened, HFL1 cells (1-week post-irradiation) showed 6 genes commonly regulated between the dose groups (Figure 7 C and D). It is also observed that a higher portion of genes is regulated in HFL1 cells treated with 10 mGy. This subset of genes might give rise to further transcriptional changes in subsequent cellular division leading to a hormesis

response (delay in senescence) in HFL1 cells 12-weeks after 10 mGy of radiation. Most of the genes that are differentially regulated by 10 mGy (1-week post-irradiation) belong to the family of MAP kinases, Insulin-like Growth Factors (IGF), and various transcriptional factors. This indicates that HFL1 cells are more responsive to 10 mGy than 100 mGy of radiation. According to the LNT model, this effect should be dose-dependent and a much higher proportion of genes should be regulated at 100 mGy. This suggests the potential existence of a threshold dose below which such radio adaptive responses can be observed where LDR could not be detrimental to HFL1 cells. This inconsistency in the LNT model is also addressed by studies using other cellular parameters [134]–[136]. Similarly, at 12-weeks post-irradiation, HFL1 cells treated with 10 mGy showed larger transcriptional regulation (62 genes) compared to 100 mGy (31 genes). 22 genes are commonly regulated between the dose groups at this time point. Most of these genes are from the family of transcriptional factors and cell cycle regulators.

Cellular senescence is a major driving factor of aging in humans. Many protein families specifically play a role in regulating senescence. One such protein family is Sirtuins. SIRT7 belongs to this family of proteins and is the least explored in terms of its role in cellular senescence [66], [67]. Strikingly, many studies have reported the role of SIRT7 in maintaining genome stability during environmental stress through participating in DNA repair pathways [66], [75], [137]. As ionization radiation exposure compromises the cellular genome stability, studying the role of SIRT7 upon LDR in HFL1 cells, especially in delaying senescence, would help in understanding pathways and identify their downstream targets for regulating senescence. Figure 8 shows that 10 mGy of radiation induces SIRT7 gene expression in HFL1 cells 12-weeks post-irradiation. Similar expression changes were also observed for genes selected through a literature review; these genes play a major role in regulating cellular senescence. Another observation is that 10 mGy also upregulated p16INK4A gene expression which is a counterintuitive observation given an established role of this gene as a promoter of cellular senescence and its wide use as a marker of

senescence. Interestingly, however, it was reported previously that $p16^{INK4A}$ /CDKN2A is required for initiating anti-inflammatory response resulting in clearance of senescent cells, suggesting a non-canonical anti-senescence role of p16. Also, the expression of CDKN2A is observed very early in the wound healing process and result in tissue remodeling in mesenchymal stem cells [138]. This evidence suggests a role of $p16^{INK4A}$ in normal cells inducing a protective bystander senescence by triggering anti-inflammatory pathways [139]. Our results highlight the complexity of molecular regulation of senescence and the possibility to suppress senescence without suppressing the p16 gene and associated circuits. The latter may have important implications in future anti-aging clinical interventions since p16 may have an important anti-cancer role which should not be compromised.

Another notable gene that was implicated by LDR is IL6, a secreted cytokine responsible for eliciting SASP during inflammation and playing a role in age-related inflammatory diseases [36], [48], [140]. LDR suppresses the expression of IL6 in HFL1 cells 12-weeks post-irradiation. This suggests that LDR may be used as an alternative for treating age-related inflammatory diseases such as arthritis. Elevated IL6 expression is also observed in COVID-19 patients in the recent pandemic [49]. LDR could be used as an alternative intervention to treat the patients suffering from the "cytokine storm" in the lung epithelium and requiring intense care. HMGB1, another secretory cytokine; NRF2 and Mn SOD2, plays a role in antioxidant activities and was also upregulated upon 10 mGy radiation. All these differentially expressed genes upon 10 mGy led to the deceleration of senescence in HFL1 cells. Further investigation of these genes through functional studies could reveal precise pathways through which they regulate the delay of senescence in HFL1 cells. Knocking down SIRT7 in HFL1 cells resulting in accelerated senescence in these cells and proliferation is also observed to be affected compared to the control (Figure 11).

To identify genes that drive senescence in SIRT7 knockdown cells, qPCR array, and individual qPCRs were performed (Figure 12 A-E). Notably, in the absence of SIRT7, SERPINB2 is highly upregulated compared to control (shC) cells. SERPINB2 is one of the potent inhibitors of the PLAU/uPA gene which is upregulated in 12-week old HFL1 cells but apart from this role, SERPINB2 has other distinct roles in regulating cellular senescence. It is known to maintain senescence by regulating p21 expression in senescent cells [141]. In nasopharyngeal carcinoma cells, its overexpression induces G2/M cell cycle arrest and halts cellular proliferation [142]. Also, in the presence of LDR and SIRT7 knockdown (Table 3 in Appendix and figure 9) SERBINB2 gene expression does not seem to inhibit PLAU gene expression and SIRT7 may be required to modulate its mRNA level for the proper proliferation of old HFL1 cells. Another observation shown in Figure 12 B and C is that of gene IGFBP3 which is highly downregulated in SIRT7 knockdown cells, consistent with previous studies where low IGFBP3 expression was shown to be a cellular senescence marker [84]. IGFBP3 is reported to interact with Plasminogen Activator Inhibitor-1 (PAI-1)/SERPINE1 during stress-induced cellular response to induce senescence in human lung fibroblast cells [143]. Similar to the activity of SERPINE1 (Figure 12 C and D), a novel regulatory role of SERPINB2/PAI-2 and IGFBP3 is suggested. In the absence of SIRT7 and $p16^{INK4A}$, higher expression of SERPINB2 might inhibit the expression of IGFBP3 driving senescence in HFL1 cells through NF-kB signaling as sirtuin proteins mediate many cellular processes through this signaling pathway.

Elevated expression of SERPINB2 can also lead to its extracellular secretion resulting in regulating secretory signaling cascades such as upregulation of HMGB1 (Figure 12F), a cytokine mostly secreted by macrophages play a role in inflammation in relative to cellular senescence [12], [77], [110]. Figure 12 E shows the overlapping genes between HFL1 cells 12 weeks post-irradiation of 10 mGy and SIRT7 knockdown cells. Although, 21 genes are commonly regulated between these groups. Among these, genes such as TWIST1, PRKCD, CDK6, CDKN2B, CDKN2A, CDKN1A,

SOD2, MYC, CCNE1, CCND1, IGFBP7 are regulated in the presences of SIRT7 gene expression. Hence, regulation of genes by SIRT7 might play a role in delaying senescence in HFL1 cells upon LDR, it is worth noting that the gene expression changes discussed above were found using one biological replicate, therefore more replicates and further validation of the identified genes are needed to confirm their role in regulating cellular senescence in HFL1 cells.

Another class of proteins called Ras proteins, induce senescence as a fail-proof mechanism to prevent normal cells from becoming transformed tumor cells. This class of proteins belongs to the oncogene family that includes HRAS; KRAS and NRAS. Elevated expression of the HRAS gene in normal cells results in cellular senescence in various cells including cancer cell lines. HRAS modulates senescence mostly by halting the cell cycle progression by regulating the expression of checkpoint and cell cycle regulatory genes through p53 or $p16^{INK4A}$ pathways [120]. Studies have shown that the upregulation of HRAS also results in improved DNA repair and immune response post-radiation [117], [118]. The results presented in Figures 14 A-B and G show the HRAS expression profile in HFL1 cells subjected to LDR and in SIRT7- knockdown HFL1 cells which shows that HRAS gene expression is significantly upregulated in the presence of SIRT7 endogenous gene expression this also could play a role delaying senescence in these cells as HRAS is also reported to regulate DNA repair mechanisms.

OIS (Figure 5B) is a time-efficient experimental approach compared to the one using replicative senescence that takes months to complete a single experiment (e.g. see the time frame in Figure 4 that goes up to 12 weeks). HRAS is overexpressed in HFL1 cells to accelerate senescence and perform a comparative study of the transcriptional profile between LDR and OIS. Figure 14 A-G shows that the HRAS overexpression (pRas) is 9-fold higher than the control of HFL1 cells (pEmpty) and the HRAS overexpression accelerates senescence in these cells. This occurs through the induction of p16 INK4A gene (Figure 14 C). Consistent with the results of other studies,

p16^{INK4A} is also elevated in pRas HFL1 cells with a higher degree of senescence, and proliferation is largely suppressed [120].

The qPCR array results and individual qPCR analysis also show that majority of genes that are affected by the overexpression of HRAS are those involved in cell cycle and checkpoint regulation (Figure 14 F-H). It is also shown that HRAS gene expression is significantly upregulated upon LDR (Figure 14A). Further studies are required with more biological replicates to test if OIS model through HRAS overexpression can be used to study the Hormesis effect of LDR in HFL1 cells. This includes

- Altered gene expression due to replicative senescence alone in 12 weeks old HFL1 cells and compare them with the genes altered in OIS model.
- If LDR or specifically 10 mGy has any significant effect such as suppression of senescence due to HRAS overexpression.

Although many genes are commonly shared between pRAS overexpression and 10 mGy treated HFL1 cells, the above-mentioned points need to be addressed as well as more replicates are needed for HRAS overexpression cells to find significantly regulated genes between the dose groups (Figure 15C in the appendix). This will help in understanding the molecular pathways of OIS in HFL1 cells and whether LDR has a significant effect on these pathways. This is crucial to apply OIS as a model to study the beneficial effects of LDR. Also, as the exposure to LDR delays replicative senescence in HFL1 cells and an overlap in molecular pathways between LDR effects on senescence and OIS itself needs to studied well in detail (Figure 14 E) to use OIS model in this study. In this way, OIS could be represented as a valuable experimental tool that will allow the identification of molecular mechanisms of LDR-induced suppression of cellular aging. These insights may have the potential to become a foundation for prospective therapies of aging-related diseases using LDR.

CONCLUSION:

My study aims to validate the existence of radiation hormesis with respect to delayed aging in human fetal lung fibroblasts and to study the regulatory molecular pathways correlating with the potential beneficial effects of low dose radiation. In this study, I observed deceleration in senescence in HFL1 cells exposed to low dose radiation and identified a unique transcriptional profile regulated by 10 mGy of radiation. Functional studies of these genes identified through the qPCR array and individual qPCRs revealed various pathways and downstream targets contributing to the delay in senescence by LDR that I measured. SIRT7 gene expression is significantly upregulated and shown to regulate cellular senescence in HFL1 cells by interacting with many transactional factors through knockdown studies in HFL1 cells. Further studies are needed to understand the pathways through which the SIRT7 gene could mediate a delay of senescence in HFL1 cells upon LDR.

Cellular senescence is regulated through secretion of cytokines such as IL6, IL8, and HMGB1 which involved in signal transductions to regulate senescence in neighboring cells. As these genes are also differentially regulated during LDR, and implicated in many age-related inflammatory diseases, understanding the biochemical association between Senescence Associated Secretory Phenotypes (SASPs) and LDR will lead to its application in the clearance of senescent cells in these ailments. Adding to this, Oncogene Induced Senescence (OIS) could be an alternative model to investigate the effect of LDR on SASPs. In this study, I found that OIS induces gene expression changes in various cell cycle and checkpoint genes. It is widely known to induce senescence through SASP secretions in primary cells and in cancer models to terminate transformation and cancer progression. Hence, OIS could be used as a model to understand the effect of LDR on these inflammatory pathways induced by SASPs and to use low dose radiation for treating aging and age-related diseases such as atherosclerosis.

REFERENCES:

[1] "Ionizing radiation, health effects and protective measures." [Online]. Available: https://www.who.int/news-room/fact-sheets/detail/ionizing-radiation-health-effects-and-protective-measures. [Accessed: 23-Apr-2020].

[2] E. Rosen *et al.*, "Acute total body ionizing gamma radiation induces long-term adverse effects and immediate changes in cardiac protein oxidative carbonylation in the rat," *PLoS One*, vol. 15, no. 6, p. e0233967, Jun. 2020, doi: 10.1371/journal.pone.0233967.

[3] C. Bredeson *et al.*, "Prospective cohort study comparing intravenous busulfan to total body irradiation in hematopoietic cell transplantation," *Blood*, vol. 122, no. 24, pp. 3871–3878, Dec. 2013, doi: 10.1182/blood-2013-08-519009.

[4] M. C. Benyunes *et al.*, "Cataracts after bone marrow transplantation: Long-term follow-up of adults treated with fractionated total body irradiation," *Int. J. Radiat. Oncol. Biol. Phys.*, vol. 32, no. 3, pp. 661–670, Jun. 1995, doi: 10.1016/0360-3016(94)00392-X.

[5] L. Koval, E. Proshkina, M. Shaposhnikov, and A. Moskalev, "The role of DNA repair genes in radiation-induced adaptive response in Drosophila melanogaster is differential and conditional," *Biogerontology*, vol. 21, no. 1, pp. 45–56, Feb. 2020, doi: 10.1007/s10522-019-09842-1.

[6] L. B. Zablotska, M. P. Little, and R. J. Cornett, "Original Contribution Potential Increased Risk of Ischemic Heart Disease Mortality With Significant Dose Fractionation in the Canadian Fluoroscopy Cohort Study," 2013, doi: 10.1093/aje/kwt244.

[7] S. Sutou, "Black rain in Hiroshima: A critique to the Life Span Study of A-bomb survivors, basis of the linear no-threshold model," *Genes and Environment*, vol. 42, no. 1. BioMed Central Ltd., 31-Dec-2019, doi: 10.1186/s41021-019-0141-8.

[8] E. J. Calabrese, "Hormetic mechanisms," *Critical Reviews in Toxicology*, vol. 43, no. 7. pp.

580–606, Aug-2013, doi: 10.3109/10408444.2013.808172.

[9] M. Doss, “Are we approaching the end of the linear no-threshold era?,” *J. Nucl. Med.*, vol. 59, no. 12, pp. 1786–1793, Dec. 2018, doi: 10.2967/jnumed.118.217182.

[10] L. Zhou *et al.*, “Validating the pivotal role of the immune system in low-dose radiation-induced tumor inhibition in Lewis lung cancer-bearing mice,” *Cancer Med.*, vol. 7, no. 4, pp. 1338–1348, Apr. 2018, doi: 10.1002/cam4.1344.

[11] H. S. Yu, Z. M. Liu, X. Y. Yu, A. Q. Song, N. Liu, and H. Wang, “Low-dose Radiation Induces Antitumor Effects and Erythrocyte System Hormesis,” *Asian Pacific J. Cancer Prev.*, vol. 14, no. 7, pp. 4121–4126, 2013, doi: 10.7314/APJCP.2013.14.7.4121.

[12] Anuranjani and M. Bala, “Concerted action of Nrf2-ARE pathway, MRN complex, HMGB1 and inflammatory cytokines - Implication in modification of radiationdamage,” *Redox Biology*, vol. 2, no. 1. Elsevier B.V., pp. 832–846, 2014, doi: 10.1016/j.redox.2014.02.008.

[13] M. E. Lomax, L. K. Folkes, and P. O’Neill, “Biological consequences of radiation-induced DNA damage: Relevance to radiotherapy,” *Clin. Oncol.*, vol. 25, no. 10, pp. 578–585, Oct. 2013, doi: 10.1016/j.clon.2013.06.007.

[14] M. Falk, E. Lukasova, and S. Kozubek, “Higher-order chromatin structure in DSB induction, repair and misrepair,” *Mutation Research - Reviews in Mutation Research*, vol. 704, no. 1–3. pp. 88–100, Apr-2010, doi: 10.1016/j.mrrev.2010.01.013.

[15] J. A. Anderson, J. V. Harper, F. A. Cucinotta, and P. O’Neill, “Participation of DNA-PKcs in DSB Repair after Exposure to High- and Low-LET Radiation,” *Radiat. Res.*, vol. 174, no. 2, pp. 195–205, Aug. 2010, doi: 10.1667/rr2071.1.

[16] K. Rothkamm and M. Löbrich, “Evidence for a lack of DNA double-strand break repair in human cells exposed to very low x-ray doses,” *Proc. Natl. Acad. Sci. U. S. A.*, vol. 100, no. 9, pp. 5057–5062, Apr. 2003, doi: 10.1073/pnas.0830918100.

[17] M. L. Hipp and G. Bauer, “Intercellular induction of apoptosis in transformed cells does not depend on p53,” *Oncogene*, vol. 15, no. 7, pp. 791–797, 1997, doi: 10.1038/sj.onc.1201247.

[18] C. Mothersill and C. Seymour, “Radiation-induced bystander effects: Evidence for an adaptive response to low dose exposures?,” in *Abstracts of the Pacific Basin Nuclear Conference*, 2004, vol. 4, no. 4, p. 103, doi: 10.2203/dose-response.06-111.mothersill.

[19] J. Hou, F. Wang, P. Kong, P. K. N. Yu, H. Wang, and W. Han, “Gene Profiling Characteristics of Radioadaptive Response in AG01522 Normal Human Fibroblasts,” *PLoS One*, vol. 10, no. 4, p. e0123316, Apr. 2015, doi: 10.1371/journal.pone.0123316.

[20] K. Premkumar, J. Nair, and B. S. Shankar, “Differential radio-adaptive responses in BALB/c and C57BL/6 mice: pivotal role of calcium and nitric oxide signalling,” *Int. J. Radiat. Biol.*, vol. 95, no. 6, pp. 655–666, Jun. 2019, doi: 10.1080/09553002.2019.1571647.

[21] K. Ogura, J. Magae, Y. Kawakami, and T. Koana, “Reduction in Mutation Frequency by Very Low-Dose Gamma Irradiation of Drosophila melanogaster Germ Cells,” *Radiat. Res.*, vol. 171, no. 1, pp. 1–8, Jan. 2009, doi: 10.1667/rr1288.1.

[22] C. M. Somers, J. Quinn, C. M. Somers, R. Sharma, J. S. Quinn, and D. R. Boreham, “Gamma radiation-induced heritable mutations at repetitive DNA loci in out-bred mice Food web structure and bioaccumulation in Great Lakes piscivorous migratory birds View project Vocal Communication in Smooth-billed Anis View project Gamma radiation-induced heritable mutations at repetitive DNA loci in out-bred mice,” *Mutat. Res.*, vol. 568, pp. 69–78, 2004, doi: 10.1016/j.mrfmmm.2004.06.047.

[23] E. I. Azzam, G. P. Raaphorst, and R. E. Mitchel, “Radiation-induced adaptive response for protection against micronucleus formation and neoplastic transformation in C3H 10T1/2 mouse embryo cells.,” *Radiat. Res.*, vol. 138, no. 1 Suppl, pp. S28-31, Apr. 1994.

[24] E. Elmore, X.-Y. Lao, R. Kapadia, E. Giedzinski, C. Limoli, and J. L. Redpath, “ Low Doses

of Very Low-Dose-Rate Low-LET Radiation Suppress Radiation-Induced Neoplastic Transformation In Vitro and Induce an Adaptive Response ," *Radiat. Res.*, vol. 169, no. 3, pp. 311–318, Mar. 2008, doi: 10.1667/rr1199.1.

[25] B. Kadenbach, R. Ramzan, and S. Vogt, "Degenerative diseases, oxidative stress and cytochrome c oxidase function," *Trends Mol. Med.*, vol. 15, no. 4, pp. 139–147, Apr. 2009, doi: 10.1016/j.molmed.2009.02.004.

[26] R. Wetzker and I. Rubio, "Hormetic signaling patterns," *Dose-Response*, vol. 10, no. 1, pp. 83–90, 2012, doi: 10.2203/dose-response.11-012.Wetzker.

[27] D. R. Spitz, E. I. Azzam, J. J. Li, and D. Gius, "Metabolic oxidation/reduction reactions and cellular responses to ionizing radiation: A unifying concept in stress response biology," *Cancer and Metastasis Reviews*, vol. 23, no. 3–4. pp. 311–322, Aug-2004, doi: 10.1023/B:CANC.0000031769.14728.bc.

[28] M. Large *et al.*, "Study of the Anti-Inflammatory Effects of Low-Dose Radiation: The Contribution of Biphasic Regulation of the Antioxidative System in Endothelial Cells.," *Strahlentherapie und Onkol.*, vol. 191, no. 9, pp. 742–749, Sep. 2015, doi: 10.1007/s00066-015-0848-9.

[29] D. I. Portess, G. Bauer, M. A. Hill, and P. O'Neill, "Low-dose irradiation of nontransformed cells stimulates the selective removal of precancerous cells via intercellular induction of apoptosis," *Cancer Res.*, vol. 67, no. 3, pp. 1246–1253, Feb. 2007, doi: 10.1158/0008-5472.CAN-06-2985.

[30] N. Aneva *et al.*, "Inflammatory profile dysregulation in nuclear workers occupationally exposed to low-dose gamma radiation," *J. Radiat. Res.*, pp. 1–12, 2019, doi: 10.1093/jrr/rrz059.

[31] B. Poljsak and I. Milisav, "Aging, Oxidative Stress and Antioxidants," in *Oxidative Stress*

and Chronic Degenerative Diseases - A Role for Antioxidants, InTech, 2013.

[32] M. Ohtsuji, F. Katsuoka, A. Kobayashi, H. Aburatani, J. D. Hayes, and M. Yamamoto, "Nrf1 and Nrf2 play distinct roles in activation of antioxidant response element-dependent genes," *J. Biol. Chem.*, vol. 283, no. 48, pp. 33554–33562, Nov. 2008, doi: 10.1074/jbc.M804597200.

[33] E. K. Lee *et al.*, "Low-dose radiation activates Nrf1/2 through reactive species and the Ca2+/ERK1/2 signaling pathway in human skin fibroblast cells," *BMB Rep.*, vol. 46, no. 5, pp. 258–263, 2013, doi: 10.5483/BMBRep.2013.46.5.199.

[34] S. Sharma, N. Singla, V. D. Chadha, and D. K. Dhawan, "A concept of radiation hormesis. Stimulation of antioxidant machinery in rats by low dose ionizing radiation," *Hell. J. Nucl. Med.*, vol. 22, no. 1, pp. 43–48, 2019, doi: 10.1967/s002449910958.

[35] G. Bauer, "Low dose radiation and intercellular induction of apoptosis: Potential implications for the control of oncogenesis," *International Journal of Radiation Biology*, vol. 83, no. 11–12. pp. 873–888, 2007, doi: 10.1080/09553000701727523.

[36] B. Dieriks, W. H. De Vos, H. Derradji, S. Baatout, and P. Van Oostveldt, "Medium-mediated DNA repair response after ionizing radiation is correlated with the increase of specific cytokines in human fibroblasts," *Mutat. Res. - Fundam. Mol. Mech. Mutagen.*, vol. 687, no. 1–2, pp. 40–48, May 2010, doi: 10.1016/j.mrfmmm.2010.01.011.

[37] H. NAKATSUKASA, M. TSUKIMOTO, Y. OHSHIMA, F. TAGO, A. MASADA, and S. KOJIMA, "Suppressing Effect of Low-Dose Gamma-Ray Irradiation on Collagen-Induced Arthritis," *J. Radiat. Res.*, vol. 49, no. 4, pp. 381–389, 2008, doi: 10.1269/jrr.08002.

[38] D. Hladik *et al.*, "Creb signaling mediates dose-dependent radiation response in the murine hippocampus two years after total body exposure," *J. Proteome Res.*, 2019, doi: 10.1021/acs.jproteome.9b00552.

[39] Y. Shibamoto and H. Nakamura, “Overview of biological, epidemiological, and clinical evidence of radiation hormesis,” *International Journal of Molecular Sciences*, vol. 19, no. 8. MDPI AG, 13-Aug-2018, doi: 10.3390/ijms19082387.

[40] W. Chen *et al.*, “Low-dose gamma-irradiation inhibits il-6 secretion from human lung fibroblasts that promotes bronchial epithelial cell transformation by cigarette-smoke carcinogen,” *Carcinogenesis*, vol. 33, no. 7, pp. 1368–1374, Jul. 2012, doi: 10.1093/carcin/bgs159.

[41] V. R. Bruce *et al.*, “Low-dose gamma-radiation inhibits benzo[A]pyrene-induced lung adenoma development in A/J mice,” *Dose-Response*, vol. 10, no. 4, pp. 516–526, 2012, doi: 10.2203/dose-response.12-040.Bruce.

[42] A. Cheda, J. Wrembel-Wargocka, E. Lisiak, E. M. Nowosielska, M. Marciniak, and M. K. Janiak, “Single Low Doses of X Rays Inhibit the Development of Experimental Tumor Metastases and Trigger the Activities of NK Cells in Mice,” *Radiat. Res.*, vol. 161, no. 3, pp. 335–340, Mar. 2004, doi: 10.1667/rr3123.

[43] H. Hayase, Y. Ohshima, M. Takahashi, and S. Kojima, “The enhancement of Th1 immunity and the suppression of tumour growth by low-dose γ-radiation,” *Int. J. Low Radiat.*, vol. 5, no. 4, pp. 275–289, 2008, doi: 10.1504/IJLR.2008.020977.

[44] M. Tsukimoto, H. Nakatsukasa, K. Sugawara, K. Yamashita, and S. Kojima, “Repeated 0.5-Gy γ Irradiation Attenuates Experimental Autoimmune Encephalomyelitis with Up-regulation of Regulatory T Cells and Suppression of IL17 Production,” *Radiat. Res.*, vol. 170, no. 4, pp. 429–436, Oct. 2008, doi: 10.1667/rr1352.1.

[45] J. Xue, J. H. Dong, G. D. Huang, X. F. Qu, G. Wu, and X. R. Dong, “NF-κB signaling modulates radiation-induced microglial activation,” *Oncol. Rep.*, vol. 31, no. 6, pp. 2555–2560, 2014, doi: 10.3892/or.2014.3144.

[46] R. Yahyapour *et al.*, “Radiation-induced inflammation and autoimmune diseases,” *Mil. Med. Res.*, vol. 5, no. 1, p. 9, Dec. 2018, doi: 10.1186/s40779-018-0156-7.

[47] D. D. Brand, K. A. Latham, and E. F. Rosloniec, “Collagen-induced arthritis,” *Nat. Protoc.*, vol. 2, no. 5, pp. 1269–1275, May 2007, doi: 10.1038/nprot.2007.173.

[48] H. Nakatsukasa, M. Tsukimoto, A. Tokunaga, and S. Kojima, “Repeated Gamma Irradiation Attenuates Collagen-Induced Arthritis via Up-regulation of Regulatory T Cells but not by Damaging Lymphocytes Directly,” *Radiat. Res.*, vol. 174, no. 3, pp. 313–324, Sep. 2010, doi: 10.1667/rr2121.1.

[49] C. Huang *et al.*, “Clinical features of patients infected with 2019 novel coronavirus in Wuhan, China,” *Lancet*, vol. 395, no. 10223, pp. 497–506, Feb. 2020, doi: 10.1016/S0140-6736(20)30183-5.

[50] B. LM, D. EJ, S. E, G. S, and M. S, “COVID-19 Autopsies, Oklahoma, USA,” *Am. J. Clin. Pathol.*, vol. 153, no. 6, 2020, doi: 10.1093/AJCP/AQAA062.

[51] J. Gu, B. Han, and J. Wang, “COVID-19: Gastrointestinal Manifestations and Potential Fecal–Oral Transmission,” *Gastroenterology*, vol. 158, no. 6. W.B. Saunders, pp. 1518–1519, 01-May-2020, doi: 10.1053/j.gastro.2020.02.054.

[52] P. Verdecchia, C. Cavallini, A. Spanevello, and F. Angeli, “The pivotal link between ACE2 deficiency and SARS-CoV-2 infection,” *European Journal of Internal Medicine*, vol. 76. Elsevier B.V., 2020, doi: 10.1016/j.ejim.2020.04.037.

[53] Q. Ruan, K. Yang, W. Wang, L. Jiang, and J. Song, “Clinical predictors of mortality due to COVID-19 based on an analysis of data of 150 patients from Wuhan, China,” *Intensive Care Medicine*, vol. 46, no. 5. Springer, pp. 846–848, 01-May-2020, doi: 10.1007/s00134-020-05991-x.

[54] S. Dong *et al.*, “Repeated 0.2-Gy γ-Ray Irradiation Attenuates the Inflammatory Process

and Endotoxin Damage Induced by Lipopolysaccharides," *Dose-Response*, vol. 17, no. 2, Apr. 2019, doi: 10.1177/1559325819836355.

[55] L. Hayflick, "The limited in vitro lifetime of human diploid cell strains," *Exp. Cell Res.*, vol. 37, no. 3, pp. 614–636, 1965, doi: 10.1016/0014-4827(65)90211-9.

[56] A. Takashima and D. V. Faller, "Targeting the RAS oncogene," *Expert Opinion on Therapeutic Targets*, vol. 17, no. 5. NIH Public Access, pp. 507–531, May-2013, doi: 10.1517/14728222.2013.764990.

[57] Z. Tu *et al.*, "Oncogenic Ras Regulates BRIP1 Expression to Induce Dissociation of BRCA1 from Chromatin, Inhibit DNA Repair, and Promote Senescence," *Dev. Cell*, vol. 21, no. 6, pp. 1077–1091, Dec. 2011, doi: 10.1016/j.devcel.2011.10.010.

[58] M. Rhinn, B. Ritschka, and W. M. Keyes, "Cellular senescence in development, regeneration and disease," *Dev.*, vol. 146, no. 20, Oct. 2019, doi: 10.1242/dev.151837.

[59] D. J. Lowe *et al.*, "Chronic irradiation of human cells reduces histone levels and deregulates gene expression," *Sci. Rep.*, vol. 10, no. 1, Dec. 2020, doi: 10.1038/s41598-020-59163-4.

[60] I. O. Velegzhaninov, A. V. Ermakova, and D. Y. Klokov, "Low dose ionizing irradiation suppresses cellular senescence in normal human fibroblasts," *Int. J. Radiat. Biol.*, vol. 94, no. 9, pp. 825–828, Sep. 2018, doi: 10.1080/09553002.2018.1492167.

[61] M. Pustovalova *et al.*, "Residual γH2AX foci induced by low dose x-ray radiation in bone marrow mesenchymal stem cells do not cause accelerated senescence in the progeny of irradiated cells," *Aging (Albany. NY).*, vol. 9, no. 11, pp. 2397–2410, 2017, doi: 10.18632/aging.101327.

[62] D. Wu, Y. Li, K. S. Zhu, H. Wang, and W.-G. Zhu, "Advances in Cellular Characterization of the Sirtuin Isoform, SIRT7," *Front. Endocrinol. (Lausanne).*, vol. 9, Nov. 2018, doi: 10.3389/fendo.2018.00652.

[63] S. Chen *et al.*, “SIRT7-dependent deacetylation of the U3-55k protein controls pre-rRNA processing,” *Nat. Commun.*, vol. 7, no. 1, pp. 1–11, Feb. 2016, doi: 10.1038/ncomms10734.

[64] M. Ding, C. Y. Jiang, Y. Zhang, J. Zhao, B. M. Han, and S. J. Xia, “SIRT7 depletion inhibits cell proliferation and androgen-induced autophagy by suppressing the AR signaling in prostate cancer,” *J. Exp. Clin. Cancer Res.*, vol. 39, no. 1, Feb. 2020, doi: 10.1186/s13046-019-1516-1.

[65] Q. He, K. Chen, R. Ye, N. Dai, P. Guo, and L. Wang, “Associations of sirtuins with clinicopathological variables and prognosis in human ovarian cancer,” *Oncol. Lett.*, vol. 19, no. 4, pp. 3278–3288, 2020, doi: 10.3892/ol.2020.11432.

[66] B. N. Vazquez, J. K. Thackray, and L. Serrano, “Sirtuins and DNA damage repair: SIRT7 comes to play,” *Nucleus*, vol. 8, no. 2, pp. 107–115, Jan. 2017, doi: 10.1080/19491034.2016.1264552.

[67] H. Jęśko, P. Wencel, R. P. Strosznajder, and J. B. Strosznajder, “Sirtuins and Their Roles in Brain Aging and Neurodegenerative Disorders,” *Neurochem. Res.*, vol. 42, no. 3, pp. 876–890, Mar. 2017, doi: 10.1007/s11064-016-2110-y.

[68] A. Kaiser *et al.*, “SIRT7: an influence factor in healthy aging and the development of age-dependent myeloid stem-cell disorders,” *Leukemia*, 2020, doi: 10.1038/s41375-020-0803-3.

[69] F. Debacq-Chainiaux, J. D. Erusalimsky, J. Campisi, and O. Toussaint, “Protocols to detect senescence-associated beta-galactosidase (SA-βgal) activity, a biomarker of senescent cells in culture and in vivo,” *Nat. Protoc.*, vol. 4, no. 12, pp. 1798–1806, Nov. 2009, doi: 10.1038/nprot.2009.191.

[70] C. Capparelli *et al.*, “CDK inhibitors (p16/p19/p21) induce senescence and autophagy in cancer-associated fibroblasts, ‘fueling’ tumor growth via paracrine interactions, without an

increase in neo-angiogenesis," *Cell Cycle*, vol. 11, no. 19, pp. 3599–3610, Oct. 2012, doi: 10.4161/cc.21884.

[71] A. G. Georgakilas, O. A. Martin, and W. M. Bonner, "p21: A Two-Faced Genome Guardian," *Trends in Molecular Medicine*, vol. 23, no. 4. Elsevier Ltd, pp. 310–319, 01-Apr-2017, doi: 10.1016/j.molmed.2017.02.001.

[72] C. H. Hsu, S. J. Altschuler, and L. F. Wu, "Patterns of Early p21 Dynamics Determine Proliferation-Senescence Cell Fate after Chemotherapy," *Cell*, vol. 178, no. 2, pp. 361-373.e12, Jul. 2019, doi: 10.1016/j.cell.2019.05.041.

[73] D. J. Baker *et al.*, "Opposing roles for p16Ink4a and p19Arf in senescence and ageing caused by BubR1 insufficiency," *Nat. Cell Biol.*, vol. 10, no. 7, pp. 825–836, Jul. 2008, doi: 10.1038/ncb1744.

[74] M. Hashimoto *et al.*, "Elimination of p19ARF-expressing cells enhances pulmonary function in mice," *JCI Insight*, vol. 1, no. 12, Aug. 2016, doi: 10.1172/jci.insight.87732.

[75] S. Paredes *et al.*, "The epigenetic regulator SIRT7 guards against mammalian cellular senescence induced by ribosomal DNA instability," *J. Biol. Chem.*, vol. 293, no. 28, pp. 11242–11250, Jul. 2018, doi: 10.1074/jbc.AC118.003325.

[76] N. Lee *et al.*, "Comparative interactomes of SIRT6 and SIRT7: Implication of functional links to aging," *Proteomics*, vol. 14, no. 13–14, pp. 1610–1622, 2014, doi: 10.1002/pmic.201400001.

[77] L. K. Fonken *et al.*, "The alarmin HMGB1 mediates age-induced neuroinflammatory priming," *J. Neurosci.*, vol. 36, no. 30, pp. 7946–7956, Jul. 2016, doi: 10.1523/JNEUROSCI.1161-16.2016.

[78] L. Koelman, O. Pivovarova-Ramich, A. F. H. Pfeiffer, T. Grune, and K. Aleksandrova, "Cytokines for evaluation of chronic inflammatory status in ageing research: Reliability and

phenotypic characterisation," *Immun. Ageing*, vol. 16, no. 1, p. 11, May 2019, doi: 10.1186/s12979-019-0151-1.

[79] J. Sun, X. Ren, and J. W. Simpkins, "Sequential Upregulation of Superoxide Dismutase 2 and Heme Oxygenase 1 by tert-Butylhydroquinone Protects Mitochondria during Oxidative Stress s," *Mol. Pharmacol. Mol Pharmacol*, vol. 88, pp. 437–449, 2015, doi: 10.1124/mol.115.098269.

[80] B. J. Willcox *et al.*, "FOXO3A genotype is strongly associated with human longevity," *Proc. Natl. Acad. Sci. U. S. A.*, vol. 105, no. 37, pp. 13987–13992, Sep. 2008, doi: 10.1073/pnas.0801030105.

[81] W. B. Ershler and E. T. Keller, "Age-Associated Increased Interleukin-6 Gene Expression, Late-Life Diseases, and Frailty," *Annu. Rev. Med.*, vol. 51, no. 1, pp. 245–270, Feb. 2000, doi: 10.1146/annurev.med.51.1.245.

[82] W. B. Ershler, "Interleukin-6: A Cytokine for Gerontolgists," *J. Am. Geriatr. Soc.*, vol. 41, no. 2, pp. 176–181, 1993, doi: 10.1111/j.1532-5415.1993.tb02054.x.

[83] F. Paré, G. Tardif, H. Fahmi, Y. Ouhaddi, J. P. Pelletier, and J. Martel-Pelletier, "In vivo protective effect of adipsin-deficiency on spontaneous knee osteoarthritis in aging mice," *Aging (Albany. NY).*, vol. 12, no. 3, pp. 2880–2896, Feb. 2020, doi: 10.18632/aging.102784.

[84] S. Hong and M. M. Kim, "IGFBP-3 plays an important role in senescence as an aging marker," *Environ. Toxicol. Pharmacol.*, vol. 59, pp. 138–145, Apr. 2018, doi: 10.1016/j.etap.2018.03.014.

[85] B. R. Binder *et al.*, "Plasminogen activator inhibitor 1: Physiological and pathophysiological roles," *News Physiol. Sci.*, vol. 17, no. 2, pp. 56–61, Apr. 2002, doi: 10.1152/nips.01369.2001.

[86] S. Wang, E. J. Moerman, R. A. Jones, R. Thweatt, and S. Goldstein, "Characterization of

IGFBP-3, PAI-1 and SPARC mRNA expression in senescent fibroblasts," *Mech. Ageing Dev.*, vol. 92, no. 2–3, pp. 121–132, Dec. 1996, doi: 10.1016/S0047-6374(96)01814-3.

[87] C. S. Whyte, G. B. Morrow, J. L. Mitchell, P. Chowdary, and N. J. Mutch, "Fibrinolytic abnormalities in acute respiratory distress syndrome (ARDS) and versatility of thrombolytic drugs to treat COVID-19," *Journal of Thrombosis and Haemostasis*. Blackwell Publishing Ltd, 2020, doi: 10.1111/jth.14872.

[88] W. A. Schroder *et al.*, "SerpinB2 inhibits migration and promotes a resolution phase signature in large peritoneal macrophages," *Sci. Rep.*, vol. 9, no. 1, pp. 1–15, Dec. 2019, doi: 10.1038/s41598-019-48741-w.

[89] V. Gorbunova, A. Seluanov, Z. Mao, and C. Hine, "SURVEY AND SUMMARY Changes in DNA repair during aging," *Nucleic Acids Res.*, vol. 35, no. 22, pp. 7466–7474, 2007, doi: 10.1093/nar/gkm756.

[90] I. A. Shaltiel, L. Krenning, W. Bruinsma, and R. H. Medema, "The same, only different - DNA damage checkpoints and their reversal throughout the cell cycle," *Journal of Cell Science*, vol. 128, no. 4. Company of Biologists Ltd, pp. 607–620, 15-Feb-2015, doi: 10.1242/jcs.163766.

[91] M. E. Lingbeek, J. J. L. Jacobs, and M. Van Lohuizen, "The T-box repressors TBX2 and TBX3 specifically regulate the tumor suppressor gene p14ARF via a variant T-site in the initiator," *J. Biol. Chem.*, vol. 277, no. 29, pp. 26120–26127, Jul. 2002, doi: 10.1074/jbc.M200403200.

[92] T. Willmer, S. Hare, J. Peres, and S. Prince, "The T-box transcription factor TBX3 drives proliferation by direct repression of the p21WAF1 cyclin-dependent kinase inhibitor," *Cell Div.*, vol. 11, no. 1, Apr. 2016, doi: 10.1186/s13008-016-0019-0.

[93] T. H. Lü, C. Rudat, I. Wojahn, A. Moon, and V. M. Christoffels, "Tbx2 and Tbx3 Act

Downstream of Shh to Maintain Canonical Wnt Signaling during Branching Morphogenesis of the Murine Lung," *Dev. Cell*, vol. 39, pp. 239–253, 2016, doi: 10.1016/j.devcel.2016.08.007.

[94] A. Suzuki, S. Sekiya, D. Büscher, J. C. I. Belmonte, and H. Taniguchi, "Tbx3 controls the fate of hepatic progenitor cells in liver development by suppressing p19ARF expression," *Development*, vol. 135, no. 9, pp. 1589–1595, May 2008, doi: 10.1242/dev.016634.

[95] P. T. Tran *et al.*, "Twist1 suppresses senescence programs and thereby accelerates and maintains mutant Kras-induced lung tumorigenesis," *PLoS Genet.*, vol. 8, no. 5, May 2012, doi: 10.1371/journal.pgen.1002650.

[96] T. K. Kim *et al.*, "Interferon regulatory factor 3 activates p53-dependent cell growth inhibition," *Cancer Lett.*, vol. 242, no. 2, pp. 215–221, Oct. 2006, doi: 10.1016/j.canlet.2005.11.003.

[97] Q. Li *et al.*, "Interferon regulatory factors IRF5 and IRF7 inhibit growth and induce senescence in immortal Li-Fraumeni fibroblasts," *Mol. Cancer Res.*, vol. 6, no. 5, pp. 770–784, May 2008, doi: 10.1158/1541-7786.MCR-07-0114.

[98] G. P. Dimri *et al.*, "A biomarker that identifies senescent human cells in culture and in aging skin in vivo," *Proc. Natl. Acad. Sci. U. S. A.*, vol. 92, no. 20, pp. 9363–9367, Sep. 1995, doi: 10.1073/pnas.92.20.9363.

[99] W. Wang *et al.*, "Sequential Activation of the MEK-Extracellular Signal-Regulated Kinase and MKK3/6-p38 Mitogen-Activated Protein Kinase Pathways Mediates Oncogenic ras-Induced Premature Senescence," *Mol. Cell. Biol.*, vol. 22, no. 10, pp. 3389–3403, May 2002, doi: 10.1128/mcb.22.10.3389-3403.2002.

[100] J. G. Bode *et al.*, "The MKK6/p38 mitogen-activated protein kinase pathway is capable of inducing SOCS3 gene expression and inhibits IL-6-induced transcription," *Biol. Chem.*, vol.

382, no. 10, pp. 1447–1453, 2001, doi: 10.1515/BC.2001.178.

[101] G. Harada, Q. Neng, T. Fujiki, and Y. Katakura, “Molecular mechanisms for the p38-induced cellular senescence in normal human fibroblast,” doi: 10.1093/jb/mvu040.

[102] Y. Xu, N. Li, R. Xiang, and P. Sun, “Emerging roles of the p38 MAPK and PI3K/AKT/mTOR pathways in oncogene-induced senescence,” *Trends in Biochemical Sciences*, vol. 39, no. 6. Elsevier Ltd, pp. 268–276, 2014, doi: 10.1016/j.tibs.2014.04.004.

[103] J. Raingeaud, A. J. Whitmarsh, T. Barrett, B. Dérijard, and R. J. Davis, “MKK3- and MKK6-regulated gene expression is mediated by the p38 mitogen-activated protein kinase signal transduction pathway.,” *Mol. Cell. Biol.*, vol. 16, no. 3, pp. 1247–1255, Mar. 1996, doi: 10.1128/mcb.16.3.1247.

[104] J. Zhao *et al.*, “ATM is a key driver of NF-κB-dependent DNA-damage-induced senescence, stem cell dysfunction and aging,” *Aging (Albany. NY).*, vol. 12, no. 6, pp. 4688–4710, Mar. 2020, doi: 10.18632/aging.102863.

[105] M. Eren *et al.*, “PAI-1-regulated extracellular proteolysis governs senescence and survival in Klotho mice,” *Proc. Natl. Acad. Sci. U. S. A.*, vol. 111, no. 19, pp. 7090–7095, May 2014, doi: 10.1073/pnas.1321942111.

[106] S. S. Khan *et al.*, “A null mutation in SERPINE1 protects against biological aging in humans,” *Sci. Adv.*, vol. 3, no. 11, p. eaao1617, Nov. 2017, doi: 10.1126/sciadv.aao1617.

[107] A. J. Ball and F. Levine, “Telomere-independent cellular senescence in human fetal cardiomyocytes,” *Aging Cell*, vol. 4, no. 1, pp. 21–30, Feb. 2005, doi: 10.1111/j.1474-9728.2004.00137.x.

[108] I. HORIKAWA, T. YAWATA, and J. C. BARRETT, “Cellular Senescence Mechanisms Independent of Telomere Shortening and Telomerase: Other Barriers to Cell Immortalization and Carcinogenesis,” *J. Anti. Aging. Med.*, vol. 3, no. 4, pp. 373–382, Jan.

2000, doi: 10.1089/rej.1.2000.3.373.

[109] A. R. Davalos *et al.*, "p53-dependent release of Alarmin HMGB1 is a central mediator of senescent phenotypes," *J. Cell Biol.*, vol. 201, no. 4, pp. 613–629, May 2013, doi: 10.1083/jcb.201206006.

[110] H. Erlandsson Harris and U. Andersson, "Mini-review: The nuclear protein HMGB1 as a proinflammatory mediator," *Eur. J. Immunol.*, vol. 34, no. 6, pp. 1503–1512, Jun. 2004, doi: 10.1002/eji.200424916.

[111] F. Olivieri, F. Prattichizzo, J. Grillari, and C. R. Balistreri, "Cellular Senescence and Inflammaging in Age-Related Diseases," *Mediators Inflamm.*, vol. 2018, 2018, doi: 10.1155/2018/9076485.

[112] I. M. Rea, D. S. Gibson, V. McGilligan, S. E. McNerlan, H. Denis Alexander, and O. A. Ross, "Age and age-related diseases: Role of inflammation triggers and cytokines," *Frontiers in Immunology*, vol. 9, no. APR. Frontiers Media S.A., 09-Apr-2018, doi: 10.3389/fimmu.2018.00586.

[113] B. Dieriks, W. De Vos, S. Baatout, and P. Van Oostveldt, "Repeated exposure of human fibroblasts to ionizing radiation reveals an adaptive response that is not mediated by interleukin-6 or TGF-β," *Mutat. Res. - Fundam. Mol. Mech. Mutagen.*, vol. 715, no. 1–2, pp. 19–24, Oct. 2011, doi: 10.1016/j.mrfmmm.2011.07.002.

[114] D. M. Nelson, T. McBryan, J. C. Jeyapalan, J. M. Sedivy, and P. D. Adams, "A comparison of oncogene-induced senescence and replicative senescence: implications for tumor suppression and aging," *Age (Omaha).*, vol. 36, no. 3, p. 9637, Jun. 2014, doi: 10.1007/s11357-014-9637-0.

[115] M. Serrano, A. W. Lin, M. E. McCurrach, D. Beach, and S. W. Lowe, "Oncogenic ras provokes premature cell senescence associated with accumulation of p53 and p16(INK4a),"

Cell, vol. 88, no. 5, pp. 593–602, Mar. 1997, doi: 10.1016/S0092-8674(00)81902-9.

[116] Q. Deng, R. Liao, B. L. Wu, and P. Sun, "High Intensity ras Signaling Induces Premature Senescence by Activating p38 Pathway in Primary Human Fibroblasts," *J. Biol. Chem.*, vol. 279, no. 2, pp. 1050–1059, Jan. 2004, doi: 10.1074/jbc.M308644200.

[117] I. Y. Chang *et al.*, "Oncogenic H-Ras up-regulates expression of Ku80 to protect cells from γ-ray irradiation in NIH3T3 cells," *Cancer Res.*, vol. 65, no. 15, pp. 6811–6819, Aug. 2005, doi: 10.1158/0008-5472.CAN-04-4065.

[118] H. J. Cho *et al.*, "Oncogenic H-ras enhances DNA repair through the Ras/phosphatidylinositol 3-kinase/Rac1 pathway in NIH3T3 cells. Evidence for association with reactive oxygen species," *J. Biol. Chem.*, vol. 277, no. 22, pp. 19358–19366, May 2002, doi: 10.1074/jbc.M200933200.

[119] K. M. Sathyan, K. R. Nalinakumari, and S. Kannan, "H-Ras mutation modulates the expression of major cell cycle regulatory proteins and disease prognosis in oral carcinoma," *Mod. Pathol.*, vol. 20, no. 11, pp. 1141–1148, Nov. 2007, doi: 10.1038/modpathol.3800948.

[120] D. X. Mason, T. J. Jackson, and A. W. Lin, "Molecular signature of oncogenic ras-induced senescence," *Oncogene*, vol. 23, no. 57, pp. 9238–9246, Dec. 2004, doi: 10.1038/sj.onc.1208172.

[121] T. J. Huot *et al.*, "Biallelic Mutations in p16INK4a Confer Resistance to Ras- and Ets-Induced Senescence in Human Diploid Fibroblasts," *Mol. Cell. Biol.*, vol. 22, no. 23, pp. 8135–8143, Dec. 2002, doi: 10.1128/mcb.22.23.8135-8143.2002.

[122] J. P. Coppé *et al.*, "Senescence-associated secretory phenotypes reveal cell-nonautonomous functions of oncogenic RAS and the p53 tumor suppressor.," *PLoS Biol.*, vol. 6, no. 12, 2008, doi: 10.1371/journal.pbio.0060301.

[123] J. Salotti and P. F. Johnson, "Regulation of senescence and the SASP by the transcription

factor C/EBPβ," *Experimental Gerontology*, vol. 128. Elsevier Inc., p. 110752, 01-Dec-2019, doi: 10.1016/j.exger.2019.110752.

[124] Y. Su *et al.*, "The protein kinase D1-mediated classical protein secretory pathway regulates the Ras oncogene-induced senescence response," 2018, doi: 10.1242/jcs.207217.

[125] E. Vénéreau, C. Ceriotti, and M. E. Bianchi, "DAMPs from cell death to new life," *Frontiers in Immunology*, vol. 6, no. AUG. Frontiers Media S.A., p. 422, 18-Aug-2015, doi: 10.3389/fimmu.2015.00422.

[126] J. S. Roh and D. H. Sohn, "Damage-associated molecular patterns in inflammatory diseases," *Immune Network*, vol. 18, no. 4. Korean Association of Immunologists, 01-Aug-2018, doi: 10.4110/in.2018.18.e27.

[127] S. Vanpatten and Y. Al-Abed, "High Mobility Group Box-1 (HMGb1): Current Wisdom and Advancement as a Potential Drug Target," *Journal of Medicinal Chemistry*, vol. 61, no. 12. American Chemical Society, pp. 5093–5107, 28-Jun-2018, doi: 10.1021/acs.jmedchem.7b01136.

[128] Y. Guéguen, A. Bontemps, and T. G. Ebrahimian, "Adaptive responses to low doses of radiation or chemicals: their cellular and molecular mechanisms," *Cellular and Molecular Life Sciences*, vol. 76, no. 7. Birkhauser Verlag AG, pp. 1255–1273, 15-Apr-2019, doi: 10.1007/s00018-018-2987-5.

[129] Y. Liu *et al.*, "Protective effects of crocetin on arsenic trioxide-induced hepatic injury: Involvement of suppression in oxidative stress and inflammation through activation of nrf2 signaling pathway in rats," *Drug Des. Devel. Ther.*, vol. 14, pp. 1921–1931, 2020, doi: 10.2147/DDDT.S247947.

[130] P. Hiebert *et al.*, "Nrf2-Mediated Fibroblast Reprogramming Drives Cellular Senescence by Targeting the Matrisome," *Dev. Cell*, vol. 46, no. 2, pp. 145-161.e10, Jul. 2018, doi:

10.1016/j.devcel.2018.06.012.

[131] A. V Ermakova and I. O. Velegzhaninov, “Low-Dose Irradiation of Human Fibroblasts Leads to Delayed Acceleration of Proliferation of Their Progeny,” *Orig. Russ. Text © A.V. Ermakova, I.O. Velegzhaninov*, vol. 62, no. 5, pp. 932–937, 2017, doi: 10.1134/S0006350917050062.

[132] Y. Le and T. Pack, “Low-dose radiation delays aging of human stem cells,” *Cytotherapy*, vol. 21, no. 5, p. e15, May 2019, doi: 10.1016/j.jcyt.2019.04.048.

[133] M. Okada *et al.*, “Single extreme low dose/low dose rate irradiation causes alteration in lifespan and genome instability in primary human cells,” *Br. J. Cancer*, vol. 96, pp. 1707–1710, 2007, doi: 10.1038/sj.bjc.6603775.

[134] S. Ulyanenko *et al.*, “Formation of γH2AX and pATM foci in human mesenchymal stem cells exposed to low dose-rate gamma-radiation,” *Int. J. Mol. Sci.*, vol. 20, no. 11, Jun. 2019, doi: 10.3390/ijms20112645.

[135] A. N. Osipov, G. Buleeva, E. Arkhangelskaya, and D. Klokov, “In vivo γ-irradiation low dose threshold for suppression of DNA double strand breaks below the spontaneous level in mouse blood and spleen cells,” *Mutat. Res. - Genet. Toxicol. Environ. Mutagen.*, vol. 756, no. 1–2, pp. 141–145, May 2013, doi: 10.1016/j.mrgentox.2013.04.016.

[136] A. N. Osipov *et al.*, “Activation of homologous recombination DNA repair in human skin fibroblasts continuously exposed to X-ray radiation,” *Oncotarget*, vol. 6, no. 29, pp. 26876–26885, 2015, doi: 10.18632/oncotarget.4946.

[137] A. Iyer-Bierhoff and I. Grummt, “Stop-and-Go: Dynamics of Nucleolar Transcription During the Cell Cycle,” *Epigenetics Insights*, vol. 12. SAGE Publications Ltd, 01-May-2019, doi: 10.1177/2516865719849090.

[138] V. Krizhanovsky *et al.*, “Senescence of Activated Stellate Cells Limits Liver Fibrosis,” *Cell*,

vol. 134, no. 4, pp. 657–667, Aug. 2008, doi: 10.1016/j.cell.2008.06.049.

[139] T. S. Chikenji *et al.*, "p16INK4A-expressing mesenchymal stromal cells restore the senescence–clearance–regeneration sequence that is impaired in chronic muscle inflammation," *EBioMedicine*, vol. 44, pp. 86–97, Jun. 2019, doi: 10.1016/j.ebiom.2019.05.012.

[140] F. Tago, M. Tsukimoto, H. Nakatsukasa, and S. Kojima, " Repeated 0.5-Gy Gamma Irradiation Attenuates Autoimmune Disease in MRL- lpr/lpr Mice with Suppression of CD3 + CD4 − CD8 − B220 + T-Cell Proliferation and with Up-regulation of CD4 + CD25 + Foxp3 + Regulatory T Cells ," *Radiat. Res.*, vol. 169, no. 1, pp. 59–66, Jan. 2008, doi: 10.1667/rr1013.1.

[141] H. H. Hsieh, Y. C. Chen, J. R. Jhan, and J. J. Lin, "The serine protease inhibitor serpinB2 binds and stabilizes p21 in senescent cells," *J. Cell Sci.*, vol. 130, no. 19, pp. 3272–3281, 2017, doi: 10.1242/jcs.204974.

[142] X.-M. Zhang, T. Wang, P. Hu, B. Li, H. Liu, and Y.-F. Cheng, "SERPINB2 overexpression inhibited cell proliferation, invasion and migration, led to G2/M arrest, and increased radiosensitivity in nasopharyngeal carcinoma cells," *J. Radiat. Res.*, vol. 60, no. 3, pp. 318–327, 2019, doi: 10.1093/jrr/rrz003.

[143] D. J. Elzi, Y. Lai, M. Song, K. Hakala, S. T. Weintraub, and Y. Shiio, "Plasminogen activator inhibitor 1 - Insulin-like growth factor binding protein 3 cascade regulates stress-induced senescence," *Proc. Natl. Acad. Sci. U. S. A.*, vol. 109, no. 30, pp. 12052–12057, Jul. 2012, doi: 10.1073/pnas.1120437109.

APPENDIX

TABLE 3: Differential gene expression from Qiagen human cellular senescence qPCR array kit. Changes in gene expression were calculated relative to age-matched untreated control cells. The regulation threshold = 2-fold. Red highlight – upregulated; Green highlight – downregulation. (Replicate 1 and 2 are the two independent biological replicates used for these experiments). Data shows the mean ± S.E.M of two independent biological replicates.

Group – 1: Differentially expressed genes in HFL1 cells 1-week post-radiation relative to UT control

TARGET GENE	SAMPLE NAME	MEAN Cq	REGULATION	DIRECTIONALITY OF CHANGE (2-fold threshold)
ALDH1A3		33.27	3.60569	Up regulated
ATM		28.9	-2.02866	Down regulated
CDK2		28.38	-2.1672	Down regulated
CREG1		30.65	-2.2171	Down regulated
EGR1		30.38	-2.65124	Down regulated
GLB1		30.37	-2.21902	Down regulated
ID1		28.32	-2.11851	Down regulated
IGFBP3		27.19	-2.45161	Down regulated
SERPINB2		29.07	-2.6656	Down regulated
SERPINE1		25.88	-2.0475	Down regulated
CCND1	**1 week**	24.04	2.16572	Up regulated
CCNE1	**10 mGy**	28.46	3.41657	Up regulated
CD44		22.49	2.12704	Up regulated
CDKN1B		27.47	2.3856	Up regulated
COL1A1		22.71	2.10328	Up regulated
E2F1		29.19	2.20532	Up regulated
E2F3		29.1	2.23541	Up regulated
EGR1		27.07	2.139	Up regulated
ETS2		27.47	2.08032	Up regulated
FN1		19.36	2.37039	Up regulated
GLB1		28.42	2.23477	Up regulated
GSK3B		25.75	2.00209	Up regulated

IGF1R		27.87	2.6009	Up regulated
IRF5		34.37	9.74584	Up regulated
IRF7		32.3	2.33832	Up regulated
MAP2K1		26.67	2.26314	Up regulated
MAP2K6		29.71	2.18806	Up regulated
PPC		20.36	-2.25555	Down regulated
RBL2		26.5	2.62634	Up regulated
SPARC		22.3	2.05638	Up regulated
TERF2		26.94	2.10789	Up regulated
TGFB111		26.87	2.14087	Up regulated
THBS1		22.14	2.03621	Up regulated
TP53		26.14	2.01584	Up regulated
ALDH1A3	**1 week** **100 mGy**	32.52	5.44704	Up regulated
CHEK2		29.03	2.03311	Up regulated
CREG1		30.43	-2.09922	Down regulated
IRF7		32.77	2.80639	Up regulated
SERPINB2		30.15	-6.25851	Down regulated
ALDH1A3		34.32	-2.69672	Down regulated
FN1		22.69	-2.04107	Down regulated
ID1		28.56	2.84775	Up regulated
IGF1		35.6	-2.45438	Down regulated

Group – 2: Differentially expressed genes in 12 weeks old HFL1 cells post radiation relative to UT control:

TARGET GENE	SAMPLE NAME	MEAN Cq	REGULATION	DIRECTIONALITY OF CHANGE (2-fold threshold
BMI1	12 weeks 10 mGy	29.96	-2.56985	Down regulated
CCNA2		32.07	-2.76972	Down regulated
CDK2		30.84	2.26609	Up regulated
CDKN1B		31.1	2.60098	Up regulated
CDKN2D		30.12	5.3755	Up regulated
COL1A1		27.05	-6.14141	Down regulated
COL3A1		27.19	-9.17125	Down regulated
CREG1		31.72	-5.78666	Down regulated
E2F1		33.26	3.03877	Up regulated
EGR1		34.99	-6.87948	Down regulated
ETS1		32.01	-2.91274	Down regulated
FN1		23.06	-5.48496	Down regulated
GSK3B		29.49	-2.70939	Down regulated
ID1		29.13	3.329	Up regulated
IGFBP3		25.56	-8.92558	Down regulated
IGFBP7		21.89	-2.48493	Down regulated
PIK3CA		29.33	-2.96977	Down regulated
PLAU		29.49	13.24821	Up regulated
PTEN		30.08	-6.37918	Down regulated
RB1		31.17	-3.59001	Down regulated

RBL1		34.09	-2.71562	Down regulated
RBL2		30.68	-2.85065	Down regulated
SIRT1		31.68	-3.13478	Down regulated
TBX2		29.62	5.98378	Up regulated
THBS1		23.75	-2.837	Down regulated
TWIST1		32.92	-2.74796	Down regulated
VIM		22.18	-5.98026	Down regulated
ALDH1A3		34.04	2.56232	Up regulated
ATM		27.39	5.76413	Up regulated
BMI1		26.09	2.65374	Up regulated
CCND1		23.41	6.31238	Up regulated
CCNE1		29.37	4.01605	Up regulated
CD44		22.41	3.5389	Up regulated
CDC25C		36.36	-2.49601	Down regulated
CDK2		27.73	4.43382	Up regulated
CDK6		26.54	2.68132	Up regulated
CDKN1A		20.82	2.52609	Up regulated
CDKN1B		30.74	2.63559	Up regulated
CDKN1C		28.29	6.21909	Up regulated
CDKN2A		23.68	6.44382	Up regulated
CDKN2B		26.25	2.34589	Up regulated
CHEK1		29.57	2.42677	Up regulated
CITED2		27.44	-2.36709	Down regulated
COL1A1		23.8	-2.49968	Down regulated
E2F1		32.77	2.1398	Up regulated

ETS1		28.17	2.03555	Up regulated
ETS2		29.28	2.73155	Up regulated
GSK3B		26.19	2.18491	Up regulated
HRAS		25.72	2.5994	Up regulated
ID1		24.58	10.80399	Up regulated
IGF1R		28.98	2.17437	Up regulated
IGFBP3		22.06	-2.96399	Down regulated
IGFBP7		17.63	3.73783	Up regulated
ING1		30.44	2.16994	Up regulated
IRF3		26.69	2.761	Up regulated
IRF5		36.39	2.81811	Up regulated
MAP2K3		24.04	2.54676	Up regulated
MAPK14		27.59	3.48254	Up regulated
MDM2		25.2	3.14179	Up regulated
MORC3		26.28	4.07294	Up regulated
MYC		25.49	2.24068	Up regulated
NBN		26.89	3.24173	Up regulated
NOX4		26.97	2.86935	Up regulated
PCNA		26.13	2.33853	Up regulated
PIK3CA		25.21	3.13266	Up regulated
PLAU		26.58	12.24542	Up regulated
PRKCD		29.92	2.48909	Up regulated
PTEN		24.85	3.15127	Up regulated
RB1		26.58	2.67996	Up regulated
RBL2		27.36	2.34647	Up regulated

SERPINB2		25.12	4.1226	Up regulated
SIRT1		27.4	2.90141	Up regulated
SOD1		21.22	4.19274	Up regulated
SOD2		24.6	3.17713	Up regulated
TBX2		26.63	10.77345	Up regulated
TERF2		28.05	2.29839	Up regulated
TGFB1I1		28.83	2.70359	Up regulated
TP53		29.07	2.02764	Up regulated
TP53BP1		25.14	4.3319	Up regulated
CCNA2		28.62	-2.5277	Down regulated
CDC25C		35.66	-3.20792	Down regulated
CDKN2B		26.52	-2.12788	Down regulated
CDKN2C		32.18	-2.58888	Down regulated
COL1A1		22.9	-3.42773	Down regulated
CREG1		29.62	-13.39203	Down regulated
ETS2		26.85	2.74007	Up regulated
FN1	12 weeks	18.85	-2.93847	Down regulated
ID1	100mGy	29.44	-3.71093	Down regulated
IGFBP3		23.61	-22.99443	Down regulated
IGFBP5		22.55	3.12898	Up regulated
IRF7		31.76	4.52293	Up regulated
MYC		25.36	-2.47684	Down regulated
PLAU		25.02	29.55876	Up regulated
SERPINB2		23.62	-2.28083	Down regulated
SERPINE1		21.9	-2.51586	Down regulated

TBX2		25.25	12.4246	Up regulated
THBS1		21.15	-4.66596	Down regulated
VIM		17.94	-3.13147	Down regulated
ABL1		30.13	-2.29934	Down regulated
AKT1		30.04	-2.1328	Down regulated
CDKN1C		30.01	2.3925	Up regulated
CDKN2B		29.52	-3.25136	Down regulated
CDKN2C		35.03	-5.31466	Down regulated
CHEK2		35.55	-11.97971	Down regulated
CITED2		27.66	-2.18972	Down regulated
COL1A1		24.79	-3.92597	Down regulated
COL3A1		25.23	-2.90553	Down regulated
CREG1		30.98	-3.88158	Down regulated
EGR1		33.08	-5.15123	Down regulated
FN1		22.79	-3.86357	Down regulated
GADD45A		29.76	-2.74516	Down regulated
ID1		27.09	2.39113	Up regulated
IGF1R		31.44	-2.011	Down regulated
IGFBP3		22.82	-3.98654	Down regulated
ING1		33.59	-3.23634	Down regulated
PLAU		29.17	2.55259	Up regulated
SERPINB2		25.3	4.58655	Up regulated
SOD2		25.27	2.51978	Up regulated
TBX2		28	5.25616	Up regulated
TBX3		34.92	-2.31026	Down regulated

A

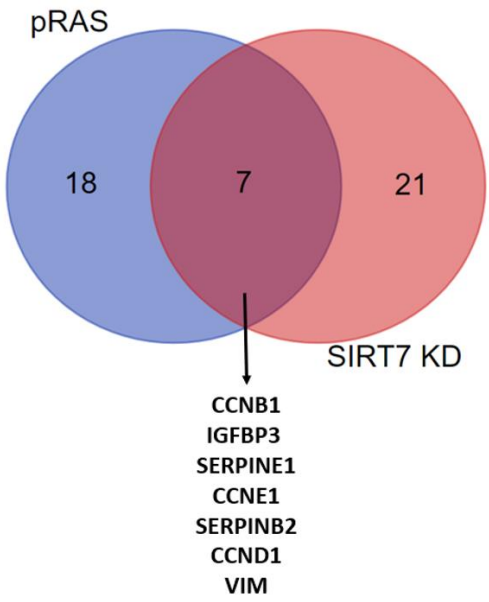

B

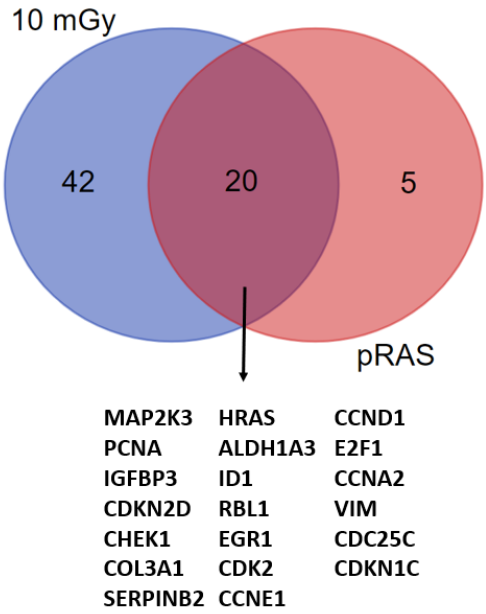

C

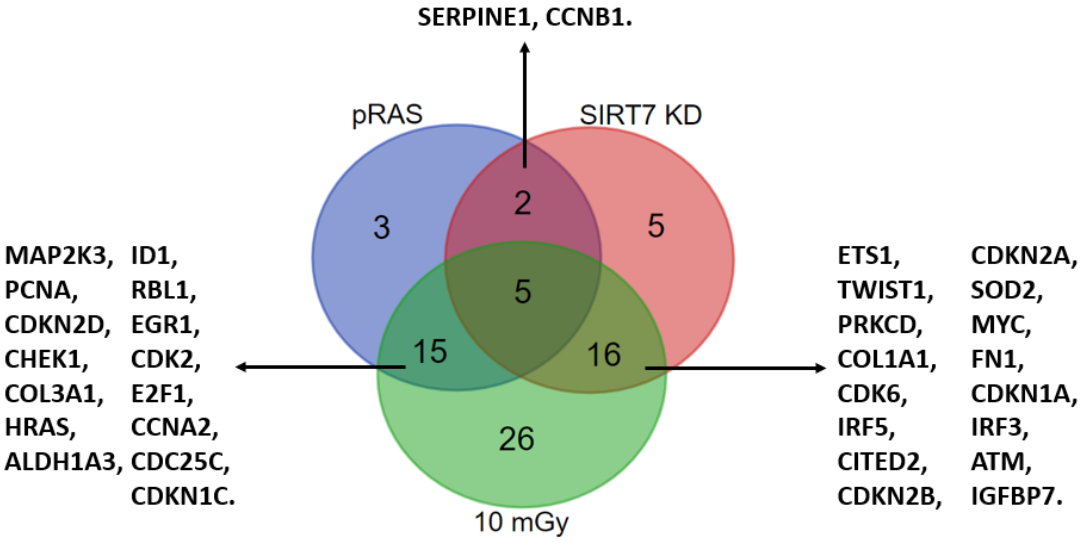

Common genes between 10 mGy, SIRT7 KD and pRAS:
IGFBP3, SERPINB2, CCNE1, CCND1, VIM.

Figure 15: Venn diagrams representation of commonly expressed genes between the dose groups: 10 mGy (where the HFL1 cells displayed a delay in senescence), SIRT7 KD HFL1 cells and HRAS overexpressed HFL1 cells (pRAS).Among the all the three groups, IGFBP3, SERPINEB2,CCNE1,CCND1, AND VIM are the genes that are regulated between all the three interventions in HFL1 cells.